

Functional consequences of chromosome holocentricity

**Dissertation
zur Erlangung des
Doktorgrades der Agrarwissenschaften (Dr. agr.)**

der

Naturwissenschaftlichen Fakultät III
Agrar- und Ernährungswissenschaften

der Martin-Luther-Universität Halle-Wittenberg

vorgelegt von

Frau M.Sc. Maja Jankowska
Geb. am 12.05.1987 in Katowice

Gutachter:

Prof. Dr. Robert Hasterok (Katowice)

Prof. Dr. Klaus Pillen

PD Dr. Andreas Houben (Gatersleben)

Datum der Verteidigung: 20.06.2016

Acknowledgements

I would like to thank my supervisor Dr habil. Andreas Houben for giving me the opportunity to be a part of the Chromosome Structure and Function group and to develop my PhD work here, for his guidance and precious remarks. Without all that support, this dissertation would certainly not be possible.

I also thank all members of the group for a truly enjoyable working atmosphere, scientific advices and for inspiring discussions. Especially, I want to thank Wei, Lala and Susann for fruitful scientific and non-scientific conversations. For the excellent technical assistance, I thank Katrin Kumke, Oda Weiss and Karla Meier.

Manny thanks to my boyfriend Bogdan for his help and giving me a lot strength and motivation to finish this work. I wish also to thank my aunt Monika and great friends Heidrun and Lutz for unconditional support, help with learning German and memorable time which we spent together. Moreover, I would like to thank all my friends who come along with me until now and thus make life a bit easier.

Niniejszą pracę pragnę zadedykować moim wspaniałym rodzicom i dziadkom, dzięki którym miałam możliwość kształcić się i zdobywać cenną wiedzę, którzy stale mnie mobilizowali i wspierali przez cały okres trwania mojej edukacji. Kocham Was!!!

Table of content

Table of content	III
List of Figures	VI
List of Tables	VII
Abstract	VIII
Zusammenfassung	IX
Abbreviations	X
1. Introduction	1
1.1. Holocentric chromosomes	1
1.2. Centromere function and structure	4
1.3. <i>Luzula elegans</i> as a model for holocentric plants.....	6
1.4. Meiosis	8
1.4.1. Meiosis in monocentric species.....	8
1.4.2. Meiosis in holocentric.....	9
1.4.3. DMC1 recombinase facilitates homologous recombination.....	12
1.5. Consequences of chromosome fragmentation	14
1.5.1. Monocentric contra holocentric after radiation	14
1.5.2. Chromosome fragments are stabilized by <i>de novo</i> formed telomeres	16
1.5.3. Karyotype evolution of holocentric chromosome species.....	18
2. Open questions and aim of the thesis	21
3. Materials and methods	22
3.1. Materials.....	22
3.2. Methods.....	24
3.2.1. Plant material and plant cultivation.....	24
3.2.2. X-ray irradiation.....	24
3.2.3. Genome size measurement by flow cytometry	25
3.2.4. Analysis of telomerase activity according to the Telomere Repeat Amplification Protocol (TRAP).....	25
3.2.5. CTAB extraction of genomic DNA.....	27
3.2.6. Fluorescence <i>in situ</i> hybridization (FISH).....	28
3.2.6.1. Probe generation for FISH	28

3.2.6.2. Nick translation of FISH probes	28
3.2.6.3. Preparation of mitotic and meiotic chromosomes for FISH	29
3.2.6.4. Fluorescence <i>in situ</i> hybridization	30
3.2.7. Indirect immunostaining	30
3.2.7.1. Preparation of meiotic chromosomes.....	30
3.2.7.2. Indirect immunostaining	31
3.2.8. Microscopy	32
3.2.9. Generation of a LeDMC1-specific antibody	32
3.2.9.1. Molecular cloning	32
3.2.9.1.1. Extraction of total RNA and cDNA synthesis	32
3.2.9.1.2. RT-PCR	33
3.2.9.1.3. LeDMC1 fragment ligation into the pSC-A-amp/kan cloning vector ..	33
3.2.9.1.4. Plasmid DNA extraction, digestion and sequencing	34
3.2.9.1.5. LeDMC1 fragment ligation into the pET-23a-d(+) expression vector	34
3.2.9.2. Recombinant protein expression and purification	34
3.2.9.2.1. LeDMC1 recombinant protein expression.....	34
3.2.9.2.2. LeDMC1 recombinant protein purification.....	35
3.2.9.3. Verification of recombinant LeDMC1 protein	36
3.2.9.3.1. Total protein extraction from flower buds.....	36
3.2.9.3.2. Coomassie staining and Western blot analysis	36
4. Results.....	38
4.1. <i>L. elegans</i> performs an inverted meiosis	38
4.1.1. Axial element, synaptonemal complex and bouquet-like configuration are present during prophase I in <i>L. elegans</i>	38
4.1.2. Three bivalent configurations occur during pre-metaphase I	41
4.1.3. Heterochromatin fibers connect non-sister chromatids	43
4.1.4. An inverted sequence of meiotic sister chromatid segregation occurs in <i>L. elegans</i>	47
4.2 Identification of the meiotic gene DMC1 in <i>L. elegans</i>	52
4.2.1. Expression profile of LeDMC1.....	57
4.2.2. Expression of recombinant LeDMC1 protein.....	58
4.2.3. Validation of LeDMC1 anti- sera	62
4.2.4. The dynamics of LeDMC1 protein during prophase I.....	64

4.2.5. LeDMC1 do not mediate the end-to-end connection between homologues in <i>L. elegans</i>	66
4.3. Karyotype of holocentric species evolves rapidly due to holocentric centromere and efficient telomere healing	67
4.3.1. X-ray radiation induced dosage dependent chromosomal aberrations	67
4.3.2. Chromosome fragments have a holokinetic centromere and are stabilized by <i>de novo</i> formed telomeres	68
4.3.3. Holocentric fragments are successfully transmitted across several generations	75
5. Discussion	80
5.1. <i>L. elegans</i> performs an inverted meiosis	80
5.1.1. Prophase I is conserved in <i>Luzula</i> species	80
5.1.2. <i>L. elegans</i> exhibits a restricted crossover frequency and localization	80
5.1.3. Centromeres of <i>L. elegans</i> are holocentric during the entire meiotic division	81
5.1.4. An inverted sequence of meiotic sister chromatid segregation in <i>L. elegans</i>	82
5.1.5. Heterochromatin fibers connect homologous non-sister chromatids.....	83
5.1.6. Chromosome end looping is likely important for telomere protection as well as to establish an end-to-end connection between homologs	87
5.2. DMC1 is present in <i>L. elegans</i> pollen mother cells.....	89
5.2.1. DMC1 exhibits a meiosis- specific expression pattern in <i>L. elegans</i>	89
5.2.2. LeDMC1 shows a line-like specific immunolabelling pattern.....	89
5.2.3. LeDMC1 localizes with CENH3 but does not mediate the meiotic end-to-end connection between homologous non-sister chromatids.....	91
5.3. Karyotype of holocentric species evolves rapidly due to holokinetic centromeres and efficient telomere healing	93
5.3.1. X-ray radiation induced dosage dependent chromosomal aberrations	93
5.3.2. Chromosome fragmentation in <i>L. elegans</i> is sequence independent.....	93
5.3.3. Chromosome fragments have holokinetic centromeres	94
5.3.4. Chromosome fragments are stabilized by <i>de novo</i> formed telomeres	95
5.3.5. Chromosome fragments are successfully transmitted across several generations	96
6. Outlook.....	99
7. References	100
List of publications related to this thesis	116
Curriculum Vitae.....	117

List of Figures

Fig. 1. Monocentric and holocentric chromosomes at mitotic anaphase. 2

Fig. 2. *L. elegans* chromosomes at mitotic metaphase. 7

Fig. 3. Model illustrating meiotic segregation events in monocentric and holocentric species (Heckmann *et al.*, 2014). 12

Fig. 4. Model on how DMC1 recombinase facilitates homologous recombination. 14

Fig. 5. Behavior of monocentric and holocentric chromosome fragments during mitotic anaphase. 16

Fig. 6. Three possible healing events for the telomere-free broken end of a chromosome (according to Matsumoto *et al.*, 1987). 18

Fig. 7. Axial elements, synaptonemal complex and bouquet configuration are formed during prophase I in *L. elegans* (Fig. 7e-h (Heckmann *et al.*, 2014)). 39

Fig. 8. Bouquet configuration is formed during prophase I in *L. luzuloides* (Heckmann *et al.*, 2014). 40

Fig. 9. Various bivalent configurations occur during pre-metaphase I (Heckmann *et al.*, 2014). 42

Fig. 10. Satellite DNA-enriched chromatin threads connect homologous non-sister chromatids in holocentric (Fig. 10a-f (Heckmann *et al.*, 2014)). 44

Fig. 11. In monocentric species satellite DNA-enriched chromatin threads connect homologous non-sister chromatids. 46

Fig. 12. Terminal satellite repeats involved in end-to-end connection are similar between *L. elegans* and closely related *L. luzuloides*. 47

Fig. 13. Separation of sister chromatids is followed by non-sister chromatid division (Heckmann *et al.*, 2014). 49

Fig. 14. Sister chromatids separate during anaphase I implying inverted meiosis in *L. elegans* (Heckmann *et al.*, 2014). 51

Fig. 15. Structural model of inverted meiosis in *L. elegans* (Heckmann *et al.*, 2014). 52

Fig. 16. Structure of the partial LeDMC1-like gene and protein. 54

Fig. 17. Alignment of the partial *L. elegans* DMC1-like protein with the DMC1 proteins of different plant species revealed that DMC1 is a highly conserved protein. 55

Fig. 18. Phylogenetic tree containing the DMC1 protein of different plant species shows *L. elegans* DMC1- like protein affiliation to the monocot family. 56

Fig. 19. DMC1-like of *L. elegans* shows transcription activity only in generative tissue. 58

Fig. 20. Restriction digestion confirmed successful cloning of LeDMC1 gene into pSC-A-amp vector. 59

Fig. 21. The DMC1 sequences from pET-23-a constructs differ only in one amino-acid compared to the DMC1 sequence coming from RNAseq database. 60

Fig. 22. SDS-PAGE gel staining and Western blot of purified LeDMC1 recombinant protein reveal the presence of recombinant protein in the sample. 62

Fig. 23. Typical signals caused by the pre-immune serum of the rabbit used to generate LeDMC1 antibody are of weak intensity.	63
Fig. 24. Western blot analysis of LeDMC1 rabbit antibodies reveal multiple bands.	64
Fig. 25. Distribution of anti-LeDMC1-specific immunosignals.	65
Fig. 26. LeDMC1 does not localize to the end-to-end association between homologues at metaphase I.	66
Fig. 27. X-radiation induces chromosome fragmentation in <i>L. elegans</i> (Jankowska et al., 2015).	68
Fig. 28. Chromosome fragments of <i>L. elegans</i> possess holocentric centromere and are stabilized by <i>de novo</i> formed telomeres.	70
Fig. 29. TRAP assay revealed telomerase activity in seedlings and flower buds of <i>L. elegans</i> (Jankowska et al., 2015).	72
Fig. 30. Determination of inhibitor factors and telomerase activity in different irradiated and non-irradiated <i>L. elegans</i> samples by the RTQ-TRAP assay.	74
Fig. 31. Holocentric fragments are stably transmitted to the next generations (Jankowska et al., 2015).	77
Fig. 32. Model illustrating possible ways of holocentric karyotype evolution based on the interplay between holokinetic centromeres and rapid telomere healing (Jankowska et al., 2015).	79
Fig. 33. Model illustrating crossover distribution along a holocentric chromosome.	81
Fig. 34. Crossover-triggered differentiation of bivalent subdomains dictates chromosome organization and behavior during meiosis.	85
Fig. 35. Scheme showing the likely dynamics of CENH3 and LeDMC1 proteins in holocentric centromeres at different stages of meiosis.	92

List of Tables

Table 1. List of primer sequences.	26
Table 2. Antibodies and their dilutions used for immunostaining	31
Table 3. Antibodies and their dilutions used for Western blot.	37

Abstract

Holocentric chromosomes occur in a number of independent eukaryotic lineages. They form centromeres along almost the entire poleward chromatid surfaces and due to this alternative chromosome structure species with holocentric chromosomes cannot use the two-step loss of cohesion during meiosis typical for monocentric chromosomes.

We provide evidence that the plant *Luzula elegans* maintains a holocentric chromosome architecture and behavior throughout meiosis. Contrary to a monopolar sister centromere orientation in monocentrics, sister centromeres in *L. elegans* behave as two distinct functional units during meiosis I mediating bipolar attachment to microtubules. During first meiosis division sister chromatids segregate and terminally linked by satellite DNA enriched chromatin threads non-sister chromatids migrated to the same cell pole. Homologous non-sister chromatids remain connected till the metaphase II and then after degradation of mentioned connection, they separated at anaphase II. Hence, the sequence of meiotic chromosome segregation in *L. elegans* is inverted. Based on anti-LeDMC1 staining, we excluded a recombination dependent end-to-end connection between homologous non-sister chromatids.

Additionally, we found that irradiation induced chromosomal fragments and rearranged chromosomes showed normal centromere activity and rapid *de novo* telomere formation at break points. Holocentric chromosome fragments and translocated chromosomes revealed the same mitotic mobility like unfragmented chromosomes and successful transmission across three generations. Hence, a combination of holocentric centromere activity and the fast formation of new telomeres at break points enable holocentric species a rapid karyotype evolution involving chromosome fission and rearrangements.

Zusammenfassung

Holozentrische Chromosomen treten in einer Reihe von unabhängigen Abstammungen in unterschiedlichen Eukaryoten auf. Diese bilden Zentromere entlang der Gesamtlänge der Schwesterchromatiden. Aufgrund dieser alternativen Chromosomenstruktur können Arten mit holozentrischen Chromosomen während der Meiose den für monozentrische Chromosomen-typischen Vorgang des Zwei-Schritt-Kohäsionsverlusts nicht verwenden. Die Ergebnisse zeigen, dass *Luzula elegans* eine holozentrische Chromosomenarchitektur während der gesamten Meiose beibehält. Im Gegensatz zu monopolar orientierten Schwesterzentromeren monozentrischer Arten, verhalten sich Schwesterzentromere in *L. elegans* wie zwei unterschiedliche Funktionseinheiten. Während der Meiose I kommt es zu einer bipolaren Mikrotubulibindung. In der Meiose I trennen sich die Schwesterchromatiden, dagegen verbleiben Nicht-Schwesterchromatiden terminal verbunden. Satelliten DNA-positive Chromatinfäden sind an dieser Verbindung beteiligt. Homologe Nicht-Schwesterchromatiden verbleiben bis zur Metaphase II verbunden. In der Anaphase II trennen sich die Nicht-Schwesterchromatiden nach Abbau der Chromatinfäden. Somit ist die Abfolge der Chromatidenteilung in *L. elegans* invertiert. Basierend auf anti-LeDMC1 Markierungen konnte eine Rekombinations-abhängige terminale Verbindung zwischen homologen Nicht-Schwesterchromatiden ausgeschlossen werden.

Zusätzlich konnte nachgewiesen werden, dass Strahlen-induzierte Chromosomenfragmente und Translokationschromosomen eine normale Zentromeraktivität besitzen. Gebrochene Chromosomen werden durch eine schnelle *de novo* Telomerbildung repariert. Chromosomenfragmente und Translokationschromosomen zeigen eine vergleichbare Mobilität wie nicht-fragmentierte Chromosomen. Fragmentierte Chromosomen konnten über drei Generationen weitervererbt werden. Die Kombination aus holokinetischer Zentromeraktivität und die effiziente Bildung neuer Telomere ermöglicht eine schnelle Evolution neuer Karyotypen in Arten mit holozentrischen Chromosomen nach Chromosomenfragmentierung und Translokationen.

Abbreviations

°C	Degree Celsius
Amp	Ampicillin
BLAST	Basic local alignment search tool
bp	Base pair
cDNA	Complementary deoxyribonucleic acid
DNA	Deoxyribonucleic acid
dNTP	Deoxyribonucleotide triphosphate
DSB	Double strand break
Fig	Figure
Gy	Gray
h	Hours
kan	Kanamycin
kDa	Kilo Dalton
M0	Radiated generation
M1	First generation of plants after radiation
M2	Second generation of plants after radiation
M	Molarity
min	Minute(s)
ml	Millilitre
mM	Milimol
µm	Micrometer
nm	Nanometer
OD	Optical density
PCR	Polymerase chain reaction
pg	Picogram
pol A	Polyadenylation site
RNA	Ribonucleic acid
rpm	Revolution per minute

sec	Second
U	Units
V	Voltage
v/v	Volume per volume
W	Watt
w/v	Weight per volume

1. Introduction

1.1. Holocentric chromosomes

Based on the centromere localization eukaryotic chromosomes can be classified into two distinct types: monocentric and holocentric chromosomes. Monocentric chromosomes form the kinetochore at a clearly defined region at the single primary constriction typically flanked by heterochromatin. Spindle microtubule attach to the kinetochore and sister chromatids segregate to the opposite poles during anaphase with the centromere leading as V-shape structures (Fig. 1a). In contrast, holocentric chromosomes possess an elongated centromere along nearly the entire length of the chromosome. Holocentric chromosomes are homogeneously condensed during mitotic metaphase having neither primary constrictions nor a heterochromatin-rich pericentromere organization. Spindle microtubules attach at many points alongside the diffused centromere and sister chromatids migrate parallel to each other at mitotic anaphase (Fig. 1b) (reviewed in Lima-de-Faria, 1949; Dernburg, 2001; Guerra *et al.*, 2010; Melters *et al.*, 2012; Heckmann and Houben, 2013). In addition to monocentric and holocentric also polycentric chromosomes occurred in plants e.g. *Pisum sativum* (Neumann *et al.*, 2012). Monocentrics are characterized by a single region containing centromere specific histone CENH3, while polycentric chromosomes possess 3 - 5 distinct regions along elongated centromeres (Neumann *et al.*, 2012). In holocentric numerous CENH3-positive regions are distributed nearly along the entire chromosome length (Nagaki *et al.*, 2005; Heckmann *et al.*, 2011).

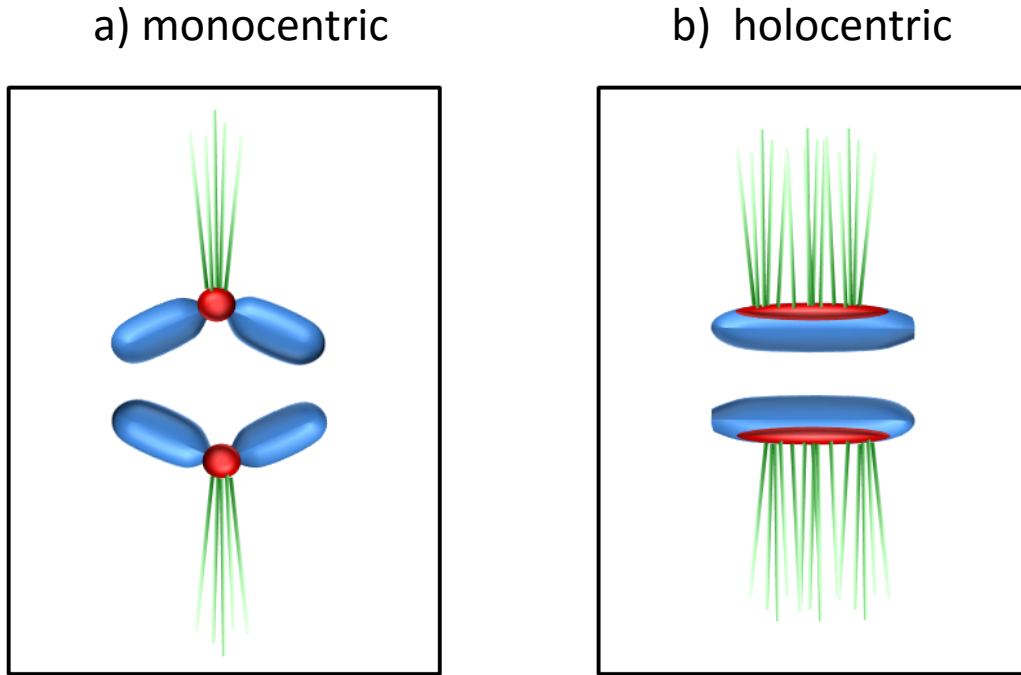


Fig. 1. Monocentric and holocentric chromosomes at mitotic anaphase.

a) Monocentric chromosomes contain a single microtubule attachment site. b) Holocentric chromosomes have a centromere which spreads over the entire length of chromosome and the spindle fibers attach at many points along the chromosome. Centromere is indicated in red, microtubule in green and chromosome in blue.

Holocentric chromosomes have been observed in various green algae, protozoans, invertebrates and different plant families (reviewed in Melters *et al.*, 2012). In the animal kingdom, holocentric chromosomes have been found only in invertebrates, including examples in the phyla Nematoda, Onychophora, Dermaptera, Ephemeroptera, Heteroptera, Thysanoptera, Sternorrhyncha, Auchenorrhyncha, Lepidoptera, Odonata, Psocoptera, Trichoptera and Zoraptera as well as in centipedes and in some Arachnids (Mola and Papeschi, 2006; Melters *et al.*, 2012). The most-well studied holocentric animal, which has a range of a model species is the nematode worm *Caenorhabditis elegans* (Dernburg, 2001; Maddox *et al.*, 2004). All known holocentric plant species belong to flowering plants (phylum Angiosperma) and include both monocots and eudicots. The holocentric monocots mainly belong to the families Juncaceae (rushes), Cyperaceae (sedges) (Malheiros *et al.*, 1947; Håkansson, 1958) and Chionographis (Tanaka and Tanaka, 1977). Holocentric eudicots exist in two genera: *Drosera* (family Droseraceae)

(Sheikh and Kondo, 1995) and *Cuscuta* (family Convulvulaceae) (Pazy and Plitmann, 1995). *Cuscuta* contains three subgenera and only one subgenus *Cuscuta* and one species in the subgenus *Grammica* are holocentric (Pazy and Plitmann, 1991, 1994, 1995).

The presence of holocentric chromosomes in unrelated taxa suggests that the phenomenon of holocentricity has arisen multiple times during eukaryotic evolution via convergent evolution, but at present there is little information on why these two distinct chromosome architectures exist (Pimpinelli and Goday, 1989; Wensch *et al.*, 1994; Dernburg, 2001; Guerra *et al.*, 2010). Different models have been proposed for the evolution of holocentric chromosomes, but it is still not clear whether holocentric or monocentric chromosomes are evolutionary older. On the one hand, the change from a localized to diffused centromere could occur for example, if the direction of kinetochore formation turns by 90⁰, then formation of centromere can run along the chromosomes axes up to the telomeric regions (Nagaki *et al.*, 2005). The 'telomere to centromere' model, proposed that centromere were derived from telomeres. Breakages of ancestral, circular genophore might activate retroelements. The retroelements could evolve from telomere or subtelomere sequences which gained the ability to interact with spindle microtubule. Consequently continuous spreading of chromosome termini sequences throughout the chromosome might occur which could explain a monocentric (telocentric) to holocentric transition during evolution (Villasante *et al.*, 2007). It has been shown that telomere like sequences are present in centromeric/pericentromeric heterochromatin in many vertebrate species (Meyne *et al.*, 1990), *Arabidopsis thaliana* (Richards *et al.*, 1991), maize (Alfenito and Birchler, 1993), potato (Tek and Jiang, 2004) and holocentric *C. elegans* (Cangiano and Lavolpe, 1993). Schrader (1974) established two models how holocentric chromosomes might be organized. The 'diffused centromere' model predicts that centromere is truly distributed along the chromosome length at mitosis while 'polycentromere' model predicts that there are a number of discrete sites dispersed along the chromosome (Schrader, 1947). Recent ultrastructural investigations validated the 'polycentromere' model (Nagaki *et al.*, 2005; Steiner and Henikoff, 2014; Wanner *et al.*, 2015) thus supporting hypothesis that holocentric chromosome could evolved from polycentric chromosomes via fusion of distinct CENH3 regions along elongated

centromeric constriction (Neumann *et al.*, 2012; Wanner *et al.*, 2015). Alternatively, the ancestral eukaryotic chromosome may have been holocentric. In this case, the restriction of kinetic activity to a specialized region must have been an evolutionary event that occurred again and again (Dernburg, 2001).

1.2. Centromere function and structure

The centromere is a protein-DNA complex cytologically visible as primary constriction in condensed metaphase chromosomes. Transiently a multi-protein complex (kinetochore) assembles at centromeres and interacts with spindle microtubules mediating the faithful transmission of the genetic material during mitosis and meiosis. The centromere is also responsible for sister chromatid cohesion/separation, checkpoint control as well as for cell cycle regulation (Choo, 1997).

The centromeres vary in size and sequence composition, from the very small 125 bp point centromeres of budding yeast *Sacharomyces cerevisiae* (Clarke and Carbon, 1985) to the several megabases of regional centromeres in higher eukaryotes (Morris and Moazed, 2007). Although centromere functions are conserved between species, with the exception of point centromeres, the DNA sequences are neither necessary nor sufficient for centromere formation (Kalitsis and Choo, 2012). Large arrays of centromeric satellite repeats interspersed with centromeric retrotransposons are the main component of many eukaryotic centromeres (Neumann *et al.*, 2011). The most plants have regional centromeres (Jiang *et al.*, 2003). Through genetic analysis and sequencing the DNA composition of centromere has been elucidated in some cereal species (reviewed in Houben and Schubert, 2003). Two conserved centromere-specific repeats, cereal centromeric sequence (CCS1) (AragonAlcaide *et al.*, 1996) and Sau3A9 (Jiang *et al.*, 1996) were found in wheat, rye, barley, maize and rice.

Centromeric DNA evolves rapidly and can differ even among closely related species (Malik and Henikoff, 2002). Until recently no centromere-specific repeat has been reported for any holocentric species (Gassmann *et al.*, 2012; Heckmann *et al.*, 2013; Steiner and Henikoff, 2014), Recent analysis of the holokinetic species *Rhynchospora pubera*

revealed the presence of a centromere specific satellite family, which interacts with CENH3-containing nucleosomes (Marques *et al.*, 2015 in preparation).

Although centromeric sequences varied between different species the protein composition of the centromere is conserved (reviewed in Malik and Henikoff, 2001; Houben and Schubert, 2003; Cooper and Henikoff, 2004; Feng *et al.*, 2015). Kinetochore is a protein complex structured of more than 90 proteins which assembles to the centromere of each chromosome during their division (Cheeseman and Desai, 2008). The majority of the protein is not present during interphase and is assembled only when the cell enters mitosis or meiosis, when the interaction with the spindle microtubule is required (reviewed in Gascoigne and Cheeseman, 2011).

CENP-A (also called CENH3) is the first centromeric protein identified in human (Palmer *et al.*, 1987). Later homologous proteins have been identified in other eukaryotes including Cse4 in budding yeast, HCP-3 in *C. elegans* (Buchwitz *et al.*, 1999), Cid in flies (Malik *et al.*, 2002), HTR12 in *A. thaliana* (Talbert *et al.*, 2002) and LnCENH3 in *Luzula nivea* (Nagaki *et al.*, 2005). As the presence of CENH3 is essential for a functional centromere, this protein is widely used as a marker to identify functionally active centromeres (Allshire and Karpen, 2008). Genetic and biochemical studies suggest that CENH3 replaces the canonical histone H3 in centromere-specific nucleosomes (Shelby *et al.*, 1997; Kalitsis and Choo, 2012). However, not all histone H3s are replaced in the centromere, more likely blocks of CENH3- and H3-associated nucleosomes are interspersed which can be observed on extended centromere fibers after immunostaining with corresponding antibodies (Blower *et al.*, 2002). Contrary to histone H3, which is extremely conserved in all eukaryotes, CENH3 shows considerable variability between species, especially in the N-terminal tail (Talbert *et al.*, 2002). Recent observations obtained from *de novo* formed centromeres showed that regions without centromeric or pericentromeric repeats can recruit CENH3 and other centromere associated proteins to assemble a functional kinetochore that promotes chromosome segregation (Saffery *et al.*, 2000; Lo *et al.*, 2001). Hence, eukaryotic centromeres except the point centromeres of *S. cerevisiae* are determined epigenetically rather than by a primary DNA sequence (Steiner and Clarke, 1994; Karpen and Allshire, 1997).

1.3. *Luzula elegans* as a model for holocentric plants

The monocot family Juncaceae is a species-rich family (450 species, 548 taxa, 8 genera) with wide-spread distribution in temperate and arctic regions in both hemispheres (Záveská Drábková, 2013). The genus *Luzula* has been considered to comprise three subgenera: *Marlenia*, *Pterodes* and *Luzula*. *Luzula* divides into seven sections: *Anthelaea*, *Atlanticae*, *Nodulosae*, *Diprophyllatae*, *Alpinae*, *Thyranochlamydeae* and *Luzula* (Bozek *et al.*, 2012; Záveská Drábková, 2013). The haploid chromosome number in the genus *Luzula* varies in a broad range and species with 3, 6–16, 18, 21, 23, 24, 26, 31, 33, 35, 36, and 42 chromosomes have been reported (reviewed in Bureš *et al.*, 2013). The structure and behavior of holocentric chromosomes have been described in different *Luzula* species, but mostly in the self-fertilizing *L. elegans* Lowe (formerly *Luzula purpurea* Link) due to the lowest chromosome count ($2n = 6$) and the largest chromosomes within the family (Nordenskiöld, 1951; Nordenskiöld 1962).

L. nivea and *L. elegans* chromosomes possess linear shaped centromeres which form parallel lines on the opposite sides of mitotic chromosomes. Each line represents an elongated kinetochore (Nagaki *et al.*, 2005; Heckmann *et al.*, 2011). Electron microscopy revealed that holocentric kinetochores of *Luzula* are rather distinct-dotted than diffuse-continuously organized (Braselton, 1971). Thus, the cytologically observed continuous metaphase centromere are the result of a visual merging of various centromere subunits at metaphase (Braselton, 1971). Recent, light and scanning electron microscopy observation of *L. elegans* chromosomes demonstrated a longitudinal groove-like structure present along each sister chromatid. The CENH3 signals are centered in the groove and extend along almost the whole chromosome length except the distal chromosome regions (Fig. 2a, c). CENH3 signals colocalized with the microtubule attachment sides (Fig. 2b, c) (Heckmann *et al.*, 2011). The longitudinal centromere-like groove is much more distinct in *L. elegans* that possesses large chromosomes compared to *L. nivea* with much smaller chromosomes (Nagaki *et al.*, 2005). It is probable that the holocentric groove is a structural accommodation for the stability of large *L. elegans* chromosomes (Heckmann *et al.*, 2011).

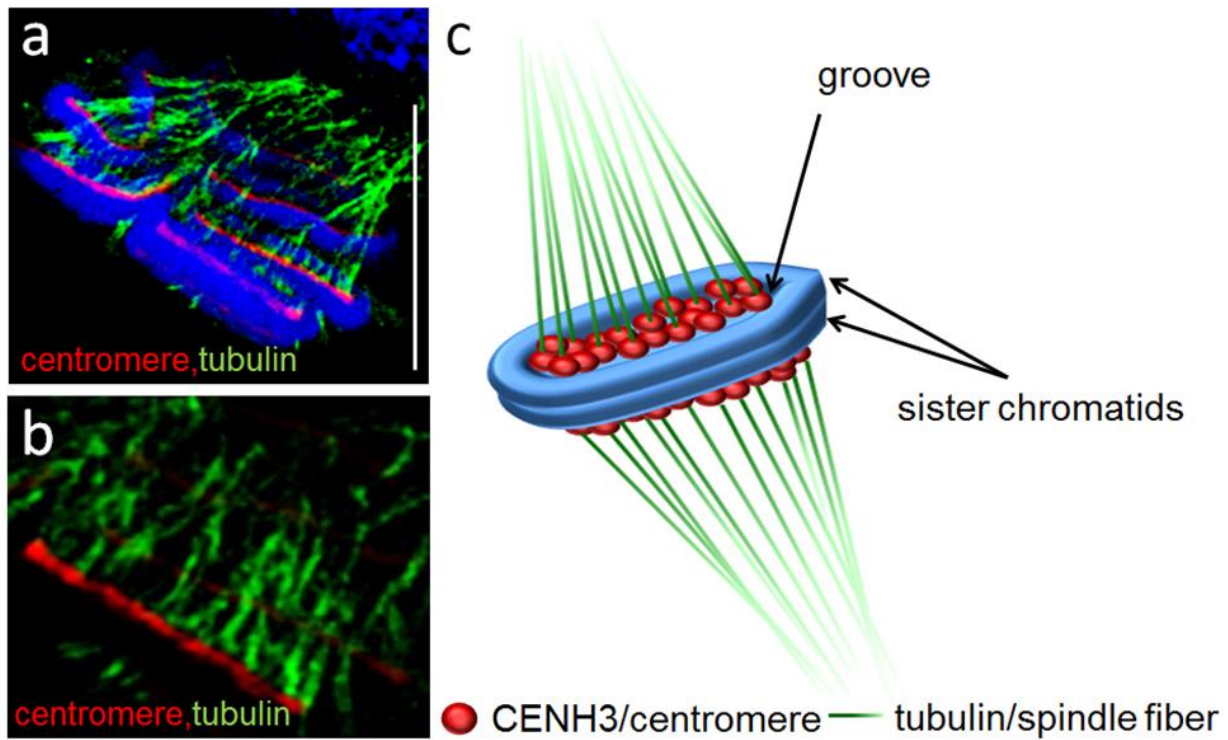


Fig. 2. *L. elegans* chromosomes at mitotic metaphase.

a) Mitotic metaphase b) enlarged holocentric centromere after immunolabelled with anti-CENH3 (red) and α -tubulins (green) revealed spindle microtubule attachment along elongated centromere. Chromatin was counterstained with DAPI (blue). Bars = 10 μ m c) Structural model of a mitotic chromosome which consists of two sister chromatids. Each chromatid exhibits a groove like structure along the chromosome axis. CENH3 (red) enriched nucleosomes are centered within the groove and interact with spindle microtubules (green).

Heckmann and coworkers (2013) analyzed the genome and chromatin organization of *L. elegans*. DNA content of *L. elegans* is equal to 7.80 pg per 2C and 61% of the genome is constituted by highly repetitive DNA (Heckmann *et al.*, 2013). This result is comparable to data obtained from monocentric plants with similar genome size (Macas *et al.*, 2007; Macas *et al.*, 2011). One third of the *L. elegans* genome is represented by transposable elements, mainly Ty1/copy from the Angle lineage, which is more frequent than in other species with similar genome content. Transposable elements are dispersed along the chromosomes length. Surprising, a low content of Ty3/gypsy repeats was observed, these sequences are characteristic for the centromeres in many monocentric plants.

Centromeric repeats were not identified suspecting that CENH3-containing nucleosomes interact with no specific high copy repeat in *L. elegans*.

L. elegans possesses a large number of satellite sequences DNA representing over 10% of the genome. 20 out of identified 122 satellite repeats were investigated by FISH method. Most of them were detected on all three pairs of chromosomes, but satellite repeats occurring on two chromosome pairs or only one were also present. *L. elegans* chromosomes are equal in size and indistinguishable by their morphology. Combination of satellite probes like LeSAT28 and LeSAT63 allowed to distinct the three pairs of chromosomes by FISH (Heckmann *et al.*, 2013). Satellites are proportionally more frequently localized to terminal (centromere free) chromosome regions (e.g. LeSAT7, LeSAT11) that in interstitial, centromere region (Heckmann *et al.*, 2013). A similar distribution of high copy repeats was observed in *Cuscuta* and some holocentric *Rhynchospora* species (Vanzela and Guerra, 2000; Guerra and Garcia, 2004) suggesting that in holocentric chromosomes the heterochromatic areas are mainly clustered at the telomeric regions with some central blocks, in contrast to the high concentration of high copy repeats found near the centromere in monocentric chromosomes (Ray and Venketeswaran, 1979).

1.4. Meiosis

1.4.1. Meiosis in monocentric species

Meiosis is a highly conserved cell division which occurs in most sexually reproducing eukaryotes. DNA replication is followed by two consecutive rounds of cell divisions, called meiosis I and meiosis II. The division results in four haploid daughter cells. Fusion of two gametes forms a zygote containing mixture of paternal and maternal chromosomes maintaining parental chromosome number (Roeder, 1997).

Prophase I is the first and the longest stage of meiosis I. It is divided into five sub-phases: leptotene, zygotene, pachytene, diplotene and diakinesis. During leptotene, paternal and maternal chromosomes search for each other and pair refers to the side-by-side alignment (Albini and Jones, 1987). Zygotene is characterized by telomere clustering at one nuclear hemisphere mirrored by the centromeres in the opposite one forming a bouquet like

configuration. The bouquet configuration precedes homologue chromosome synapsis (the intimate association) facilitated by a proteinaceous structure – the synaptonemal complex (SC) assembly (Scherthan *et al.*, 1996; Bass *et al.*, 1997). The SC serves to binds two homologues chromosomes by formation of a central element (CE) between the two axial elements (AEs), later called lateral elements (LEs) resulting in a typical tripartite structure (Heyting, 1996). During pachytene non-sister chromatids exchange genetic material in the manner of crossover. Following that, bouquet configuration disperses, SC degrades and homologues desynapse. However, crossovers create physical stable connections between homologs (visible as chiasma) that in association with sister chromatid cohesion hold the homologues together in stable pairs – bivalents. Homologues condense progressively through diplotene and diakinesis and reach their fullest condensation at metaphase I (John, 1990).

In monocentric species during this stage sister centromeres are fused and mono-oriented thereby face in the same direction. During anaphase I cohesion between sister chromatid arms is released while centromeric cohesion is protected until anaphase II (Nasmyth, 2001; Marston *et al.*, 2004; Sakuno and Watanabe, 2009). This allows release of chiasmata. As a result sister chromatids remain together but homologues can separate during anaphase I. The first meiosis division was in details reviewed in (Gerton and Hawley, 2005; Hamant *et al.*, 2006). The reductional meiosis I is followed by an equational meiosis II. In meiosis II sister kinetochores are bi-oriented and face the opposite spindle poles, therefore sister chromatids separate in anaphase II when centromeric cohesion is released (Fig. 3a) (Nasmyth, 2001; Marston *et al.*, 2004; Sakuno and Watanabe, 2009). This standard meiotic sequence based on two-step release of sister chromatids cohesion is characteristic for most monocentric species and represents the so called conventional or pre-reductional meiosis (John, 1990).

1.4.2. Meiosis in holocentric

In contrast, organisms with holocentric chromosomes, which do not have a localized centromere cannot rely on a single predefined site to regulate sister chromatid co-orientation and the two-step loss of cohesion during meiosis. Therefore holocentric

organisms required special adaptation to allow correct segregation of genetic material to each gamete.

The nematode *C. elegans* is a holocentric organism in which meiosis has been best studied (Phillips and Dernburg, 2006; Wignall and Villeneuve, 2009; Dumont *et al.*, 2010). Each of the six *C. elegans* chromosome pairs usually undergoes one crossover resulting in cruciform bivalents. Localization of crossover is random (Barnes *et al.*, 1995), but as common for holocentric species, predominantly present at the distal/terminal chromosome region (Halkka, 1964; White, 1973; Nokkala *et al.*, 2004). Crossover divided bivalent onto long and short arms which harbor distinct complements of proteins (Schwarzstein *et al.*, 2010). Subsequently long arms are oriented towards the spindle poles and short arms very tightly condense thus are no longer visible (Albertson and Thomson, 1993). The kinetochore components (CENP-C, KNL-1, BUB-1, HIM-10, NDC-80, Nuf2, MIS-12) accumulate around end of the long arms of cruciform, independent of the centromere-specific histone HCP-3 distribution (ortholog of CENH3) (Monen *et al.*, 2005; Nabeshima *et al.*, 2005; Dumont *et al.*, 2010). In spermatocytes, each end acts functionally as a kinetochore and provides a restricted spindle microtubule attachment site (Fig. 3b). Therefore meiotic chromosome reminds a 'telekinetic' like behavior typical for monocentric. In oocytes, bivalents are ensheathed by microtubule bundles running parallel to their long axes. Homologues segregation appears to be driven by growth of microtubules between separating homologues (Fig. 3c) (Albertson and Thomson, 1993; Shakes *et al.*, 2009; Wignall and Villeneuve, 2009; Dumont *et al.*, 2010; Schwarzstein *et al.*, 2010). In *C. elegans* meiotic chromosome segregation is driven by a two-steps pattern of cohesion lost similarly like in monocentric species. During meiosis I cohesion is released in between the short arms enabling homologues separation and subsequently, during meiosis II, cohesion is lost between the long arms enabling sister chromatid separation (Kaitna *et al.*, 2002; Rogers *et al.*, 2002; Nabeshima *et al.*, 2005; Schwarzstein *et al.*, 2010).

An alternative solution to deal with holocentricity during meiosis is to invert the order of chromosome segregation in the manner that sister chromatids segregated during meiosis I and homologues during meiosis II (Fig. 3d) (Nordenskiöld, 1961; Chandra, 1962). During inverted meiosis (called also post-reductional) bivalents are oriented with their long axes

perpendicular to the spindle and it is supposed that all sisters chromatid cohesion is lost till telophase I (John, 1990). The inverted order of chromosome segregation has been demonstrated in different holocentric species e.g., mealybug (Hemiptera), some dragonflies, arachnids (Chandra, 1962; Bongiorno *et al.*, 2004; Viera *et al.*, 2009) and in plants family Juncaceae (Malheiros *et al.*, 1947; Castro *et al.*, 1949; LaCour, 1953; Brown, 1954; Kusanagi, 1962; Nordenskiöld, 1962), Cyperaceae (Da Silva *et al.*, 2005; Cabral *et al.*, 2014) and Convolvulaceae (genera *Cuscuta*) (Pazy and Plitmann, 1987, 1994). Despite the widespread prevalence of inverted meiosis, the molecular mechanisms underlying this alternative order of chromosome segregation remains unknown. Moreover, in many species e.g. in Heteroptera restricted kinetochore activity and inverted meiosis can coexist in the same cell making analysis more difficult (Viera *et al.*, 2009).

Regardless the differences in chromosome division, for a genetic perspective gametes produced by all types of meiosis are indistinguishable from each other (Mola and Papeschi, 2006).

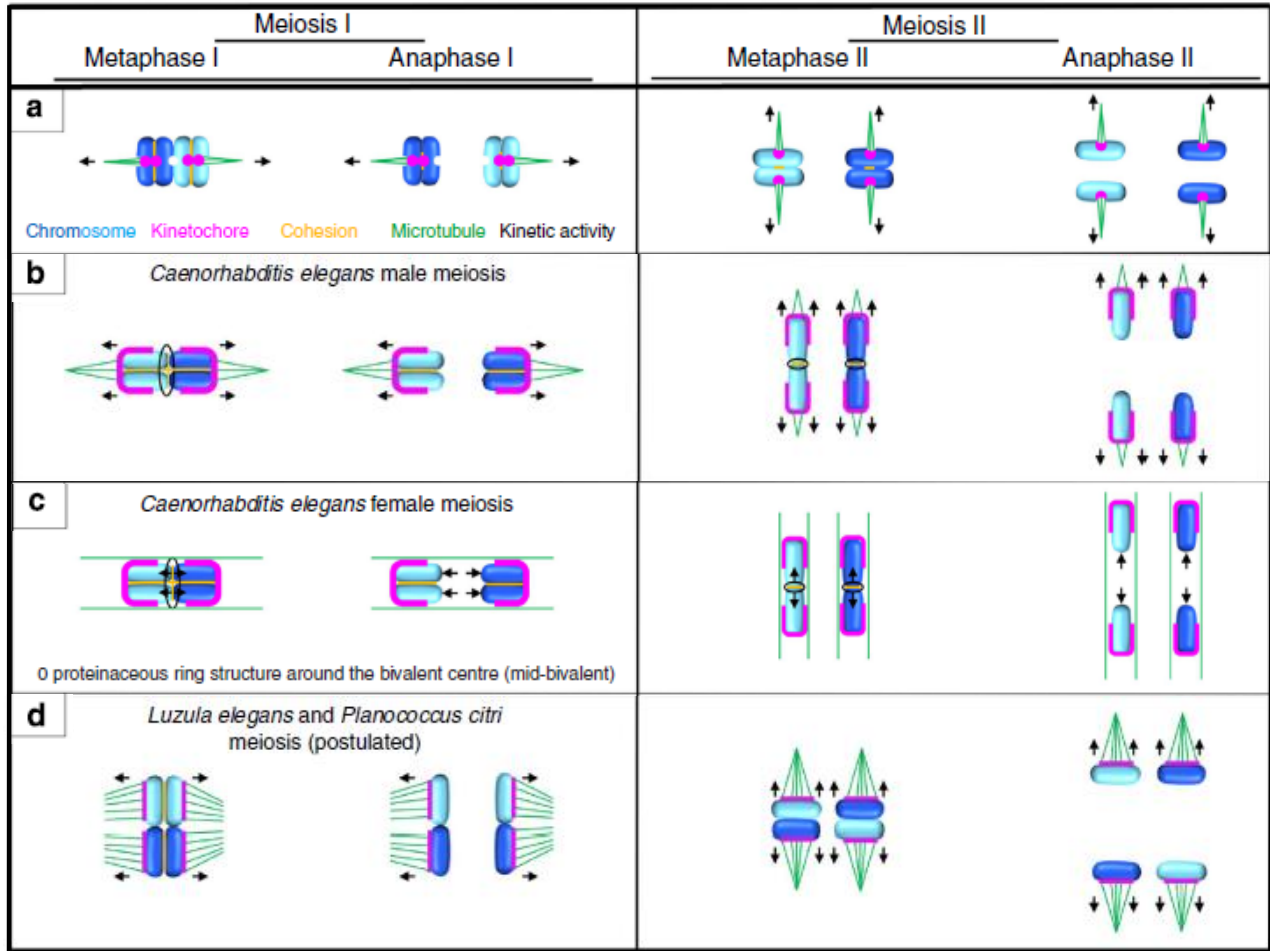


Fig. 3. Model illustrating meiotic segregation events in monocentric and holocentric species (Heckmann *et al.*, 2014).

a) Monocentric species perform a pre-reductional meiosis. Several options exist to deal with holocentricity during meiosis: b, c) ‘telokinetic’ like behavior, d) inverted meiosis.

1.4.3. DMC1 recombinase facilitates homologous recombination

Reciprocal recombination (crossover) is a genetic material exchange between two non-sister chromatids of homologous chromosomes during prophase I. This process has got two major roles: to promote accurate chromosome segregation during reductional division and to create genetic variability of sexually reproducing populations (Schuermann *et al.*, 2005). The number and distribution of crossovers differ from species to species, but there is at least one crossover per bivalent which is termed the obligate crossover (Jones, 1984; Schuermann *et al.*, 2005). The distribution of recombination sites is not random, often occurs in gene-rich as well as in GC-rich chromosomes regions, but it is mainly excluded

from the centromeres and telomeres in monocentric species (Schnable *et al.*, 1998; Gerton *et al.*, 2000; Borde *et al.*, 2004).

Meiotic recombination is initiated in leptotene by the formation of double strand breaks (DSBs) which are catalyzed by the conserved type II topoisomerase SPO11 (Fig. 4a, b) (Szostak *et al.*, 1983; Giroux *et al.*, 1989; Keeney *et al.*, 1997). DNA processing by the Mre11/Rad50/Nibrin complex at the sites of DSBs generating single-stranded overhangs (ssDNA) (reviewed in Raynard *et al.*, 2008). The ssDNA tails can be coated with the strand exchange proteins like RAD51 (Radiation sensitive 51) and DMC1 (Disrupted meiosis cDNA1) to form nucleoprotein filaments (Fig. 4c). Both recombinases have been identified in plants as well as a range of other organisms (Hamant *et al.*, 2006). Eukaryotic RAD51 and DMC1 are homologues of the bacterial recombinase RecA (Bishop *et al.*, 1992b; Shinohara *et al.*, 1992). RAD51 is required in both mitotic and meiotic cell division, whereas DMC1 has only a meiotic function (Bishop *et al.*, 1992b; Yamamoto *et al.*, 1996). DMC1 shares about 50% amino acid sequence identity with RAD51 and is well conserved among various organisms (Bishop *et al.*, 1992b; Habu *et al.*, 1996). During meiotic DSBs RAD51 and DMC1 form an independent complex by asymmetric assembly at either end of the DSBs (Fig. 4c) (Shinohara and Shinohara, 2004; Kurzbauer *et al.*, 2012). Both proteins form helical filaments on ssDNA of the same filament structure (Sheridan *et al.*, 2008) but interact with different meiotic proteins (Dresser *et al.*, 1997). It has been long speculated that the two ends of a meiotic DSBs have distinct role during meiotic DNA repair. DMC1 nucleoprotein filament formed at one side of the meiotic DSB may search for a repair template and promote ssDNA invasion into homologues duplex DNA (Fig. 4d). While the RAD51 coated nucleoprotein filament formed at the other DSB side may be temporary retained to avoid a deleterious second invasion into another DNA template. The final products of DMC1 facilitated meiotic recombination are either crossovers or non-crossovers (Fig. 4e). These findings led to the model that RAD51 and DMC1 play unique, different role during DSBs repair nevertheless they cooperate to achieve effective meiosis recombination (Dresser *et al.*, 1997; Hunter and Kleckner, 2001; Blat *et al.*, 2002; Shinohara and Shinohara, 2004; Kurzbauer *et al.*, 2012).

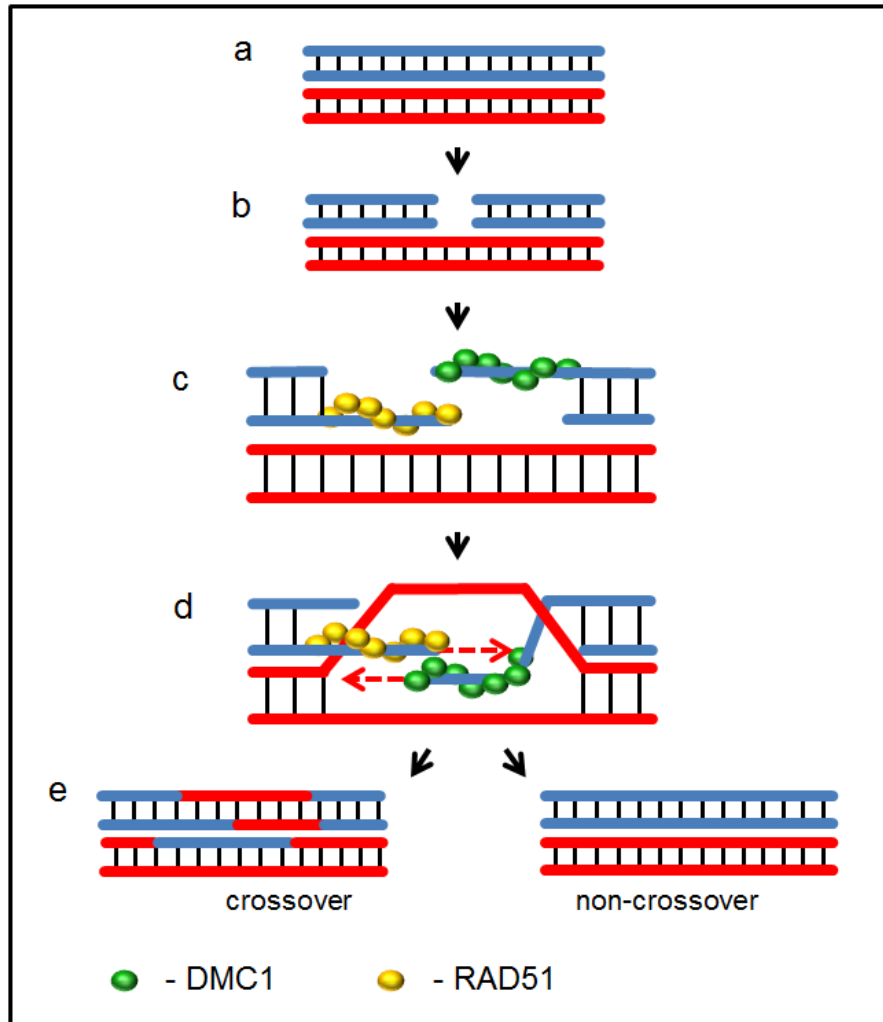


Fig. 4. Model on how DMC1 recombinase facilitates homologous recombination.

a, b) Meiosis recombination is initiated by DSB formation. c) The DMC1 protein assembles to one of the ssDNA while the Rad51 to the opposite ssDNA strand. d) The DMC1-nucleoprotein filament search for sequence similarity along homolog and promote ssDNA invasion into the DNA template. e) DMC1 promoted meiosis recombination might result either in crossover or non-crossover.

1.5. Consequences of chromosome fragmentation

1.5.1. Monocentric contra holocentric after radiation

Nowadays the centromere type can be easily confirmed by FISH or immunostaining methods which enable detection of centromere specific repeats or kinetochore proteins (Nietzel *et al.*, 2001; Houben and Schubert, 2003). In the past, chromosome fragmentation

induced by ionizing radiations (e.g. γ -, X-rays) and UV irradiation was used to distinguish between centromere types. Fragmentation of monocentric chromosomes causes the formation of centric and acentric fragments (Fig. 5a). Due to the absence of the centromeres acentric fragments do not possess a spindle microtubule attachment region and are consequently lost during mitosis which might lead to lethal mutations. In contrast, breakage of holocentric chromosomes generates mainly fragments possessing an active centromere and therefore almost all fragments segregate normally in somatic cells (Fig. 5b) (Hughes-Schrader and Ris, 1941).

In addition, radiation induced chromosome rearrangements like reciprocal translocations in holocentric species do not result in dicentric chromosomes, which often fail to segregate in monocentric species if both centromeres are active (McClintock, 1939; Bauer, 1967). Therefore, radiation of holocentric species rarely results in anaphase bridges and micronuclei formation (Hughes-Schrader and Ris, 1941; Nordenskiöld, 1964; Pazy and Plitmann, 1994). Hughes-Schrader and Ris (1942) were one of the first authors who noticed that chromosome fragments induced by x-ray behave mitotically like unbroken chromosomes, the same confirmed holocentric chromosome nature of *Steatococcus* (Hughes-Schrader and Ris, 1941). Afterwards, radiation was used to proof the existence of holokinetic centromeres in different species of green algae (Godward, 1954), plants (Håkansson, 1954), nematodes (Albertson and Thomson, 1982) and arthropods (Tempelaar, 1979).

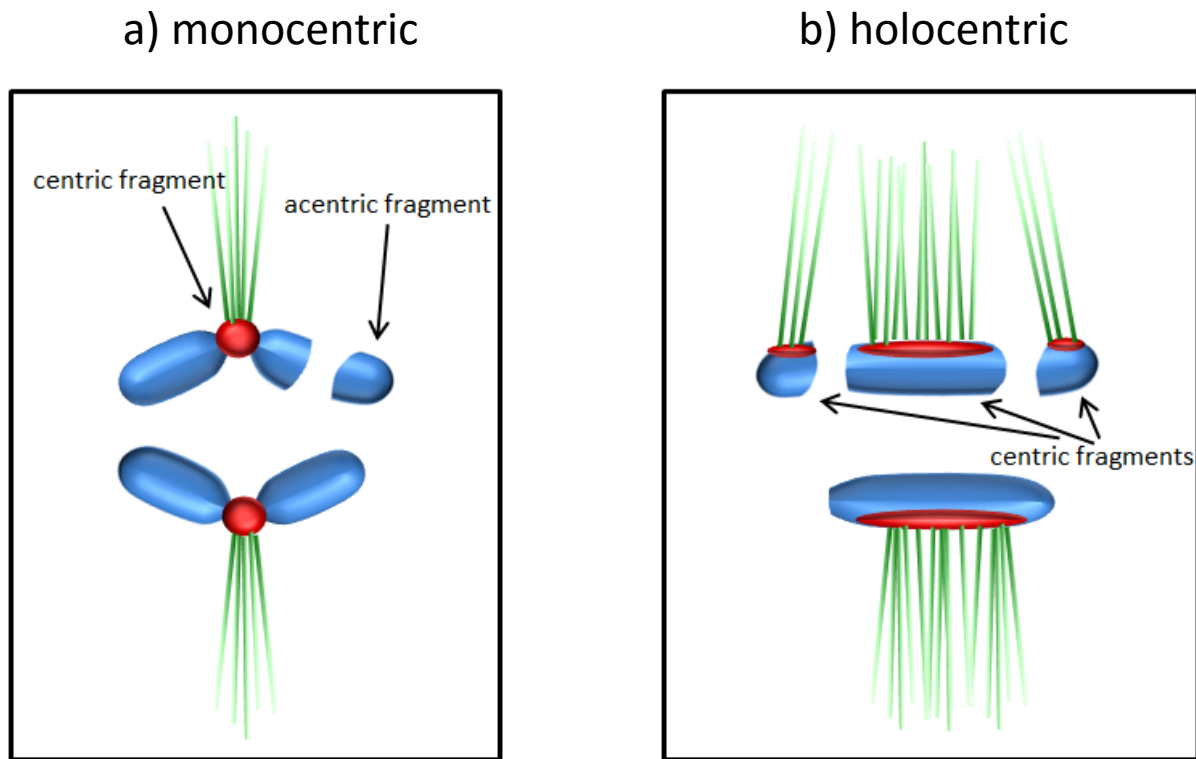


Fig. 5. Behavior of monocentric and holocentric chromosome fragments during mitotic anaphase.

a) Breakage of a monocentric chromosome results in centric and acentric fragments. An acentric DNA fragment cannot segregate due to the absence of a centromere and its inability to attach to spindle microtubule. b) Holocentric chromosome possesses a centromere spread over the total length of chromosome, consequently all chromosome fragment exhibit a part of the centromere and can attach to spindle fibers during cell division. Centromere is indicated in red, microtubule in green and chromosome/fragment in blue.

1.5.2. Chromosome fragments are stabilized by *de novo* formed telomeres

Hermann Muller and Barbara McClintock demonstrated that broken monocentric chromosomes are highly unstable. Broken ends seem to be sticky and tend to fuse with each other causing dicentric and ring chromosomes which subsequently cause repeated chromosome breakage by breakage–fusion-bridges (BFB). However, break points can be healed and therefore aberrations are prevented (Muller, 1938; McClintock, 1941, 1942). Chromosome fragments can be stabilized by adding telomeres to the broken chromosome ends (McClintock, 1941; Day *et al.*, 1993). Telomeres are composed of telomere specific

DNA sequence and various proteins. In most species telomere repeats are highly conserved, tandem repeats of 6 - 8 bp motifs. Often they are associated with other tandem repeats, which are species specific.

Telomeres not only cap and protect physical ends of linear eukaryotic chromosomes but also participate in regulation of cell division and cellular senescence (Blackburn, 1991; Wright and Shay, 1992; Zakian, 1995). They are involved in DNA replication control, meiosis bouquet configuration formation as well as in gene expression modulation (Day *et al.*, 1993). Telomeres are synthesized by a specialized reverse transcriptase-like enzyme - telomerase, which can replenish already existing telomeres or add new telomeric sequence directly to non-telomeric DNA for example at the ends of chromosome fragments (Fig. 6a) (Melek and Shippen, 1996). Telomeres are added gradually and might require passing through a certain number of cell cycles and/or through certain developmental stage (Tsujiimoto, 1993; Britt-Compton *et al.*, 2009). Alternatively chromosome broken end can be repaired by telomerase-independent mechanism – telomere capture. In this case broken chromosomes are stabilized by the transfer of telomeres from unbroken chromosomes to the broken ends via subtelomeric cryptic translocations (Fig. 6b) (Meltzer *et al.*, 1993; Slijepcevic and Bryant, 1998). It is assumed that subtelomeric DNA sequence might predispose broken chromosome for telomeric capture. Telomeric association between non-homologues chromosomes of similar subtelomeric repetitive sequence could lead to mispairing of telomeres in meiosis or mitosis and this mispairing might occasionally resolve as a chromosome nonreciprocal translocation (Brown *et al.*, 1990). Lastly, recombination between broken and its intact homologues chromosome may result in chromosome end stabilization (Fig. 6c) (Meltzer *et al.*, 1993; Slijepcevic and Bryant, 1998; Lundblad, 2002).

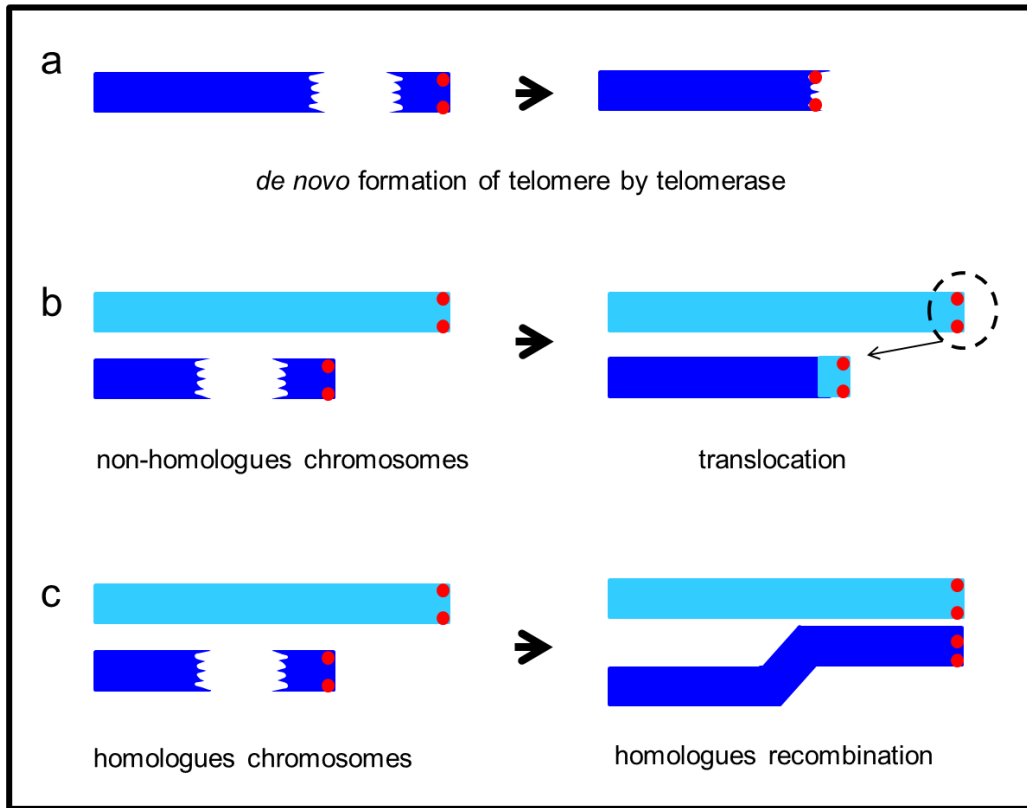


Fig. 6. Three possible healing events for the telomere-free broken end of a chromosome (according to Matsumoto *et al.*, 1987).

a) *De novo* formation of a telomere by telomerase may take place at a broken end. b) Broken chromosome can acquire a new telomere by a translocation involving another, non-homologous chromosome. c) Healing events can be based on recombination between a broken chromosome end and its intact homologous chromosome.

1.5.3. Karyotype evolution of holocentric chromosome species

Chromosomes evolve by the modification, acquisition, deletion and/or rearrangement of genetic material. Defining the forces that have affected the eukaryotic genome is fundamental to our understanding of biology and evolution (species origin, survival and adaptation) (Eichler and Sankoff, 2003). Chromosome evolution has been a driving force in speciation and diversification in diverse groups of organisms (Stebbins Jr, 1950; Grant, 1981; Coyne and Orr, 2004).

Holocentric chromosomes are well known for a rapid karyotype evolution (Bureš *et al.*, 2013). It has been speculated that stably inherited chromosome fragments and lack of

dicentric translocation products are the reasons why number and size of chromosomes may vary considerably and may be tolerated in species with holocentric chromosomes (Nordenskiöld, 1962, 1963; Nordenskiöld, 1964; LaChance and Degrugillier, 1969).

The Juncaceae along with its sister family Cyperaceae are one of the best examples of numerical variation in the karyotype with holokinetic chromosomes (Záveská Drábková, 2013). In the genus *Luzula* the haploid chromosome number varies in a broad range and species with 3, 6–16, 18, 21, 23, 24, 26, 31, 33, 35, 36, and 42 chromosomes are reported (Nordenskiöld, 1951; Kuta *et al.*, 2004; Záveská Drábková, 2013). A comparable situation was found for *Cyperus* species or holocentric butterflies with nearly continuous numbers of chromosomes from 5 to 134 (reviewed in Bureš *et al.*, 2013). Even within one holocentric species the number of chromosomes can vary between different individuals as shown for *Carex blepharicarpa* with $2n = 26 - 32$ and 41 (Hoshino and Okamura, 1994), *Rhynchospora nervosa* with $2n = 20$ and 30 (Luceño *et al.*, 1998) or *Eleocharis kamtschatica* $2n = 41 - 47$ (Yano and Hoshino, 2006).

Variability in holocentric chromosome number is usually associated with changes in chromosome size. In the genus *Luzula* a negative correlation between chromosome number and chromosome size was found. When the chromosome number is doubled from 12 to 24, the length of chromosomes is about halved (Nordenskiöld, 1951). Similarly, in *Juncus biglumis* two cytotypes with $2n = 60$ and $2n = 120$ were observed. Chromosomes of cytotype $2n = 60$ are about twice as big as the chromosomes of the cytotype with $2n = 120$ while the relative DNA content differs by only 6% between both cytotypes (Schönswetter *et al.*, 2007). Interestingly, in *Luzula* hybrids derived from parent species possessing either small or large chromosomes meiotic pairing occurs between one large and two half-sized chromosomes (Nordenskiöld, 1961). The existence of different chromosome numbers and sizes of related species suggests an important role of so called chromosome ‘fusion and fission’ events in the evolution of holocentric species (Malheiros-Garde and Garde, 1950; Nordenskiöld, 1951). However, the term ‘chromosome fusion’ should be used with caution as fusion *sensu stricto* implies the combination of two chromosomes without any loss of chromatin, which is usually prevented by telomeres (Schubert and Lysak, 2011). Interstitial telomere repeats as indication of translocations with a breakpoint inside telomere repeat arrays were found in

the spike rush *Eleocharis subarticulata* (Da Silva *et al.*, 2005). In contrast, other holocentric species e.g. aphids (Monti *et al.*, 2011), *Luzula luzuloides* (Fuchs *et al.*, 1995) *Rynchospora tenuis* (Vanzela *et al.*, 2003) and *Mamestra brassicae* (Mandrioli, 2002) do not display interstitial telomeres. Likely, most of the so-called 'fusion' events are based on translocations and subsequent loss of small translocation products and thus of lost telomeres of the terminally truncated 'fused' chromosomes.

In addition to chromosome fragmentation and translocation, polyploidy and proliferation/removal of high copy sequences are mechanisms involved in the karyotype evolution of holocentric species (Kuta *et al.*, 2004; Bačič *et al.*, 2007; Zedek *et al.*, 2010; Bozek *et al.*, 2012; Závěská Drábková, 2013). The positive, linear correlation between increasing chromosome number and DNA content was found in *Eleocharis* (Zedek *et al.*, 2010), *Drosera* (Rivadavia *et al.*, 2003) and *Luzula*. In genus *Luzula* diploids ($2n = 12$ e.g. *Luzula campestris*), tetraploids ($2n = 24$ e.g. *Luzula divulgata*), hexaploids ($2n = 36$ e.g. *Luzula multiflora*) and octoploids ($2n = 48$ e.g. *Luzula congesta*) with the same chromosome size and approximately proportionally increased genome contents were found (Bačič *et al.*, 2007).

2. Open questions and aim of the thesis

The present work aimed to:

1) Elucidate the mechanisms of meiotic chromosome division in the holocentric plant species *L. elegans*.

Accurate partitioning of the genetic material during meiosis is essential for all species with sexual reproduction to propagate. Chromosome depending on the centromere type (monocentric, holocentric), use different strategies for their division. To uncover the mechanisms that allow the holocentric plant species *L. elegans* the correct course of meiosis, the distribution of centromere-specific proteins, microtubules, telomeres and different satellite repeats at different stages of meiosis was evaluated. Furthermore to understand the nature and composition of the crucial meiotic component which allows the end-to-end association between homologues the recombination-specific LeDMC1 protein was identified and traced during meiosis.

2) To gain insight into mechanisms which are responsible for the rapid karyotype evolution in species with holocentric chromosomes.

Holocentric species are well known for a rapid karyotype evolution. In holocentrics, chromosome rearrangements such as fragmentation or reciprocal translocation do not result in acentric and dicentric fragments which often fail to segregate properly. To decipher the mechanism that allows holocentric species an accelerated karyotype evolution via chromosome breakage and translocation we ask whether rapid chromosome healing of chromosome fragments enables their successful mitotic and meiotic transmission.

3. Materials and methods

3.1. Materials

Following chemical reagents and enzymes were used in the experiments for this thesis:

β -Mercaptoethanol	Carl Roth GmbH & Co. KG, Karlsruhe
2-Amino-2-hydroxymethyl-propane-1,3-diol (Tris)	Carl Roth GmbH & Co. KG, Karlsruhe
3-Morpholinopropanesulfonic acid (MOPS)	Carl Roth GmbH & Co. KG, Karlsruhe
4',6-diamidino-2-phenylindole (DAPI)	Serva Elektrophoresis GmbH, Heidelberg
10 x PCR buffer, 12 mM MgCl	Qiagen GmbH, Hilden
10 x reaction buffer G	Thermo Scientific GmbH, Bremen
Acetic acid	Carl Roth GmbH & Co. KG, Karlsruhe
Acetocarmine	Morphisto, Frankfurt am Main
Acrylamide	AppliChem GmbH, Darmstadt
Ammonium persulphate (APS)	Carl Roth GmbH & Co. KG, Karlsruhe
Bis-acrylamide (AA:BIS)	AppliChem GmbH, Darmstadt
Boric acid	Carl Roth GmbH & Co. KG, Karlsruhe
Bovine serum albumin (BSA)	New England Biolabs, Frankfurt am Main
Bromphenol blue	Sigma-Aldrich Chemie GmbH, Taufkirchen
Cellulase	CalBioChem/ Merck KGaA, Darmstadt
Cellulase Onozuka R10	Duchefa, Haarlem (NL)
Citric acid	Carl Roth GmbH & Co. KG, Karlsruhe
Chloroform	Carl Roth GmbH & Co. KG, Karlsruhe
Coomassie R250	Serva Elektrophoresis GmbH, Heidelberg
Cetyltrimethyl ammonium bromide (CTAB)	Sigma-Aldrich Chemie GmbH, Taufkirchen
Cytohelicase	Sigma-Aldrich Chemie GmbH, Taufkirchen
Disodium phosphate	Carl Roth GmbH & Co. KG, Karlsruhe
Dithiothreitol (DTT)	AppliChem GmbH, Darmstadt
DNase I Ambion TURBO	Invitrogen GmbH, Karlsruhe
DNA Polymerase I	Thermo Scientific GmbH, Bremen
dNTP MIX 10mM	Bioline GmbH, Luckenwalde
Double-distilled water (ddH ₂ O)	IPK laboratory
DyNAzymell DNA polymerase	Thermo Scientific GmbH, Bremen
Ethylenediaminetetraacetic acid (EDTA)	Carl Roth GmbH & Co. KG, Karlsruhe
Ethylene glycol tetraacetic acid (EGTA)	Carl Roth GmbH & Co. KG, Karlsruhe
Ethanol	Carl Roth GmbH & Co. KG, Karlsruhe
FastStart SYBR Green I master mix	Carl Roth GmbH & Co. KG, Karlsruhe
Formaldehyde	Carl Roth GmbH & Co. KG, Karlsruhe
Formamide	Carl Roth GmbH & Co. KG, Karlsruhe
GeneRuler™ 1 kb Plus DNA Ladder	Thermo Scientific GmbH, Bremen

GelStar Nucleic Acid Gel Stain	Lonza GmbH, Switzerland
Glycerin	Carl Roth GmbH & Co. KG, Karlsruhe
Glycerol	Carl Roth GmbH & Co. KG, Karlsruhe
High-Fidelity DNA Polymerase (Phusion)	Carl Roth GmbH & Co. KG, Karlsruhe
Hydrochloric acid	Carl Roth GmbH & Co. KG, Karlsruhe
Nonmetabolisable Isopropyl β -D-1-thiogalactopyranoside (IPTG)	Carl Roth GmbH & Co. KG, Karlsruhe
Isoamylalcohol	Merck KGaA, Darmstadt
Leupeptin	Sigma-Aldrich Chemie GmbH, Taufkirchen
Magnesium chloride	Carl Roth GmbH & Co. KG, Karlsruhe
Magnesium sulfate	Carl Roth GmbH & Co. KG, Karlsruhe
Milk powder	Carl Roth GmbH & Co. KG, Karlsruhe
Monosodium phosphate	Carl Roth GmbH & Co. KG, Karlsruhe
Ni-NTA agarose gel	Qiagen GmbH, Hilden
<i>NotI</i> enzyme	Thermo Scientific GmbH, Bremen
PageRuler Prestained Protein Ladder	Thermo Scientific GmbH, Bremen
Paraformaldehyde	Sigma-Aldrich Chemie GmbH, Taufkirchen
Pectolyase	Sigma-Aldrich Chemie GmbH, Taufkirchen
Pepsin	Carl Roth GmbH & Co. KG, Karlsruhe
Pepstatin A	Sigma-Aldrich Chemie GmbH, Taufkirchen
Phenol	Carl Roth GmbH & Co. KG, Karlsruhe
Phenylmethylsulfonyl fluoride	Sigma-Aldrich Chemie GmbH, Taufkirchen
Phusion HF buffer	Carl Roth GmbH & Co. KG, Karlsruhe
Pipes	Carl Roth GmbH & Co. KG, Karlsruhe
Polyvinylpyrrolidone	Sigma-Aldrich Chemie GmbH, Taufkirchen
Potassium glutamate	Sigma-Aldrich Chemie GmbH, Taufkirchen
Propidium iodide	Sigma-Aldrich Chemie GmbH, Taufkirchen
<i>SacI</i> enzyme	Thermo Scientific GmbH, Bremen
Salmon sperm DNA	Promega, Mannheim
Sodium dodecyl sulphate (SDS)	Carl Roth GmbH & Co. KG, Karlsruhe
Sodium bisulfide	Sigma-Aldrich Chemie GmbH, Taufkirchen
Sodium chloride	Carl Roth GmbH & Co. KG, Karlsruhe
Sodium citrate	Carl Roth GmbH & Co. KG, Karlsruhe
Spermidine	Sigma-Aldrich Chemie GmbH, Taufkirchen
<i>Taq</i> DNA polymerase	Qiagen GmbH, Hilden
Tetramethylethylenediamine (Temed)	Carl Roth GmbH & Co. KG, Karlsruhe
Tri-sodium citrate dihydrate	Carl Roth GmbH & Co. KG, Karlsruhe

Triton X-100
Tween-20
Ribonucleoside-vanadyl complex
RNase A
Vector mounting medium

AppliChem GmbH, Darmstadt
Serva Elektrophoresis GmbH, Heidelberg
New England Biolabs, Frankfurt am Main
Qiagen GmbH, Hilden
Vector laboratories Inc., Burlingame (CA)

3.2. Methods

3.2.1. Plant material and plant cultivation

Seeds of *Luzula elegans* (Lowe) ($2n = 6$) (Vouchers at the Herbarium Gatersleben: GAT 7852-7856) and of *Luzula luzuloides* (Lam.) ($2n = 12$) (kindly provided by the Botanical Garden of the Martin Luther University, Halle-Wittenberg), were germinated on wet filter-paper under long-day conditions (16 h light/8 h dark, 20°C/18°C). Next, seedlings were transferred to soil and cultivated for 6-8 weeks under short-day conditions (8 h light/16 h dark, 20°C/18°C). Subsequently, the plants were transferred for at least 3 months to vernalizing conditions (10 h light/14 h dark, 4°C). Afterwards plants returned to long-day conditions (13 h light/11 h dark, 20°C/16°C) to induce flowering.

Seeds of barley (*Hordeum vulgare* L. cv. Morex) and rye (*Secale cereale* L. cv. Petkuser Sommerroggen) were germinated for 4 days on wet filter-paper at room temperature in darkness. Subsequently, plantlets were transferred to soil and vernalized for 6 weeks (10 h light/14 h dark, 4°C). Finally, plants were grown at long-day conditions (16 h light/8 h dark, 22°C/16°C) to induce flowering.

3.2.2. X-ray irradiation

For x-ray irradiation experiment, three leaf stage plantlets of *L. elegans* (28 days old) were irradiated with various doses ranking from 10 to 30 Gy with an x-ray apparatus (Yxlon). The dose rate amounted to 0.9 Gy/min. Subsequently, plantlets were treated according to standard cultivation condition for *L. elegans* (as described in the chapter 3.2.1.). The M1 offspring was a selfing product of irradiated plants.

3.2.3. Genome size measurement by flow cytometry

Genome size of *L. elegans* plants was estimated as described previously by Fuchs *et al.*, 2008 using either a FACStar^{PLUS} flow cytometer (BD Biosciences) equipped with an argon-ion laser INNOVA 90C (Coherent) adjusted to 514 nm or a CyFlow Space flow cytometer (Now Sysmex) equipped with a 532 nm solid-state laser. *Pisum sativum* 'Viktoria, Kifejtő Borsó' (Genebank Gatersleben accession number PIS 630; 2C = 9.09 pg (Doležel *et al.*, 1998) was used as an internal reference standard. Briefly, small fragment of young leaf tissue of *L. elegans* was chopped with a razor blade in ice-cold Nuclear isolation buffer (Galbraith *et al.*, 1983) and subsequently filtered through a 35 µm mesh. Around 10,000 nuclei per sample were analyzed. Each measurement was repeated at least two times on different days.

Nuclear isolation buffer

45 mM Magnesium chloride
30 mM Sodium citrate
20 mM MOPS
0.1% Triton X-100
1% Polyvinylpyrrolidone
DNase-free RNase (50 µg/ml)
Propidium iodide (50 µg/ml)

3.2.4. Analysis of telomerase activity according to the Telomere Repeat Amplification Protocol (TRAP)

Three leaf stage plantlets and flower buds of *L. elegans* and 7 days old seedlings of *A. thaliana* were manually grounded with a mortar and pestle in ice-cold Extraction W buffer (Fitzgerald *et al.*, 1996; Sykorova *et al.*, 2003). Crude extracts obtained after centrifugation were 5× and 10× diluted for analysis of telomerase activity as described by Fitzgerald *et al.* (1996) and Fajkus *et al.* (1998). Briefly, 1 µl of 10 µM substrate primer TS21 (sequence listed in the Table 1) was mixed with 1 µl of diluted crude protein extract. Elongation of the primer by the telomerase proceeded for 45 min at 26°C in 25 µl of TRAP reaction buffer. Telomerase was heat inactivated for 5 min in 94°C. 1 µl of 10 µM reverse primer TelPr (sequence listed in the Table 1) and 2 U of DyNAzymell DNA polymerase were added to crude protein extract and extension products were amplified in PCR (95°C/3 min, 35 cycles at (95°C/30s, 65°C/30s, 72°C/30s) 72°C/5min

final elongation and hold at 4°C). Samples of TRAP reactions were analyzed on 12.5% polyacrylamide gel (PAGE) (40% AA:BIS (19:1), 5 x TBE, 30% APS, Temed, ddH₂O) in 0.5 x TBE buffer which was run for 3h at 300 V. Gels were stained by GelStar Nucleic Acid Gel Stain and signals were visualized using the LAS-3000 system (FujiFilm).

The real-time quantitative version of the TRAP assay (RTQ-TRAP) was performed as described in Herbert *et al.* (2006). Briefly, 10 µl of FastStart SYBR Green I master mix was mixed with 0.5 µl of 10 µM primer TS21, 0.5 µl of 10 µM primer TelPr, 8 µl of ddH₂O and 1 µl of the crude extracts. For the control-quantitative real-time TRAP assay (control-RTQ-TRAP) reaction mix was prepared as follow: 10 µl of FastStart SYBR Green I master mix was mixed with 0.5 µl of 10 µM primer CAMV (sequence listed in the Table 1), 0.5 µl of 10 µM primer TelPr, 1 µl of plasmid R6 (plasmid with 6 telomeric repetitions), 7 µl of ddH₂O, and 1 µl of the crude extracts. In both cases amplification (30 cycles of 26°C/45s, 94°C/15s, 94°C/30s, 60°C/1min) and fluorescence measurements were performed using real-time cycler Rotorgene6000 (Qiagen). Relative telomerase activity was calculated by the ΔCt method (Pfaffl, 2004).

Extraction W buffer

50 mM Tris-acetate (pH 7.5)
 5 mM Magnesium chloride
 100 mM Potassium glutamate
 20 mM EGTA (pH 8.0)
 1.5% Polyvinylpyrrolidone
 10% Glycerol
 1 mM DTT
 0.1-0.2 mM Phenylmethylsulfonyl fluoride
 0.6 mM Ribonucleoside-vanadyl complex
 1µg/ml Pepstatin A
 2µg/ml Leupeptin

TRAP reaction buffer

50 mM Tris-acetate (pH 8.3)
 50 mM Potassium glutamate
 0.1% Triton X-100
 1 mM Spermidine
 1 mM DTT
 50 µM of each dNTP
 5 mM Magnesium chloride
 10 mM EGTA (pH 8.0)
 100 ng/µl BSA

10 x TBE buffer

1 M Tris
 1 M Boric acid
 0.02 M EDTA

Table 1. List of primer sequences. Frame indicates restriction enzyme sites and underlined sequences represent protection sites.

primer name	5' to 3' sequence
CAMV	ATTCGTCTTCAAAGCAAGTGG
LeDMC1_F	GAATTC GAG CTC GTT GAT GTT AAA TTT GAG GAT CAG G
LeDMC1_R	TATCAAAT GCGGCCGC GTC TTT AGC ATC GAC GAT TCC
LeGAPDH_F	GTTTGTGGTTGGTGTGAACG
LeGAPDH_R	CCTCCTTGATAGCAGCCTTG
LeSAT7_F	TTGRRRAATTTTRAAAATCTGAACCGAT
LeSAT7_R	GTAAGCACGATTTAGCWAGGTC
LeSAT11_F	GTACTTTGTGTGTTTAGAATTG
LeSAT11_R	CGAKAGAAATTGCGTAAGTG
LeSAT28_F	CCCGAAACTAGAAATCAAGATG
LeSAT28_R	TTCCCTAAAACAGAAAATCTGC
Telo_F	CCCTAA
Telo_R	TTAGGG
TelPr	CCGAATTC AACCCCTAAACCCTAAACCCTAAACCC
TS21	GACAATCCGTCGAGCAGAGTT
M13_F	TTGTAAAACGACGGCCAGTG
M13_R	GGAAACAGCTATGACCATG

3.2.5. CTAB extraction of genomic DNA

1 g of leaf tissue or flower buds was grounded in liquid nitrogen and incubated with 15 ml of 2 x CTAB buffer for 1 hour at 65°C. When the sample cooled down to room temperature, 20 ml of chloroform/isoamylalcohol (24:1 v/v) was added and intensively mixed for 15 min. Next, the probe was centrifuged for 15 min at 8000 rpm and the supernatant was mixed with 2/3 volumes of isopropanol to hook out the DNA. The DNA was cleaned two times with ice cold 70% ethanol, eluted in 500 µl ddH₂O and treated with 5 µl RNase A (10 mg/ml). The resulting extract was washed with phenol, phenol:chloroform (1:1 v/v) and chloroform and precipitated with 100% ethanol overnight at -20°C. Subsequently, genomic DNA (gDNA) was dried and dissolved in ddH₂O.

2 x CTAB buffer

100 mM Tris-hydrochloride (pH 8.0)
20 mM EDTA (pH 8.0)
2% CTAB
1.4M Sodium chloride
0.5% Sodium bisulfide
1% β-Mercaptoethanol

3.2.6. Fluorescence *in situ* hybridization (FISH)

3.2.6.1. Probe generation for FISH

FISH probes were ordered as 5'Alexa 488-labelled oligonucleotides (LeSAT63: 5'GTAGGGGTAATCATGATATTTTCATGTTTTGCAGCTCTCTTATTAAC3') (Eurofins Genomics) or were generated by PCR with *Tag* DNA polymerase using gDNA as a template. Sequence of primers for satellite repeats (LeSAT7, LeSAT11, LeSAT28) were designed according to Heckmann *et al.*, (2013) (sequence listed in the Table 1). Telomere probe was produced with minor changes according to Ijdo *et al.*, 1991 using Telo_F and Telo_R primers (sequence listed in the Table 1). Annealing temperature was 55°C and 60°C for satellite and telomere primers respectively. All DNA probes, except oligonucleotides were purified using GeneJet PCR Purification Kit (Thermo Scientific GmbH).

Probes for subtelomeric repeats of *S. cereale* pSc119.2 (Cuadrado *et al.*, 1997) and *H. vulgare* HvT01 (Nasuda *et al.*, 2005) were kindly provided by Susann Hesse and Lala Aliyeva-Schnorr, Gatersleben.

3.2.6.2. Nick translation of FISH probes

FISH probes were labelled with ChromaTide Texas Red-12-dUTP (Invitrogen), Alexa Fluor 488-5-dUTP (Invitrogen) or Cy5-dUTP (GE Healthcare Life Sciences) by nick translation according to Kato *et al.* 2006. Briefly, 1 – 3 µg of gDNA was mixed with 10 x NT buffer, dNTP mix with decreased dTTP, β-Mercaptoethanol, labeled dUTP, 0.025 U DNase and 20 U DNA Polymerase I. Nick translation was performed for 90 min at 15°C followed by 10 min at 65°C.

10 x NT buffer

0.5 M Tris-hydrochloride (pH 7.5)
50 mM Magnesium chloride
0.05% BSA

3.2.6.3. Preparation of mitotic and meiotic chromosomes for FISH

Mitotic chromosome spreads from plantlets fixed in ethanol:acetic acid (3:1, v/v) fixative were performed by squashing method according to Houben *et al.*, (1999). Briefly, acetocarmine stained root and apical meristems of seedlings were isolated and transferred to 5 µl of 45% acetic acid on the clean slide. A coverslip was placed onto the droplet and the preparation was squashed between folded filter paper and frozen in liquid nitrogen. After the coverslip was removed with a razor blade, slide was washed in ethanol-acetic acid (3:1, v/v) and placed into 100% ethanol for 20 min. Subsequently, the slide was air dried at room temperature and kept at 4°C until hybridization.

Meiotic chromosome spreads were prepared from ethanol:acetic acid (3:1, v/v) fixed flower buds according to Heckmann *et al.*, (2014). Briefly, after washing three times in water and three times in Citric buffer each for 5 min, anthers were isolated and digested in enzyme mix for 30 min at 37°C. Maceration was stopped by washing two times for 5 min in Citric buffer and then in water. Six anthers were placed into a drop of ice-cold 60% acetic acid on a slide and crushed carefully with a metal needle. 60% ice-cold acetic acid was added to the cell suspension, mixed with a needle and incubated for 2 min at room temperature. Once more, ice-cold 60% acetic acid was added and the slide was placed on a hot plate (45°C) for 2 min. On the hot plate, the drop was slightly moved by the metal needle without touching the slide. Afterwards the slide was removed from the hot plate and freshly-prepared ice-cold ethanol:acetic acid (3:1, v/v) was added to precipitate the nuclei suspension on the slide. After 30 sec, the suspension was discarded and more ice-cold ethanol-acetic acid was added to the slide. The slide was placed in 60% acetic acid for 10 min and finally washed in 100% ethanol. After air drying, slide was kept at 4°C until hybridization.

Citric buffer (pH 4.8)

0.01 M Citric acid
0.01 M Tri-sodium citrate dihydrate

enzyme mix

0.7% Cellulase Onozuka R10
0.7% Cellulase
1% Pectolyase
1% Cytohelicase
10 mM Citric buffer

3.2.6.4. Fluorescence *in situ* hybridization

FISH was performed as described earlier (Heckmann *et al.*, 2013). Briefly, slides were rinsed in 2 x SSC for 5 min, treated with 0.1% pepsin in 1 N hydrochloric acid for 6 min at 37°C and again washed twice in 2 x SSC each for 5 min. For post-fixation, slides were incubated in 2.5% formaldehyde in 2 x SSC for 10 min and subsequently washed three times in 2 x SSC for 4 min each. Next, slides were dehydrated in 70%, 90% and 100% ethanol for 2 min each time and air dried for around 1 hour. Hybridization mixture was denatured together with the chromosomal DNA on a hot plate for 2 min at 80°C on untreated slides and for 3 min on slides after immunodetection. Hybridization was performed overnight in a moist chamber at 37°C. Subsequently, slides were washed in 2 x SSC for 20 min at 58°C and dehydrated in 70%, 90% and 100% ethanol each time for 2 min. Finally, the slides were air-dried at room temperature and counterstained with DAPI solution. The slides were stored at 4°C in darkness.

20 x SSC (pH 7.0)

3 M Sodium chloride
300 mM Tri-sodium chloride dehydrate

4 x Hybridization buffer (FISH)

40% 20 x SSC
4% 1M Tris-hydrochloride (pH 8.0)
0.8% 0.5M EDTA
5.6% Salmon sperm DNA
49.6% ddH₂O

hybridization mixture

50% Deionized formamide
25% 4 x Hybridization buffer (FISH)
15% Fluorescent probes
10% ddH₂O

DAPI solution

1 µg DAPI
1 ml Vector mounting medium

3.2.7. Indirect immunostaining

3.2.7.1. Preparation of meiotic chromosomes

Meiotic chromosome spreads were prepared by squashing method (Houben *et al.*, 1999). Briefly, flower buds were fixed for 45 min in ice-cold 4% paraformaldehyde either in 1 x PBS buffer or in 1 x MTSB buffer in a case to preserve microtubules. Flower buds were washed three times for 5 min each in ice cold 1 x PBS/MTSB buffer and subsequently anthers were isolated. Six anthers were gently placed onto a slide into a drop of 1 x PBS/MTSB buffer, squashed between the glass slide and cover slip and frozen in liquid nitrogen. The coverslip was removed with a razor blade and slide was placed in 2%

paraformaldehyde in 1 x PBS/MTSB buffer for 10 min for post-fixation. Finally, the slide was washed three times for 5 min in 1 x PBS/MTSB buffer and immediately used for immunostaining.

10 x PBS buffer (pH 7.4)

1.3 M Sodium chloride
70 mM Disodium phosphate
30 mM Monosodium phosphate

10 x MTSB buffer (pH 7.2)

50 mM Pipes
2 mM EGTA
2 mM Magnesium sulfate

3.2.7.2. Indirect immunostaining

Immunostaining was performed as described in Houben *et al.*, (2007). Briefly, the slides were incubated for 30 min in blocking solution at room temperature. After two washes in 1 x PBS/MTSB buffer each for 5 min, slides were incubated with primary antibodies diluted in antibody solution (Table 2) overnight at 4°C. Next, slides were rinsed in 1 x PBS/MTSB buffer for 10 min and incubated with secondary antibodies diluted in antibody solution (Table 2) for 1 hour at 37°C in darkness. Finally, slides were washed in 1 x PBS/MTSB buffer and counterstained with DAPI solution.

blocking solution

1 x PBS/MTSB buffer
3% BSA
0.1% TritonX-100

antibody solution

1 x PBS/MTSB buffer
1% BSA
0.1% TritonX-100

Table 2. Antibodies and their dilutions used for immunostaining.

name	dilutions
primary antibodies	
rabbit anti-LnCENH3 (Nagaki <i>et al.</i> , 2005)	1:100
mouse anti- α -tubulin (clone DM 1A, Sigma)	1:200
rabbit anti-Zyp1 (Higgins <i>et al.</i> , 2005)	1:250
rabbit anti-Asy1 (Armstrong <i>et al.</i> , 2002)	1:250
rabbit anti-H2A120phos (Abcam, ab111492)	1:1000
rabbit anti-LeDMC1 antisera from rabbi 1, 2, or 3	1:150
secondary antibodies	
Cy3-conjugated anti-rabbit IgG (Dianova)	1:300
fluorescein isothiocyanate-conjugated anti-mouse Alexa 488 antibody (Molecular Probes)	1:300

3.2.8. Microscopy

Wide-field fluorescence microscopic images were recorded using an Olympus BX61 microscope (Olympus) equipped with an ORCA-ER CCD camera (Hamamatsu). 3D-deconvolution microscopy was employed to reduce the out-of-focus blur. Image stacks of 10-11 slices per specimen were acquired, and the maximum intensity projections were processed with the program AnalySIS (Soft Imaging System). All images were collected in gray scale and pseudo-colored with Adobe Photoshop CS5 (Adobe). To achieve an optical resolution of >100 nm Structured Illumination Microscopy (SIM) was applied using a C-Apo 63x/1.2W Korr objective of an Elyra microscope system (Zeiss).

3.2.9. Generation of a LeDMC1-specific antibody

3.2.9.1. Molecular cloning

3.2.9.1.1. Extraction of total RNA and cDNA synthesis

Total RNA was isolated from 100 mg of leaves and flower buds using the TRIzol method according to Chomczynski and Sacchi (1987). Contamination from gDNA was removed by treating RNA with RNase-free DNase I. The absence of gDNA in RNA sample was assayed with PCR using LeGAPDH_F and LeGAPDH_R specific primers (sequence listed in the Table 1). The reaction mix was prepared according to the standard PCR protocol (2.5 µl of 10 x PCR buffer, 2 µl of 10 mM dNTPs, 1 µl of the LeGAPDH forward and reverse primer, 0.25 µl of *Taq* polymerase, 17.25 µl of ddH₂O and 1 µl of RNA). The PCR conditions were: 95°C/3 min, 25 cycles at (95°C/30s, 58°C/30s, 72°C/30s), 72°C/10 min final elongation and hold at 4°C. The absence of PCR product meaning the absence of gDNA contamination was confirmed by electrophoresis on a 1.2% agarose gel (100V, 60 min) in 0.5 x TAE buffer. Subsequently the cDNA was synthesized from 1 µg of RNA using Reverse Aid H Minus First Strand cDNA Synthesis Kit (Thermo Scientific GmbH).

50 x TAE buffer (8.2)

24.2% Tris
5.7% Acetic acid
0.5 M EDTA

3.2.9.1.2. RT-PCR

The cDNA from flower buds was used as a template for RT-PCR amplification of the LeDMC1 sequence with LeDMC1_F and LeDMC1_R primer pair (sequence listed in the sequence listed in the Table 1). The primers were designed to have *SacI* and *NotI* restriction enzyme sites as well as protection site to allow efficient cloning. The PCR mix contained: 4 µl of 5 x Phusion HF buffer, 0.4 µl of 10 mM dNTP, 1 µl of each 0.4 µM LeDMC1 specific primers, 0.2 µl of Phusion DNA polymerase, 12.7 µl of ddH₂O and 0.7 µl of cDNA). The cycling protocol was: 95°C/3 min, 35 cycles at (95°C/30s, 57°C/30s, 72°C/40s), 72°C/ 10 min final elongation and hold at 4°C. To ensure high fidelity of the amplification the Phusion DNA Polymerase was used although this polymerase does not add poly A tail to the end of the PCR product. To ensure proper further cloning poly A tail was added to the obtained PCR product (2 µl of 10 x PCR buffer, 15 µl of product from PCR with Phusion DNA Polymerase, 2 µl of dNTP, 1 µl of *Taq* polymerase). The reaction processed in 72°C for 30 min. The size and the concentration of the product were determined via 1.2% agarose gel electrophoresis (100V, 60 min) in 0.5 x TAE buffer. GeneRuler™ 1 kb Plus DNA Ladder was used as a size marker. Subsequently, the band of proper for LeDMC1 molecular mass was isolated from the agarose gel using a Spin DNA Extraction Kit (Invisorb).

3.2.9.1.3. LeDMC1 fragment ligation into the pSC-A-amp/kan cloning vector

The amplified fragment of LeDMC1 was cloned into the pSC-A-Amp/kan cloning vector using the Strata Clone^{MT} PCR Cloning Kit (Thermo Scientific GmbH). The ligation mix contained: 3 µl of StrataClone^{MT}Buffer, 2 µl of PCR product (5 - 50 ng) and 1 µl Vector Mix amp/kan. The reaction was incubated for 5 min at room temperature. The construct was transformed via heat-shock to a competent *E.coli* strain Strata CloneTM SoloPak^R Competent Cells. Transgenic colonies (refers pSC-DMC1) were identified by colony PCR using standard PCR conditions (described in the chapter 3.2.9.1.1) and the M13 primer pair (sequence listed in the Table 1).

3.2.9.1.4. Plasmid DNA extraction, digestion and sequencing

Plasmid pSC-DMC1 was isolated from recombinant *E. coli* colonies using the JETstar™ Plasmid Purification Midi Kit 2.0 (Genomed). Correct size of the insert was checked by double restriction enzyme digestion using *SacI* and *NotI* enzymes. The digestion mix contained: 1 µl of 10 x reaction buffer G, 1 µl of *SacI* enzyme, 1 µl of *NotI* enzyme, 5 µl of plasmid solution and 2 µl of ddH₂O. Reaction was incubated at 37°C overnight. The digested plasmid was separated by electrophoresis on a 1.2% agarose gel (100V, 60 min) in 0.5 x TAE buffer. The correct sequence of the inserted DNA was confirmed by sequencing by the Eurofins Company. Sequence analysis was performed with the Software SeqMan Pro from the DNASTAR Lasergene 10 Core Suite.

3.2.9.1.5. LeDMC1 fragment ligation into the pET-23a-d(+) expression vector

The LeDMC1 fragment with correct sequence was isolated from the agarose gel using Invisorb^R Spin DNA Extraction Kit (Invitek). Fragment of interest was sub-cloned into the expression vector pET-23a-d(+) (Novagen) thus ensuring a translational fusion with a His-tag at the C-terminal part of recombinant proteins. The ligation mix contained: 2 µl of 10 x T4 DNA Ligase buffer, 8 µl of digested with *SacI* and *NotI* enzymes pET-23a-d(+) vector (50 – 100 ng), 2 µl of T4 DNA and 8 µl of LeDMC1 fragments (50 – 100 ng). The reaction was proceeded overnight at 4°C. Correct pET-23a-DMC1 cloning was confirmed by PCR with the M13 primer pair (as described in 3.2.9.1.3.) and sequencing by the Eurofins Company. The obtained pET-23a-DMC1 construct was transformed to electrocompetent *E. coli* strain BL21 (DE3) employing a Micro Pulser (BioRad) at 2500 V.

3.2.9.2. Recombinant protein expression and purification

3.2.9.2.1. LeDMC1 recombinant protein expression

Culture of BL21 *E.coli* containing the pET-21a-DMC1 construct was incubated with shaking in LB medium at 37°C until the OD₆₀₀ reach 0.5 – 0.8. The protein expression was induced by adding into the culture IPTG to a final concentration of 5 mM. The culture was

then incubated with shaking for 3 hours at 37°C. The induced cells were harvested by centrifugation at 8000 g for 15 min at 4°C.

LB medium (pH 7.0)

10% (w/v) Bacto-tryptone
5% (w/v) Bacto-yeast-extract
10% (w/v) Sodium chloride
0.2% (w/v) Ampicillin (50 mg/ml)

3.2.9.2.2. LeDMC1 recombinant protein purification

The recombinant LeDMC1 protein containing His-tag was purified under native conditions using Purification of His-tag Proteins Kit (Macherey-Nagel). Briefly, the harvested cell pellet was resuspended thoroughly in 40 ml of Binding buffer containing 10 mM imidazol. The bacterial suspension was sonicated (10 times for 15 s bursts (12 W) with a 15 s break in between each burst) on ice and centrifuged at 8000 g for 30 min at 4°C. The supernatant was collected as a crude extract for protein purification. Subsequently the crude extract was gently mixed with earlier equilibrated Ni-NTA agarose gel for 1 hour at room temperature. The mixture was sedimented by centrifugation at 500 g for 5 min and the supernatant was decanted. To remove unbound proteins the gel was washed two times each with 800 µl of Washing buffer containing 20 mM imidazole. The mixture was sedimented by centrifugation at 500 g for 5 min and the supernatant was decanted. Finally, the recombinant proteins were eluted from the gel by adding 80 µl of Elution buffer containing 250 mM imidazol. The mixture was sedimented by centrifugation at 500 g for 5 min and the supernatant containing recombinant LeDMC1 protein was collected. Elution step was repeated five times. To confirm that the purified protein is LeDMC1 Coomassie staining and Western blot analysis were performed.

NPI-10 Binding buffer (pH 0.8)

50 mM Sodium dihydrogen phosphate
300 mM Sodium chloride
10 mM Imidazole

NPI-20 Washing buffer (pH 0.8)

50 mM Sodium dihydrogen phosphate
300 mM Sodium chloride
20 mM Imidazole

NPI-250 Elution buffer (pH 0.8)

50 mM Sodium dihydrogen phosphate
300 mM Sodium chloride
20 mM Imidazole

3.2.9.3. Verification of recombinant LeDMC1 protein

3.2.9.3.1. Total protein extraction from flower buds

Approximately 100 µg of flower buds and leaves of *L. elegans* were ground up in liquid nitrogen. 250 µl of 1 x DTT buffer was added to the samples which were incubated with shaking for 20 min in 65°C. Next, samples were centrifuged at 13000 rpm for 5 min. The supernatants containing total protein extract were collected and store in - 20°C.

1 x DTT buffer

112 mM Sodium carbonate

112 mM DTT

4% SDS

24% Sucrose

4mM EDTA

0.01% Bromphenol blue

3.2.9.3.2. Coomassie staining and Western blot analysis

About 10 µg of the total protein extract from flower buds and leaves and recombinant LeDMC1 protein was separated by Tricine-SDS-Polyacrilamide gel (Tricine SDS-PAGE) electrophoresis (Schagger and Vonjagow, 1987) with 10% acrylamide (stacking gel: 50% acrylamide, 20% SDS buffer, 1.3% APS, 0.13% Temed, ddH₂O, bromophenol blue (dram); separating gel: 50% acrylamide, 20% SDS buffer, 50% glycerin, 0.7% APS, 0.7% Temed, ddH₂O). Sample was denaturated for 5 min at 95°C prior to the loading on the gel. The electrophoresis was run for 2 h at 100 V in 1 x Cathode buffer. PageRuler Prestained Protein Ladder was used as a size marker. For Coomassie staining the gel was incubated for 1 hour in Coomassie blue stain buffer with slight shacking. Next, the gel was de-stained with 20% methanol and 7% acetic acid solution until products were visible.

For Western blot, the separated proteins from SDS-PAGE gel were transferred to a nitrocellulose membrane (Merck Millipore) using electroblotting pads (Phase) at 0.8 mA/cm² for 1.5 hour. The membrane was blocked in a blocking solution for 1 hour and subsequently was incubated with the primary antibody diluted in 1 x PBST (Table 3) overnight at 4°C. Next day the membrane was washed three times in 1 x PBST and the fluorescent labelled secondary antibody diluted in 1 x PBST (Table 3) was applied for 1 hour at room temperature. After binding of the secondary antibody the membrane was

washed three times in 1 x PBST and fluorescent signals were detected using an Odyssey Scanner (LI-COR Biosciences).

SDS buffer (pH 8.5)

3 M Tris
0.3% SDS

Coomassie blue stain buffer

0.1% Coomassie blue G-250
10% Methanol
10% Acetic acid glacial

1 x PBST (pH 7.5)

1 x PBS
0.1% Tween-20

5 x Cathode buffer

500 mM TRIS
500 mM Tricine
0.5% SDS

Blocking solution

1 x PBST
5% milk powder

Table 3. Antibodies and their dilutions used for Western blot.

name	dilutions
primary antibodies	
mouse anti-6xHis-tag (Sigma)	1:1000
rabbit anti-LeDMC1 antisera from rabbi 1, 2 or 3	1:200
secondary antibodies	
goat anti-Rabbit IRDye ^R 800CW (Odyssey)	1:5000
goat anti-Mouse IRDye ^R 680RD (Odyssey)	1:5000

4. Results

4.1. *L. elegans* performs an inverted meiosis

4.1.1. Axial element, synaptonemal complex and bouquet-like configuration are present during prophase I in *L. elegans*

To test whether the early stages of prophase I are conserved among monocentric and holocentric species the presence of the axial elements and synaptonemal complex (SC) using anti-ASY1 and anti-ZYP1 antibodies were evaluated. ASY1 is a structural protein of chromosome axes involved in synapsis and SC assembly (Armstrong *et al.*, 2002). ASY1 is in *L. elegans* initially detected in pollen mother cells during premeiotic interphase as numerous punctate foci distributed over the chromatin (Fig. 7a). As prophase I progresses the signals appear to increase in number continuously (Fig. 7b) till the end of a zygotene when the signal extends almost over the entire chromosome length (Fig. 7c). The protein ZYP1 is a component of the transverse filaments of SC which spans the gap between the lateral elements. An anti-ZYP1 antibody is used as a marker to detected synapsed homologous chromosomes (Higgins *et al.*, 2005). Cross-reactivity of anti-ZYP1 demonstrated presence of a synaptonemal complex at early zygotene in *L. elegans* nuclei (Fig. 7d).

To follow the behaviour of chromosomes during prophase I the number and the distribution of terminal satellite (LeSAT7) localized at the both ends of each chromosome together with the distribution of telomeres was analysed. During the meiosis interphase 12 signals of analysed satellite probe were observed which together with telomeres were randomly distributed in the all nuclear volume (Fig. 7e). At the early leptotene the number of LeSAT7 reduced and was between 9 and 7 what indicated the beginning of chromosome pairing. Signals for terminal satellites and telomeres were distributed mostly on the limited area of the nuclei (Fig. 7f). During zygotene a meiosis-typical bouquet-like configuration occurred. All terminal satellites and telomere signals were clustered together in the one nuclear hemisphere (Fig. 7g). Later, at pachytene 6 signals for LeSAT7 were observed indicating that all tree bivalents are paired. LeSAT7 and telomere signals become more dispersed in the whole nuclei (Fig. 7h). At diakinesis chromatin

condensation gradually progresses. Some homologs separated at the one end due to formation of rod-like bivalent causing an increase of terminal satellite signals.

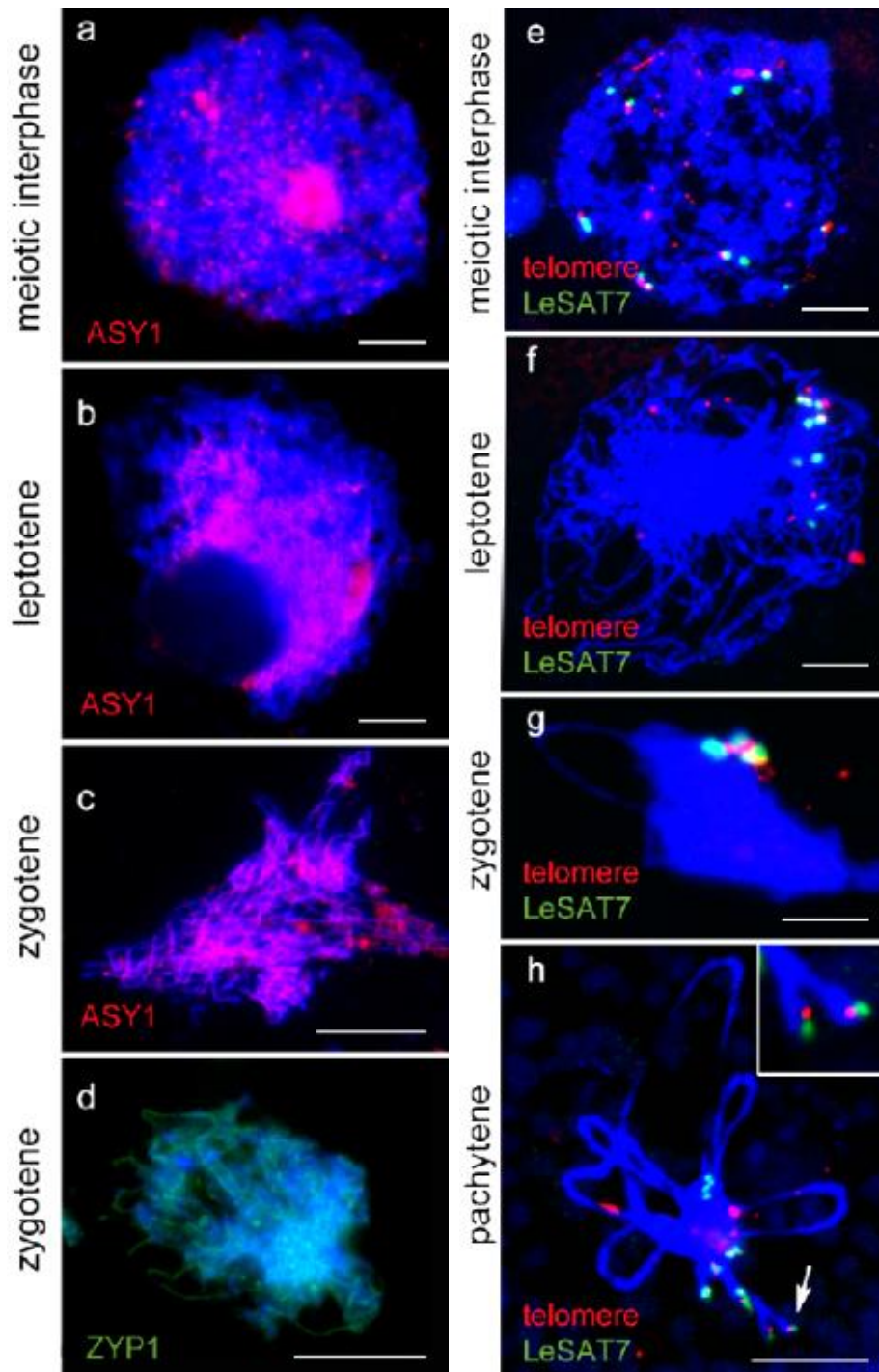


Fig. 7. Axial elements, synaptonemal complex and bouquet configuration are formed during prophase I in *L. elegans* (Fig. 7e-h (Heckmann *et al.*, 2014)).

a) Premeiotic interphase, b) leptotene, c) zygotene cells immunolabelled with anti-ASY1 (red) antibody reveals gradual axial element formation. d) Immunodetection of the synaptonemal complex transverse filament using anti-ZYP1 (green) antibody. e) Meiotic interphase, f) leptotene, g) zygotene, h) pachytene nuclei labelled with the subterminal satellite DNA LeSAT7 (green) and telomere (red) probes by FISH. g) Note a zygotene-typical bouquet-like configuration as indicated by clustering of LeSAT7 and telomere signals in one nuclear hemisphere. Inset and arrow (h) show the onset of desynapsis at the end of paired homologous chromosomes during pachytene. Chromatin was counterstained with DAPI (blue). Bars = 10 μ m.

In order to test whether closely related species *L. luzuloides* also revealed a bouquet-like configuration, the position of telomeres was evaluated by FISH. During meiosis interphase 24 telomere signals were randomly localized in the entire nuclei (Fig. 8a). Along with the prophase I progressing, a telomere signals become more and more compact till zygotene stage where all telomeres are clustered together in the one nuclear hemisphere forming a bouquet like configuration (Fig. 8b).

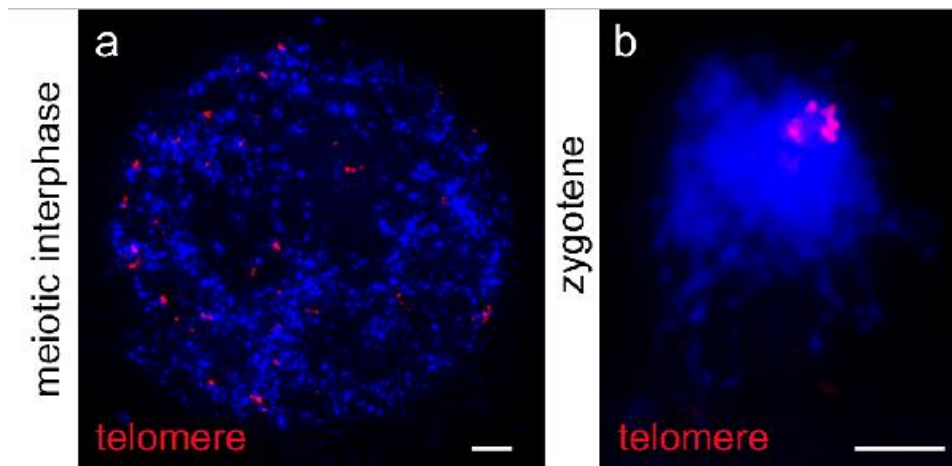


Fig. 8. Bouquet configuration is formed during prophase I in *L. luzuloides* (Heckmann et al., 2014).

a) Meiotic interphase and b) zygotene after FISH with an *Arabidopsis*-type-specific telomeric probe (red) in *L. luzuloides*. b) Typical zygotene telomere-mediated bouquet – like configuration of chromosomes take place, as observed by clustered telomeres in one nuclear hemisphere. Chromatin was counterstained with DAPI (blue). Bars = 10 μ m.

As indicated by the presence of a bouquet like configuration and the distribution of Zyp1- and Asy1-immunolabelling patterns, a signal distribution in *Luzula* species is similar to those described for species with monocentric chromosomes suggesting that the early stage of meiosis are conserved between monocentric and holocentric species.

4.1.2. Three bivalent configurations occur during pre-metaphase I

To distinguish the chromosome pairs of *L. elegans* a combination of two satellite repeats previously identified by Heckmann et al. (2013) was used as an *in situ* hybridization probes. LeSAT28 mark chromosomes number 1 and 2 and LeSAT63 localized to chromosome number 2 (Fig. 9a). At diakinesis, two predominant bivalent configurations are apparent. 43.0% and 47.3% out of 289 analyzed bivalents displayed a rod- (Fig. 9b) and ring- (Fig. 9c) like structure respectively. 9.7% of all bivalents represented a cruciform type bivalent (Fig. 9d). Each of the different homologous chromosome pairs can form ring, rod and cruciform bivalent with no obvious preference regarding the occurrence of one or the other configuration existing between the bivalents (Fig. 9b, c, d). To address the question whether both ends of a given chromosome can take part in bivalent association, LeSAT28 satellite was used as a marker to discriminate chromosomes ends within one bivalent. Among 50 examined rod bivalents 54% of them were associated by the end negative for marker probe (Fig. 9e) and in 46% connection was mediated by the end carrying the marker (Fig. 9f) indicating that each end of a chromosome can take part in bivalent association.

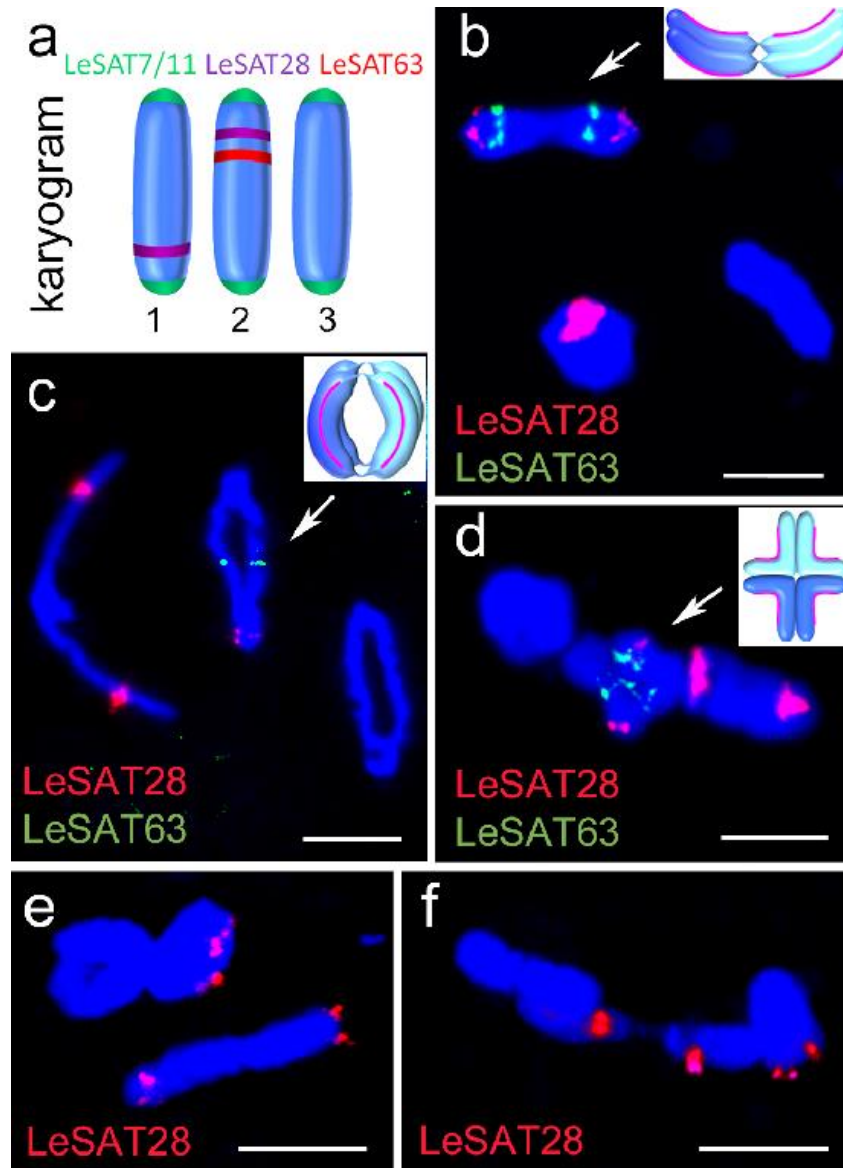


Fig. 9. Various bivalent configurations occur during pre-metaphase I (Heckmann *et al.*, 2014).

a) Karyogram of *L. elegans* showing the distribution of utilized satellite repeats. b-d) Each homologues chromosomes pair can form a ring, rod and cruciform- like bivalent configuration as shown by FISH with LeSAT28- (red) and LeSAT63- (green) specific probes. Chromosome end negative (e) or positive (f) for chromosome end marker (LeSAT28) can mediate the association with its homologous partner. Chromosomes were counterstained with DAPI (blue). Bars = 10 μ m.

4.1.3. Heterochromatin fibers connect non-sister chromatids

To decipher the nature of the terminal connection between homologous chromosomes FISH was performed using an *Arabidopsis*-type telomere probe. Analysis revealed eight telomere signals per rod bivalent, two at the end of each homologous chromosome and four in the middle. DAPI- positive region between the telomere of homologues reflecting an end-to-end association of homologous chromosomes was found (Fig. 10a). Centromere- specific CENH3 signals occur along the entire length of chromatids except for the distal chromosomal regions involved in the end-to-end connection (Fig. 10b, c). It was observed that homologous non-sister chromatids forming rod bivalent are connected to each other by chromatin threads. At early metaphase I always two, thin (<0.5 μm) and up to 6 μm long fibers occur. A comparable interchromatid connection was not observed in *L. elegans* mitotic cells. To reveal the end-to-end composition, we asked whether terminal-enriched satellite repeats colocalize with threads. FISH with LeSAT7-, LeSAT11- and LeSAT28- specific hybridization probes showed that this repetitive sequence localize to the chromatin threads (Fig. 10d, e, f, g). Interestingly, terminal satellites are localized distal to the *Arabidopsis*-type telomeres both in metaphase I (Fig. 10e, f) and in metaphase II (Fig. 13g). The telomeres are not localized at the morphological chromosome termini and seem to be fold back.

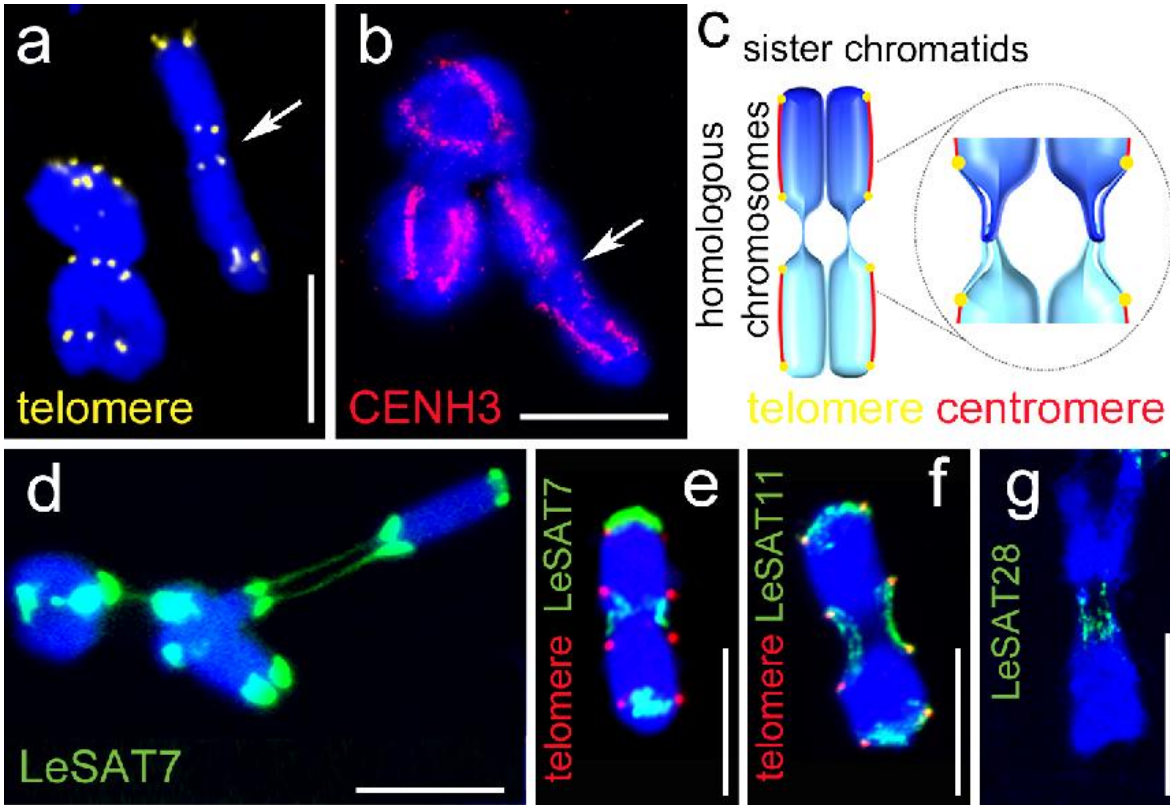


Fig. 10. Satellite DNA-enriched chromatin threads connect homologous non-sister chromatids in holocentric (Fig. 10a-f (Heckmann *et al.*, 2014)).

a) Eight telomere signals both in ring and rod bivalents revealed FISH with an Arabidopsis-type-specific telomere probe (yellow). Arrow indicates end-to-end association between homologous chromosomes of a rod bivalent. b) Rod and ring bivalents after detection of CENH3 (red) by immunolabelling. Arrow shows the CENH3-free end-to-end association of the homologous chromosomes in rod-like bivalent. c) Model of an end-to-end associated rod bivalent. Inset shows proposed structure of the end-to-end connection. Telomeric regions loop back to facilitate the observed internal telomere localization. d, e) Satellites LeSAT7, f) LeSAT11 and g) LeSAT28 mediate end-to-end association. Note, heterochromatin fibers differ in length between homologues (d, e, f, g). The bivalents were labelled with LeSAT7 (green), LeSAT11 (green), LeSAT28 (green) and Arabidopsis-type telomere (red) probes and counterstained with DAPI (blue). Bars = 10 μ m.

For comparison with monocentric species the end-to-end connections of rod-bivalents were investigated in rye (*S. cereale*) and barley (*H. vulgare*). To mark this region FISH was performed using a probe combination of Arabidopsis-type telomere and the subtelomeric specific repeats pSc119.2 (Cuadrado *et al.*, 1997) for rye and the same

telomeric probe together with the repeat HvT01 (Nasuda *et al.*, 2005) for barley. Some of the 7 bivalents formed rod configurations where homologs were connected to each other by chromatin thread. In contrast to *L. elegans* only one fiber per one end-to-end association was present. In 41% (n = 22) of rye rod bivalents (Fig. 11a) and in 25% (n = 16) of barley rod bivalents (Fig. 11b) terminal-enriched satellite repeats colocalized within fibers which run in between the telomeres of homologs. In the remaining cases examined subtelomere repeats were not involved in end-to-end association (Fig. 11a, c). As presented on the model (Fig. 11d) one fiber might be a result of association between non-sister chromatids mediated by proteins involved in chiasmata resolution. These findings suggest that holocentric and monocentric can use different mechanisms to facilitate homologues connection although in both cases terminal satellite repeats are involved.

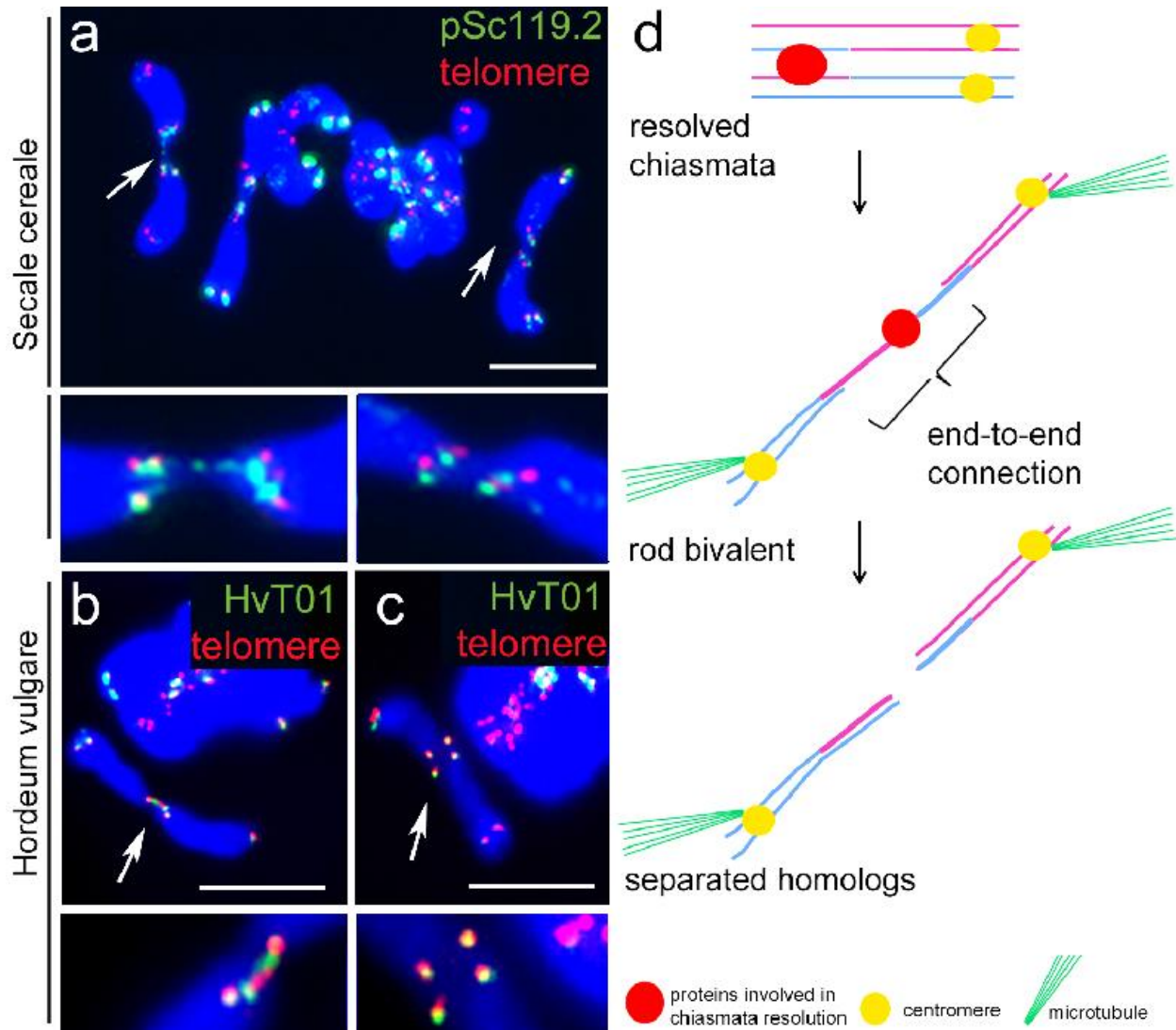


Fig. 11. In monocentric species satellite DNA-enriched chromatin threads connect homologous non-sister chromatids.

Meiotic metaphase I chromosomes of rye (a) and barley (b, c). In rod bivalents one fiber enriched in subtelomeric repeats pSc119.2 (rye) and HvT01 (barley) connects homologous chromatids and mediate their association. Arrows and inserts indicate two possible connection types – with and without fibers enriched in subtelomeric repeats like pSc119.2 (rye) or HvT01 (barley). d) Model shows proposed recombination dependent origin of fibers in monocentric. Proteins involved in chiasmata resolution connect non-sister chromatids in a position where crossover took place. Subsequently, spindle microtubules interact with centromere and pull homologs in the opposite directions stretching rich in proteins end-to-end association of rod bivalent. As a result, one fiber in between homologues is observed. After dissociation of proteins involved in chiasmata resolution from the end-to-end connection, homologues separated during anaphase I. The bivalents were labelled with pSc119.2 (green), HvT01 (green) and Arabidopsis-type telomere (red) probes and counterstained with DAPI (blue) Bars = 10 μ m.

To test the presence of satellite repeats in related holocentric species PCR with primers specific for selected *L. elegans* terminal satellites involved in the end-to-end connection (LeSAT11, LeSAT27, LeSAT28 and LeSAT7) and genomic DNA of *L. elegans* (Fig. 12a) and *L. luzuloides* (Fig. 12b) was performed. LeSAT11, LeSAT28 and LeSAT7 terminal satellite repeats show similar PCR patterns implying the occurrence of similar satellite repeats in both holocentric species.

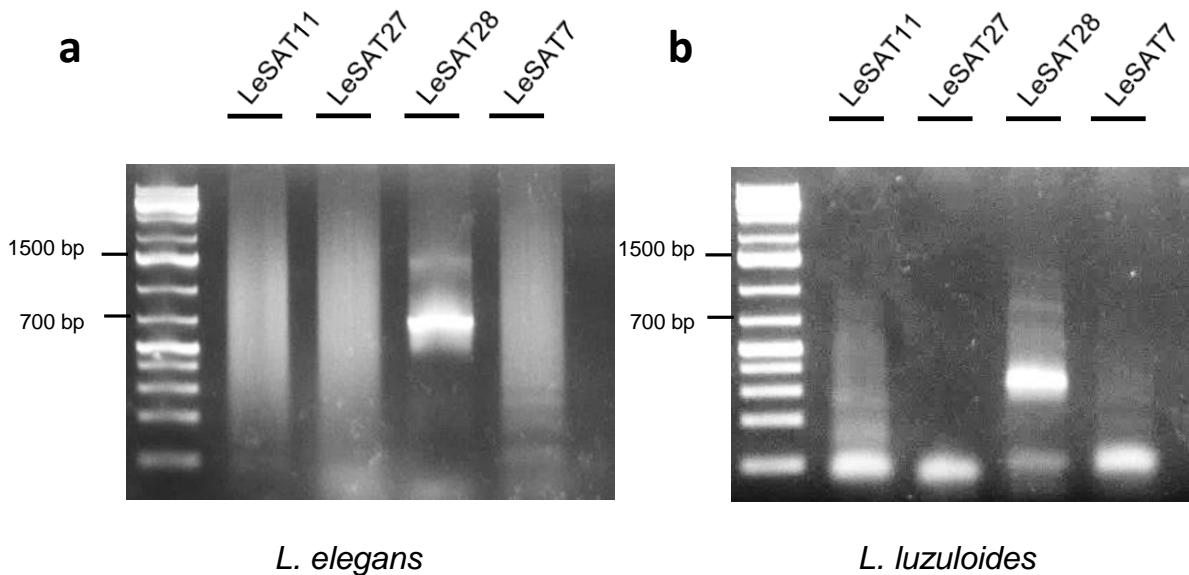


Fig. 12. Terminal satellite repeats involved in end-to-end connection are similar between *L. elegans* and closely related *L. luzuloides*.

PCR with genomic DNA from *L. elegans* (a) and *L. luzuloides* (b) with primers specific for *L. elegans* terminal satellite repeats involved in end-to-end connection of homologous chromosomes during meiosis. PCR patterns for LeSAT11, LeSAT28 and LeSAT7 are similar in both holocentric species.

4.1.4. An inverted sequence of meiotic sister chromatid segregation occurs in *L. elegans*

In order to test whether *L. elegans* performs an 'inverted meiosis' the segregation of chromatids during gamete formation was studied in detail. During first meiotic metaphase three bivalents are oriented with their longitudinal axes perpendicular to the spindle (Fig. 13a). CENH3 and H2AThr120ph immunolabelling revealed four, distinct linear centromeres per bivalent, reflecting two pairs of individual sister centromeres (Fig. 10b,

13a). Sister centromeres appear as a parallel axes showing bi-orientation and behaving as a two distinct functional units. Spindle microtubules are attached at various sites along the whole-longitudinal centromeres (Fig. 13a). Microtubule coming from one spindle pole are attached to the end-to-end associated homologous non-sister chromatids enabling equational sister chromatids division. Chromosomes initiate the migration to the poles at the onset of anaphase I. At this stage sister chromatids separate to opposite cell poles and non-sister chromatids migrate together to the same pole (Fig. 13b). We detected thin heterochromatin fibers, rich in subtelomeric satellite repeats connecting non-sister chromatids in 95% of the analyzed anaphase I cells (Fig. 13c). At the end of anaphase I a large number of long microtubules are localized in between separated chromatids enabling two distinct 'interkinesis-like' nuclei formation (Fig. 13d). During telophase I chromatid decondensation progresses and spindle microtubules disappear (Fig. 13e). After short prophase II non-sister chromatids align at the metaphase II plate perpendicular to the spindle axis (Fig. 13f). Heterochromatin threads running between telomeres of non-sister chromatids are observed at metaphase II (Fig. 13g). During anaphase II, when end-to-end connection is resolved, non-sister chromatids segregate holokinetically forming four daughter cells (Fig. 13h). Our data indicated a holocentric centromere organization throughout all stages of meiosis in *L. elegans*. To proof correct course of inverted meiosis FISH with two chromosome- specific markers – LeSAT7 and LeSAT28 was performed. Every daughter cell shows six FISH signals for LeSAT7 and two signals for LeSAT28 confirming correct genome haploidization (Fig. 13i).

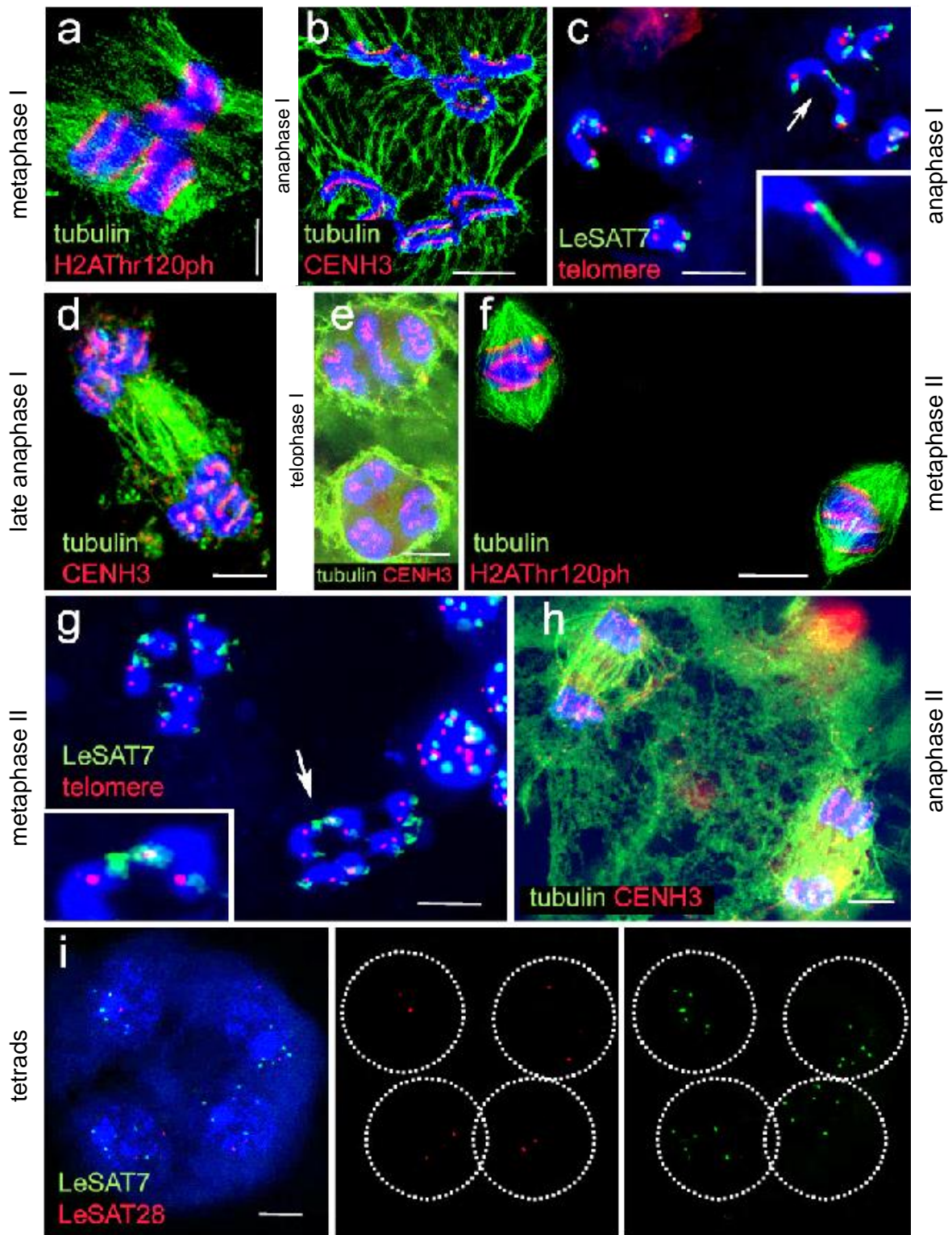


Fig. 13. Separation of sister chromatids is followed by non-sister chromatid division (Heckmann *et al.*, 2014).

Detection of centromeres by immunolabelling using antibodies recognizing H2AThr120ph or CENH3 (red) and α -tubulins (green) during a) metaphase I, b, d) anaphase I, e)

telophase I, f) metaphase II and h) anaphase II. (Pictures d, e and h are kindly provided by S. Heckmann). Distribution of subterminal LeSAT7 (green) and telomere (red) repeats at a) anaphase I, g) metaphase II, as well as of chromosome-specific markers LeSAT7 (green) LeSAT28 (red) in tetrads after FISH. Arrows in c and g indicate LeSAT7-enriched chromatin fibers connecting non-sister chromatids. i) Equal number of LeSAT7 and LeSAT28 signals in daughter cells indicates proper meiosis segregation. Chromosomes were counterstained with DAPI (blue). Bars = 10 μ m.

To gain further evidence of the inverted order of chromatids segregation chromosome segregation in individual plant possessing X-ray induced chromosome fragments was analyzed by FISH. Breakage of one chromosome of pair 1 resulted in two chromosome fragments of a different size (Fig. 14a) enabling distinguishing between sister (the same length) and non-sister (different length) chromatids during meiosis (Fig. 14b). This heteromorphic chromosome pair provided an ideal test system to mark one homolog and then monitor chromosome separation during meiosis. At metaphase I three bivalents (one heteromorphic) and one chromosome fragment were observed. Heteromorphic bivalent consists of the long chromosome fragment of pair 1 end-to-end connected with the unbroken homologous chromosomes while the remaining small chromosome fragment of pair 1 is unpaired (Fig. 14c). All analyzed anaphase I cells clearly showed mirror images of all chromosomes, including chromosome fragments. During anaphase I end-to-end connection occurs between different in length chromatids demonstrating that sister chromatids separate already during meiosis I and non-sisters migrate together to the same cells poles proving occurrence of inverted meiosis in *L. elegans* (Fig. 14d).

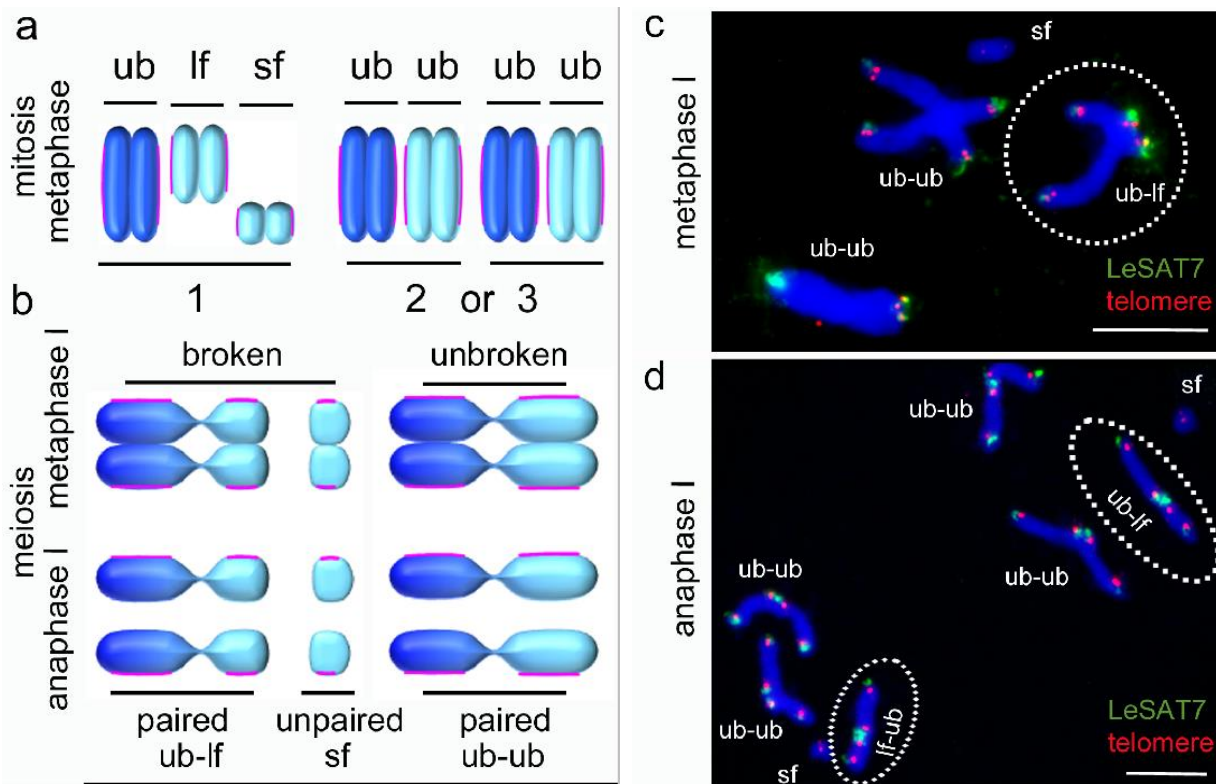


Fig. 14. Sister chromatids separate during anaphase I implying inverted meiosis in *L. elegans* (Heckmann et al., 2014).

a.) Karyogram depicting chromosomes in a plant carrying two chromosome fragments of a different size (lf – long fragment, sf – short fragment, ub – unbroken homologous chromosome). b) Schemata of broken (lf and sf) and unbroken (ub) bivalent behavior during metaphase I and anaphase I. b, c) Large chromosome fragment forms end-to-end connection with its homolog (encircled) whereas the small fragment remains unpaired at metaphase I. b, d) End-to-end connected chromatids of a different length (ub-lf, encircled) migrate to the same cell pole illustrating that at meiosis I sister chromatids are separated and not homologues. The chromatids of sf divided, too c, d) FISH with LeSAT7 (green) and telomere (red) probes. Chromosomes were counterstained with DAPI (blue). Bars = 10 μ m.

All gained results indicated that, the first meiosis division in *L. elegans* is equational and the second meiotic division is reductional as shown in the model (Fig. 15). Thus, we supported previous assumptions that *L. elegans* chromosomes perform inverted sequence of meiosis (inverted meiosis) in order to deal with holocentricity during meiosis.

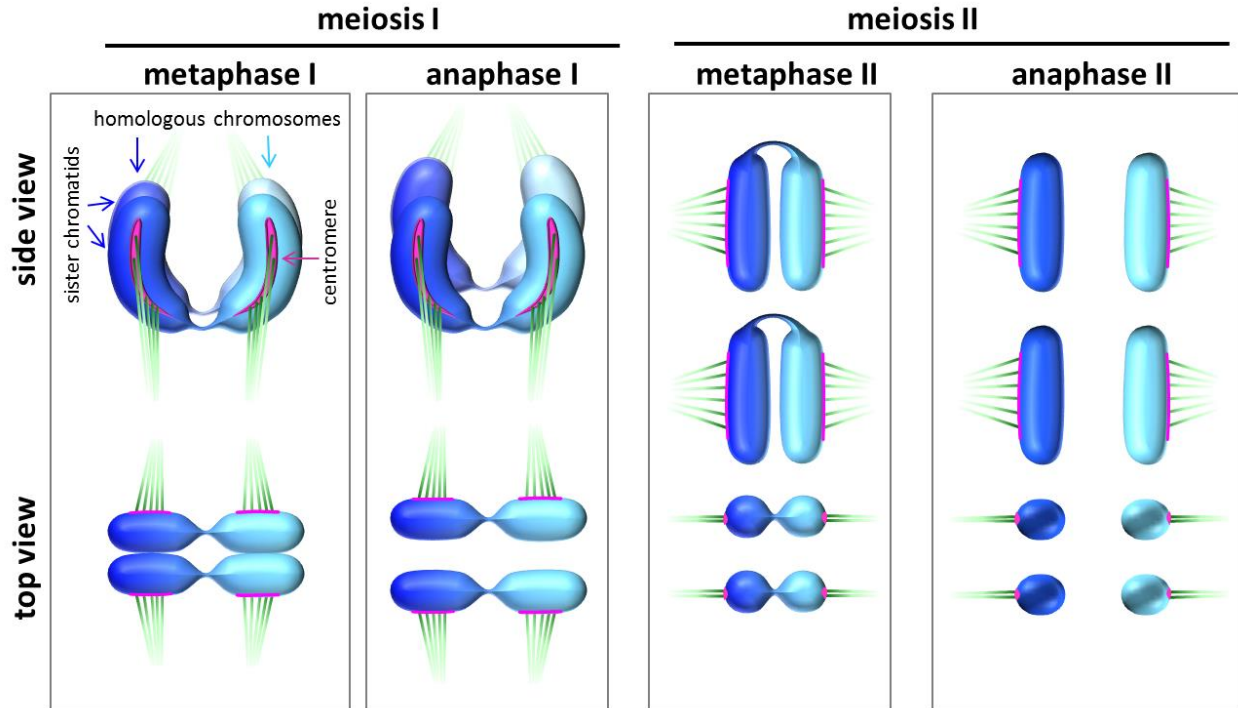


Fig. 15. Structural model of inverted meiosis in *L. elegans* (Heckmann et al., 2014).

End-to-end associated holocentric homologs align at metaphase I in such a manner that sister chromatids separated during anaphase I and non-sister chromatids migrated together to the same cell pole. Non-sister chromatids are terminally linked by satellite DNA-enriched chromatin threads until metaphase II. During meiosis II, after resolution of end-to-end connection non-sister chromatids are holokinetically separated. Thus, an inverted sequence of meiotic events compared to the typical reductional-equational sequence observed in monocentric organisms take place.

4.2 Identification of the meiotic gene DMC1 in *L. elegans*

To uncover the mechanism of inverted meiosis, in particular the nature of the end-to-end connection between homologous chromosomes, a number of available plant meiotic-specific antibodies (*A. thaliana*: DMC1, Rad51, MLH1; barley: HvMLH3; kindly provided by James Higgins, Birmingham) were tested for cross reactivity in *L. elegans*. Unfortunately, none of the tested antibodies was informative. Therefore, the meiotic transcriptome was determined based on next generation sequence reads obtained from mRNA isolated from staged pollen mother cells of *L. elegans*. Next generation sequencing of meiotic transcriptome was performed by the company Fasteris. Sequence assembly and gene prediction was done in cooperation with Dr. K. X. Mayer (MIPS, Munich).

To test whether end-to-end connection between non-sister chromatids is recombination dependent, we looked for the DMC1-like gene in *L. elegans* pollen mother cells transcriptome. Among the *in silico* annotated hits of the transcriptome the nematode *Trichinella spiralis* (tr|E5S116|E5S116_TRISP) DNA repair and recombination protein RecA sequence was found, which is a DMC1 homologue. Therefore, this sequence was considered as a *L. elegans* DMC1-like gene. The nucleotide length of the partial *L. elegans* DMC1-like gene is 1023 bp, corresponding to 341 amino acids (Fig. 16a, b) with a predicted molecular weight of 37.15 kDa (http://web.expasy.org/compute_pi/). BLAST analysis revealed that *L. elegans* DMC1 gene is not a complete sequence since a stop codon is missing. The partial protein sequence of *L. elegans* DMC1 (LeDMC1) was aligned via Cluster W method with DMC1 protein sequences of *Oryza sativa*, *Zea mays*, *Triticum aestivum* and *Brachypodium distachyon*. The alignment revealed a large similarity between the examined proteins (Fig. 17) manifested also in a numerous conserve domains (Fig. 16b). Some domains have multiple functions and are absolutely necessary for homologues recombination like 'Helix-Hairpin-Helix' (HHH_5) which is non-sequence specific binding domain present in variety of DNA repair proteins (Doherty *et al.*, 1996) or 'ATPases Associated with diverse cellular Activitie' (AAA_25) which contains several conserved motifs including those necessary for ATP binding and hydrolysis, the Walker A and Walker B motifs, respectively (Dougan *et al.*, 2002; Erzberger and Berger, 2006). Rad51_DMC1_radA domain is a single- stranded DNA binding domain which catalyzed recombination reaction using ATP- dependent DNA binding activity or 'recomb_DMC1' domain which shows a recombinase activity only in meiosis (reviewed in <http://www.ncbi.nlm.nih.gov/Structure/cdd/wrpsb.cgi?RID=WG WV0APY01R&mode=all>).

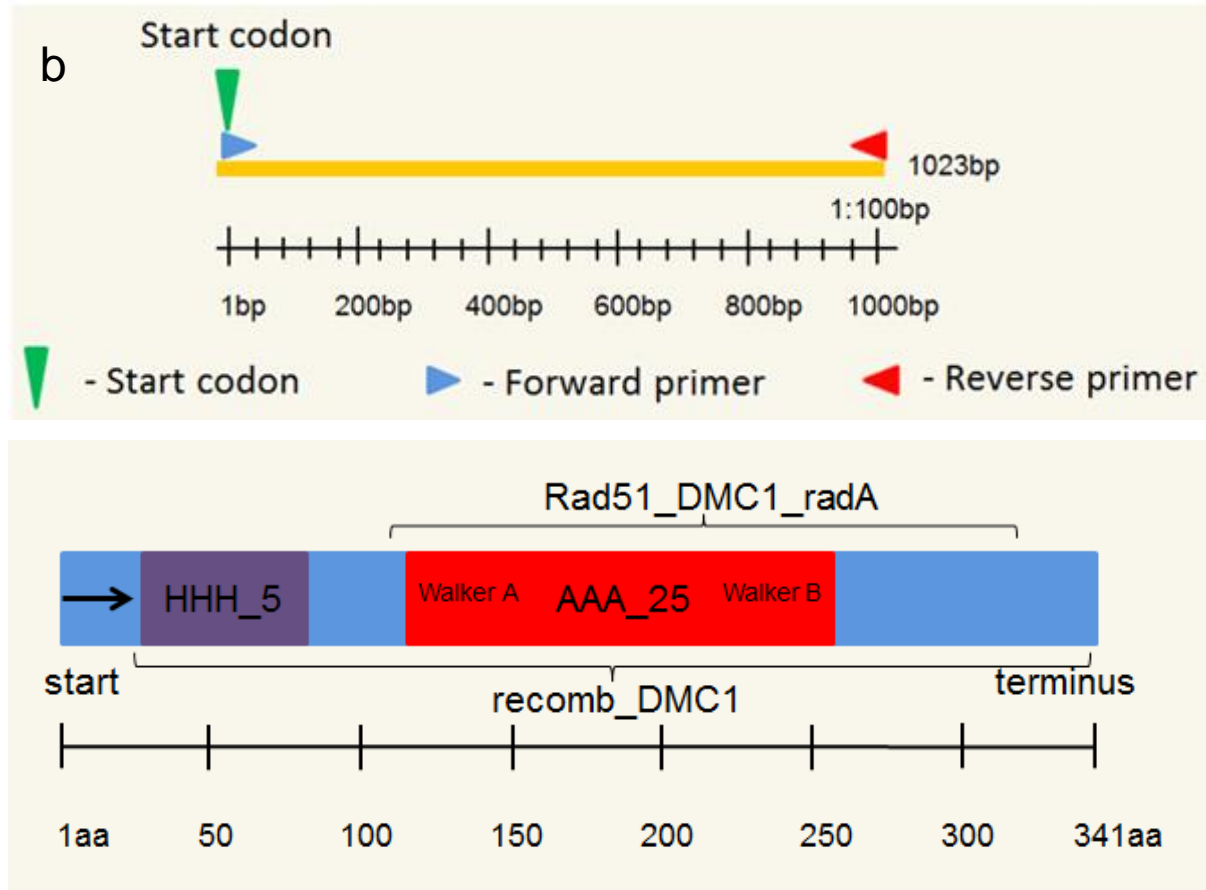


Fig. 16. Structure of the partial LeDMC1-like gene and protein.

Models show the general features of partial LeDMC1-like a) gene and b) protein. a) The nucleotide length of the partial LeDMC1-like gene is 1023 bp. A start codon (green arrowhead) is present but stop codon is absent. Blue and red arrowhead indicate the position of forward and reverse primers respectively. b) The length of partial LeDMC1-like protein is 341 aa. A number of conserved domains (HHH_5, AAA_25, Rad51_DMC1_radA, recomb_DMC1) are present.

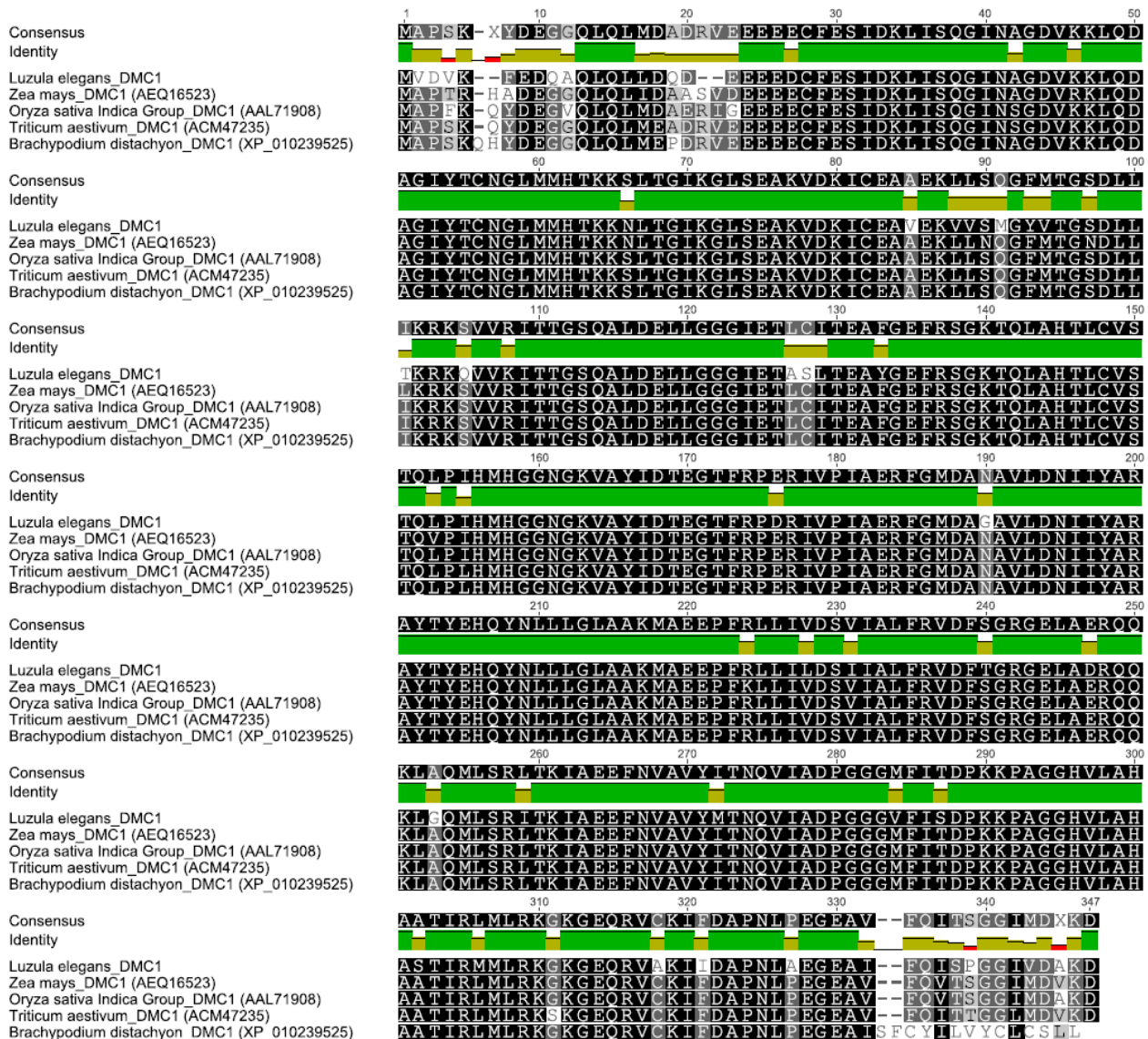


Fig. 17. Alignment of the partial *L. elegans* DMC1-like protein with the DMC1 proteins of different plant species revealed that DMC1 is a highly conserved protein.

Alignment of the partial DMC1-like protein of *L. elegans* with the DMC1 proteins of *Z. mays*, *O. sativa*, *T. aestivum* and *B. distachyon* shows high interspecies homology. The height and the color of the bar below the amino acid sequence represent the identity, green means that the residue at the position is the same across all sequences, yellow is for less than complete identity and red refers to very low identity at the given position. The protein sequences were obtained from NCBI database.

Next, a phylogenetic study was conducted to further characterize DMC1-like protein of *L. elegans*. A phylogenetic genetree was calculated with the program Geneious 7.0.6.

(Biomatters Ltd). The tree is divided in two major branches representing monocots and eudicots. DMC1-like protein of *L. elegans* clusters with DMC1 proteins of monocots (Fig. 18). The prevalence of DMC1 proteins both in monocots and dicots suggests the presence of DMC1 protein in their common ancestor and a major role in plant development.

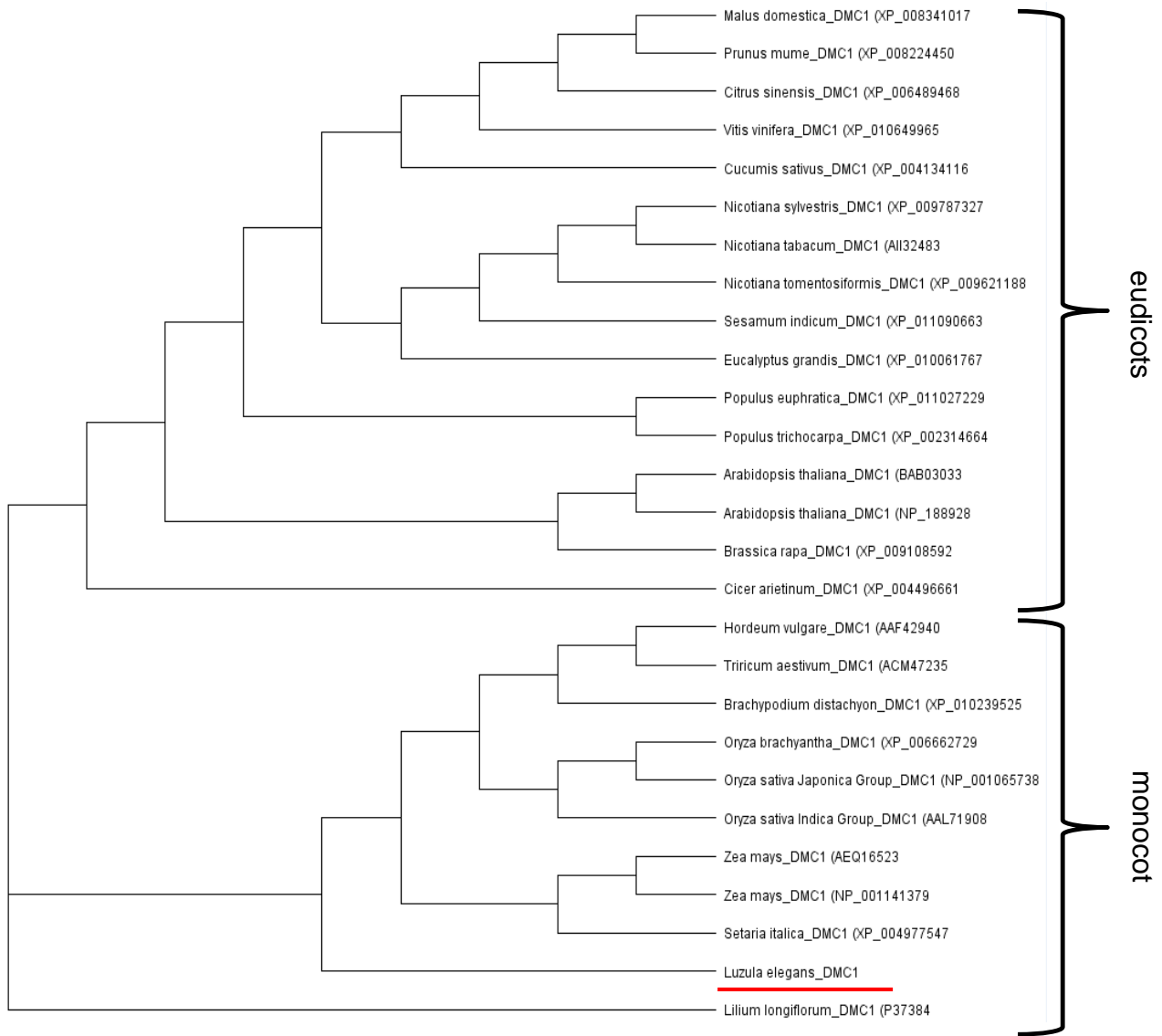


Fig. 18. Phylogenetic tree containing the DMC1 protein of different plant species shows *L. elegans* DMC1-like protein affiliation to the monocot family.

The phylogenetic tree shows the relationship between the monocot and eudicots DMC1 protein. DMC1-like protein of *L. elegans* clusters with DMC1 of monocots.

All *in silico* gained results confirmed that the chosen sequence encodes proper LeDMC1 protein. Therefore, the selected sequence can be used for future analysis aiming to test whether end-to-end connection between non-sister chromatids is recombination dependent.

4.2.1. Expression profile of LeDMC1

To test whether the DMC1 gene of *L. elegans* shows high transcriptional activity in meiotic tissue as described for yeast (Schwacha and Kleckner, 1997), plants (Vignard *et al.*, 2007) mouse and human (Habu *et al.*, 1996) transcription analysis was performed. RNA isolated from young leaves and anthers was converted into cDNA and subsequently used for semi-quantitative RT-PCR. As a control RT-PCR was performed with primers specific for glyceraldehyde 3-phosphate dehydrogenase (GAPDH) of *L. elegans* (kindly provided by Wei Ma, IPK Gatersleben). GAPDH is a gene which is stably and constitutively expressed in most tissues and cells. Thus is considered as a housekeeping gene and commonly used as a quantity control of cDNA during quantitative PCR (Dundas and Ling, 2012). As indicated in the Fig. 19a cDNA that comes from leaves and anthers were of equal amount.

Quantification of DMC1-like transcriptome of *L. elegans* was performed with the primer pair LeDMC1_F and LeDMC1_R designed with the online design tool Primer3 (<http://primer3.ut.ee/>). Primers positions are indicated in the model (Fig. 16a) and sequences are listed in the Table 1. LeDMC1 shows transcription activity only in generative tissue – anthers (Fig. 19b), no activity was found in vegetative leaf tissue. Hence, we demonstrated that DMC1 of *L. elegans* is a meiosis- specific protein.

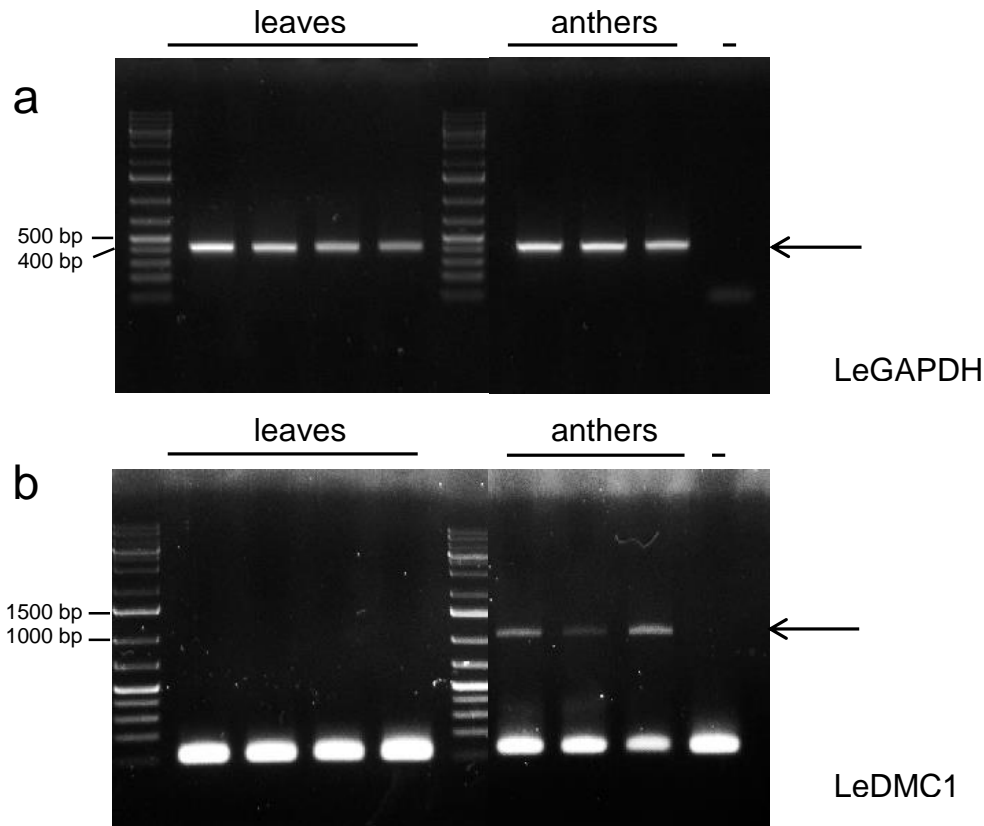


Fig. 19. DMC1-like of *L. elegans* shows transcription activity only in generative tissue.

PCR was performed with cDNA of *L. elegans* isolated from leaves and anthers. a) Equal amount of cDNA from different tissues was shown by amplification using a LeGAPDH-specific primer pair. b) DMC1 transcription activity in different tissues. DMC1 transcripts were only observed in anthers undergoing meiosis. -) negative control (no cDNA in the reaction). Arrows indicate the specific bands. Lengths of the expected amplicons are indicated.

4.2.2. Expression of recombinant LeDMC1 protein

To produce a LeDMC1-specific antibody the LeDMC1 341 amino acid- long sequence was selected for recombinant protein production. cDNA of anthers was used as a template for RT-PCR amplification of the desired region with LeDMC1_F forward primer and LeDMC1_R reverse primer (Fig. 16a, Table 1). The primers were designed to have *SacI* and *NotI* restriction enzyme sites as well as protection site (Table 1). A 6 base pairs protection site was added before the recognition site to increase cleavage efficiency by the inhibition of primer dimers and hairpin loops formation (https://www.neb.com/~media/NebUs/Files/Chart%20image/cleavage_oligonucleotides_

old.pfd). Subsequently, PCR products were cloned into the pSC-A-amp cloning vector and transformed into Strata Clone Solo Pack competent cells. Recombinant colonies (refers pSC-DMC1) were identified by colony PCR using a M13 primer pair. Restriction analysis after plasmid DNA purification gave two bands of ~ 1000 bp and ~5000 bp, which corresponded to the expected size of LeDMC1 gene and pSC-A-amp vector respectively (Fig. 20). Finally, pSC-DMC1 plasmids with the right size of DMC1 gene were sequenced by the Eurofins Company to confirm they had correct sequence.

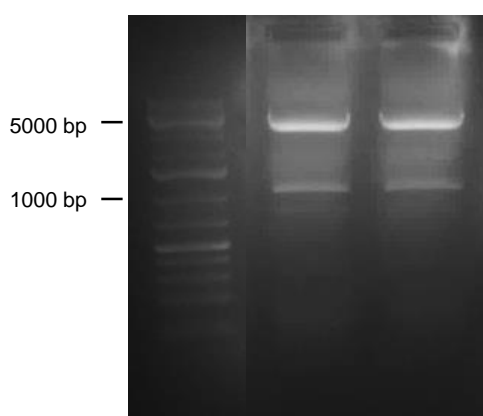


Fig. 20. Restriction digestion confirmed successful cloning of LeDMC1 gene into pSC-A-amp vector.

Digestion of recombinant plasmids pSC-A-amp with *SacI* and *NotI* enzymes revealed two bands with the length of ~ 1000bp and ~5000bp corresponding to the DMC1 gene and pSC-A-amp vector size respectively. Lengths of the expected restriction fragments are indicated.

Comparison of sequences from pSC-DMC1 plasmids with LeDMC1 sequence from our RNAseq database revealed one amino acid change in the position 116 (Isoleucine-valine) in all pSC-DMC1 plasmids (Fig. 21). We assumed that one amino-acid change will not affect specificity of the future polyclonal antibody.

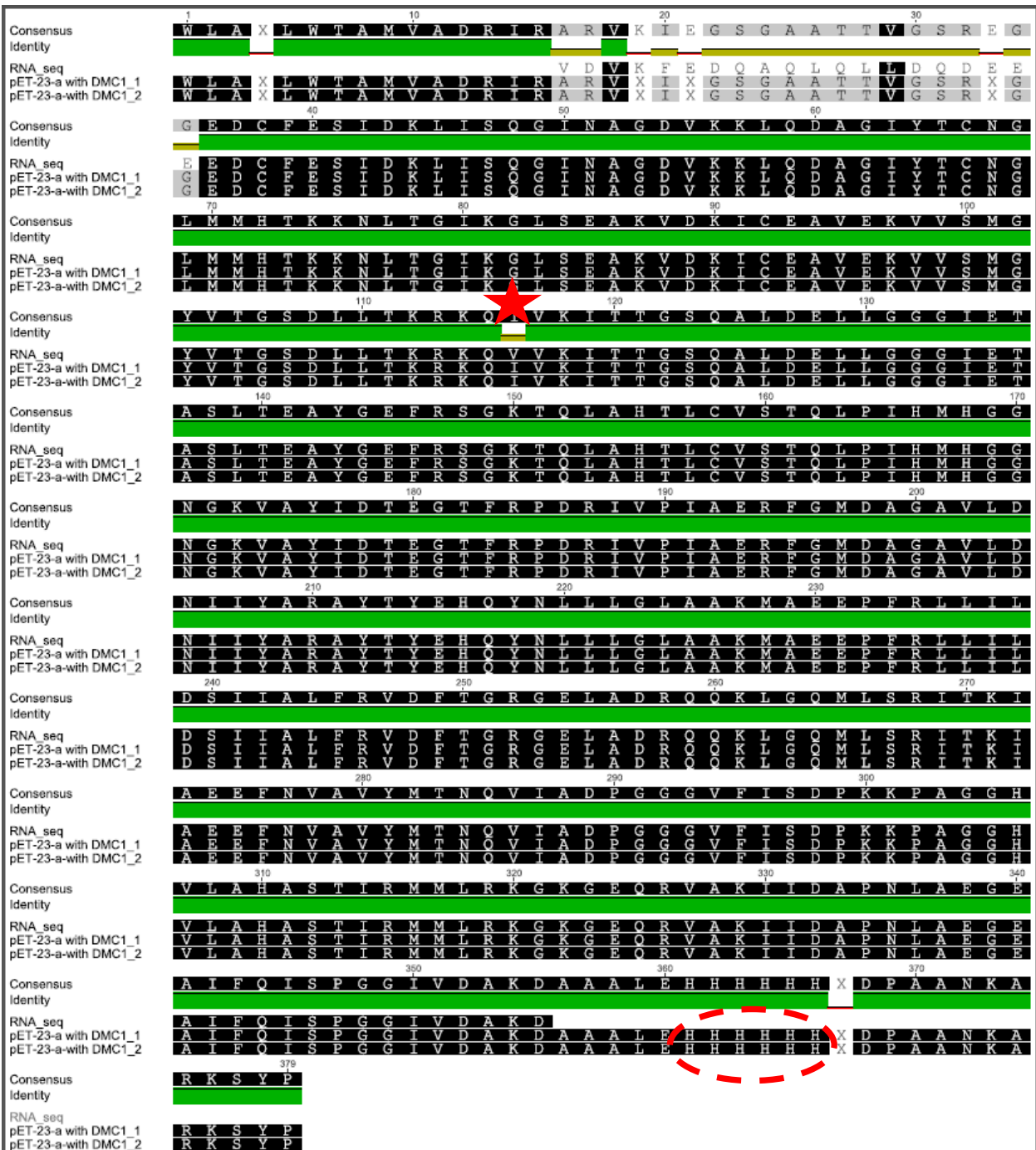


Fig. 21. The DMC1 sequences from pET-23-a constructs differ only in one amino-acid compared to the DMC1 sequence coming from RNAseq database.

The amino acid Cluster W alignment of DMC1 sequence coming from RNAseq database (protein_RNAseq) with the two DMC1 construct sequences after sequencing (pET-23-a with DMC1_1, pET-23-a with DMC1_2) differ only in one amino-acid in the position 116 (red star). Note C-terminal polyhistidine (6xHis) tag in the DMC1 construct (circled). The bar below the amino acid sequence represents the identity, green means that the residue

at the position is the same across all sequences, yellow is for less than complete identity and red refers to very low identity at the given position.

To construct the plasmid for protein expression, pSC-DMC1 plasmid was digested with *SacI* and *NotI* and subsequently the DMC1 fragment was ligated into the pET-23a vector. Correct pET-23a-DMC1 sequence was confirmed by PCR with M13 primer pair and sequencing. Plasmid pET-23a-DMC1 was transformed into the *E. coli* strain BL21 (DE3) competent cells. Exponentially growing cultures of transgenic bacteria were used for IPTG induction of recombinant protein expression for 3 hours at 37°C. Recombinant protein was expressed as a fusion protein containing a C-terminal polyhistidine (6xHis) tag which allows efficient protein purification (Fig. 21). DMC1 recombinant protein was purified under native conditions using nickel matrix of Ni-NTA agarose and subsequently checked by SDS-PAGE gel. Coomassie Blue staining showed a faint band around 40 kDa (Fig. 22a), which was consistent with the predicted calculation (http://web.expasy.org/compute_pi/). To confirm that the expressed protein is the LeDMC1 recombinant protein a Western blot with an anti-histidine tag antibody was performed. The results showed a single band with molecular weight of ~40 kDa as expected for LeDMC1 recombinant protein (Fig. 22b).

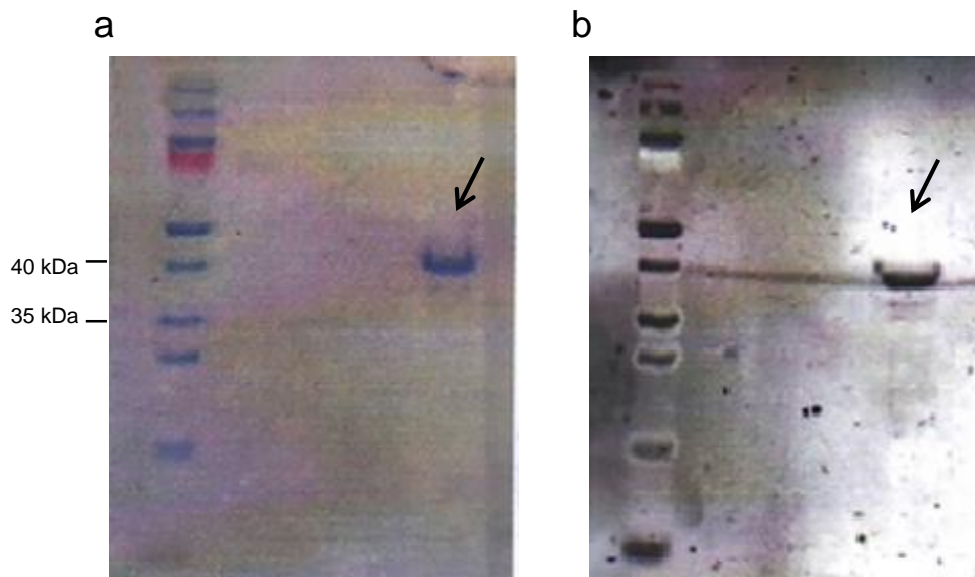


Fig. 22. SDS-PAGE gel staining and Western blot of purified LeDMC1 recombinant protein reveal the presence of recombinant protein in the sample.

LeDMC1 recombinant protein showed the expected molecular weight (~40 kDa), as evidenced by a) SDS-PAGE gel staining and b) by the Western blot detecting His-tag. Note: arrows show expressed protein. Lengths of the expected recombinant protein are indicated.

4.2.3. Validation of LeDMC1 anit- sera

In order to differentiate between specific and unspecific signals the pre-immune sera of five rabbits were used for indirect immunostaining experiments first. The signals caused by the pre-immune sera were weak and diffused in the cytoplasm and nuclei (Fig. 23). Three rabbits with the weakest immunostaining pattern were chosen for immunization. The recombinant protein was sent to the Pineda Company (Berlin) to raise the anti-LeDMC1 antibody in the selected rabbits.

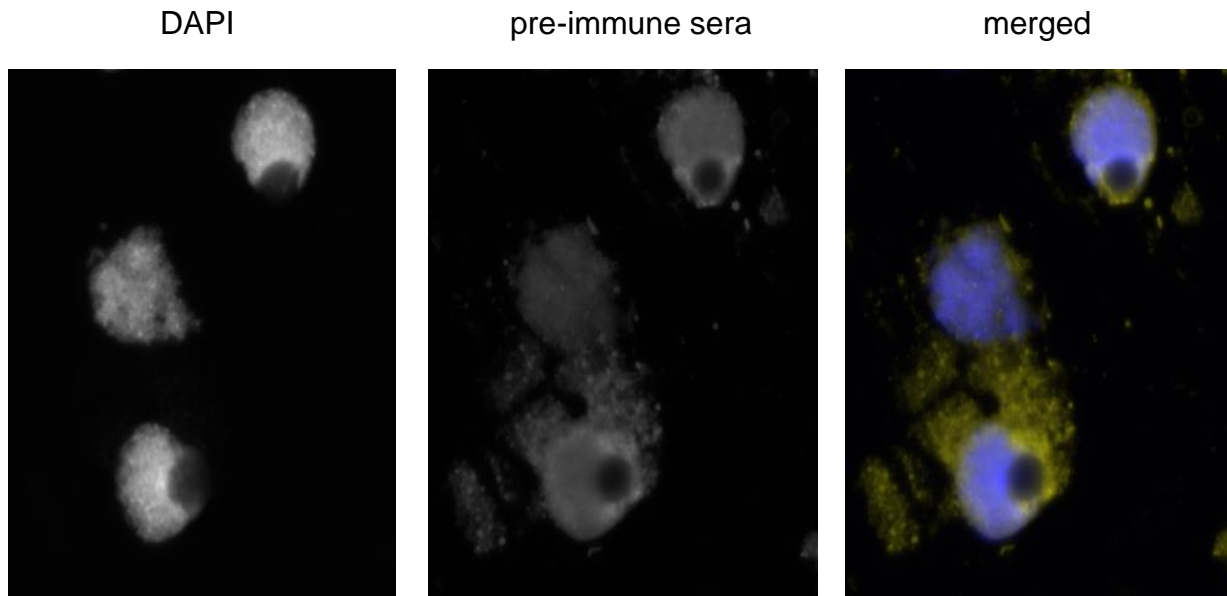


Fig. 23. Typical signals caused by the pre-immune serum of the rabbit used to generate LeDMC1 antibody are of weak intensity.

Immunostaining of prophase I nuclei with pre-immune serum of rabbit (yellow) which was subsequently used to raise the antibody against LeDMC1. Signals from pre-immune serum caused a uniform staining in cytoplasm and nuclei. Nuclei were counterstained with DAPI (blue).

To test the specificity of the obtained LeDMC1 rabbit antibodies Western blot analysis was performed. None of the tested recombinant antibodies could specifically recognize DMC1 protein in total protein extracts from leaves and anthers of *L. elegans*. However, detection of LeDMC1 recombinant protein (which we used for immunization) was successful (Fig. 24).

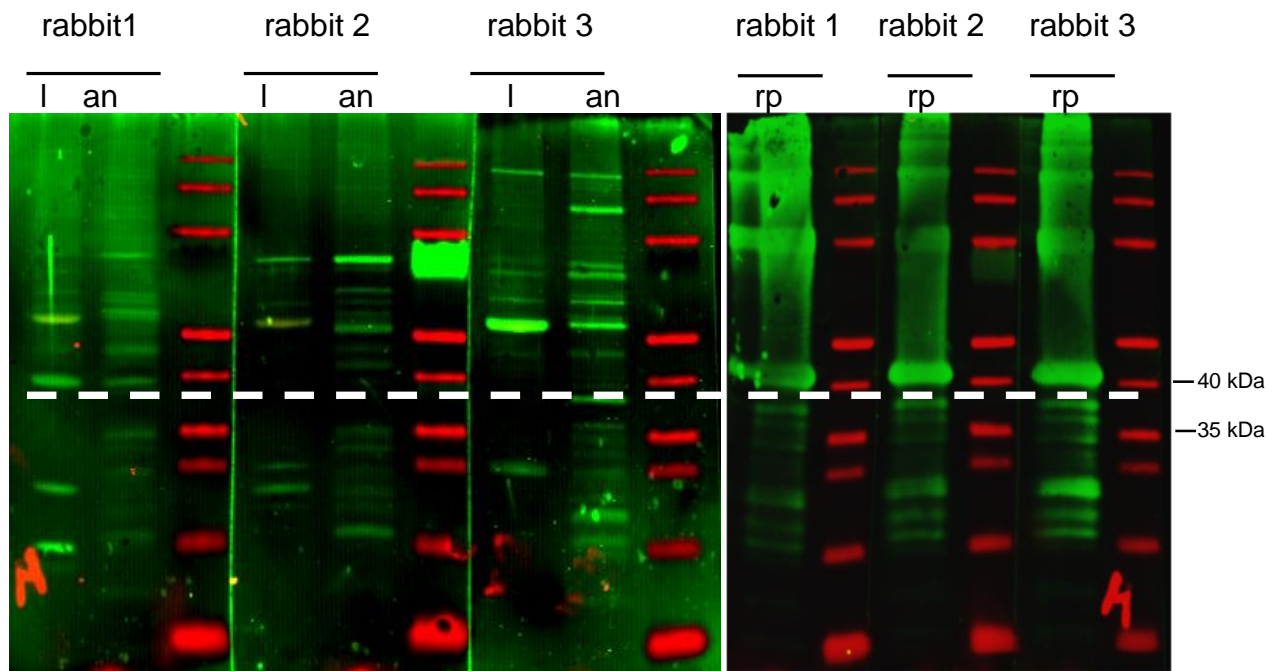


Fig. 24. Western blot analysis of LeDMC1 rabbit antibodies reveal multiple bands.

Three different LeDMC1 antisera (rabbit 1, rabbit2, rabbit3) were checked by Western-blot analysis for their specificity with total protein extract from leaves (l) and anthers (an) as well as with recombinant protein (rp). In green are bands caused by antisera and protein marker is in red. Lengths of the expected protein are indicated by a dotted line.

4.2.4. The dynamics of LeDMC1 protein during prophase I

To investigate whether the generated antibody recognize DMC1 on chromosomes, immunolocalization studies were carried out. DMC1 is a meiosis specific protein which interacts with DSBs (Bishop *et al.*, 1992b). As expected, DMC1 was absent on mitotic metaphase chromosomes while the CENH3 antibody successfully labelled mitotic chromosomes (Fig. 25a). LeDMC1 is initially detected in pollen mother cells during early leptotene as dispersed and numerous small foci (Fig. 25b). While prophase I progresses the signals gradually linearized as we observed in late leptotene (Fig. 25c) and zygotene (Fig. 25d). Interestingly, the linear pattern for DMC1 labelling is not found in other species (Sheridan *et al.*, 2008; Kurzbauer *et al.*, 2012). To confirm the specificity of generated antibody, the LeDMC1 antibody cross-reactivity was tested in rye. As expected, during the prophase I dot- like signals were randomly distributed through the total nuclear volume

(Fig. 25e). In contrast to the LeDMC1 pattern observed in *L. elegans*, lines have been never detected in prophase I of rye. Therefore we concluded that LeDMC1 line like pattern is typical for *L. elegans*.

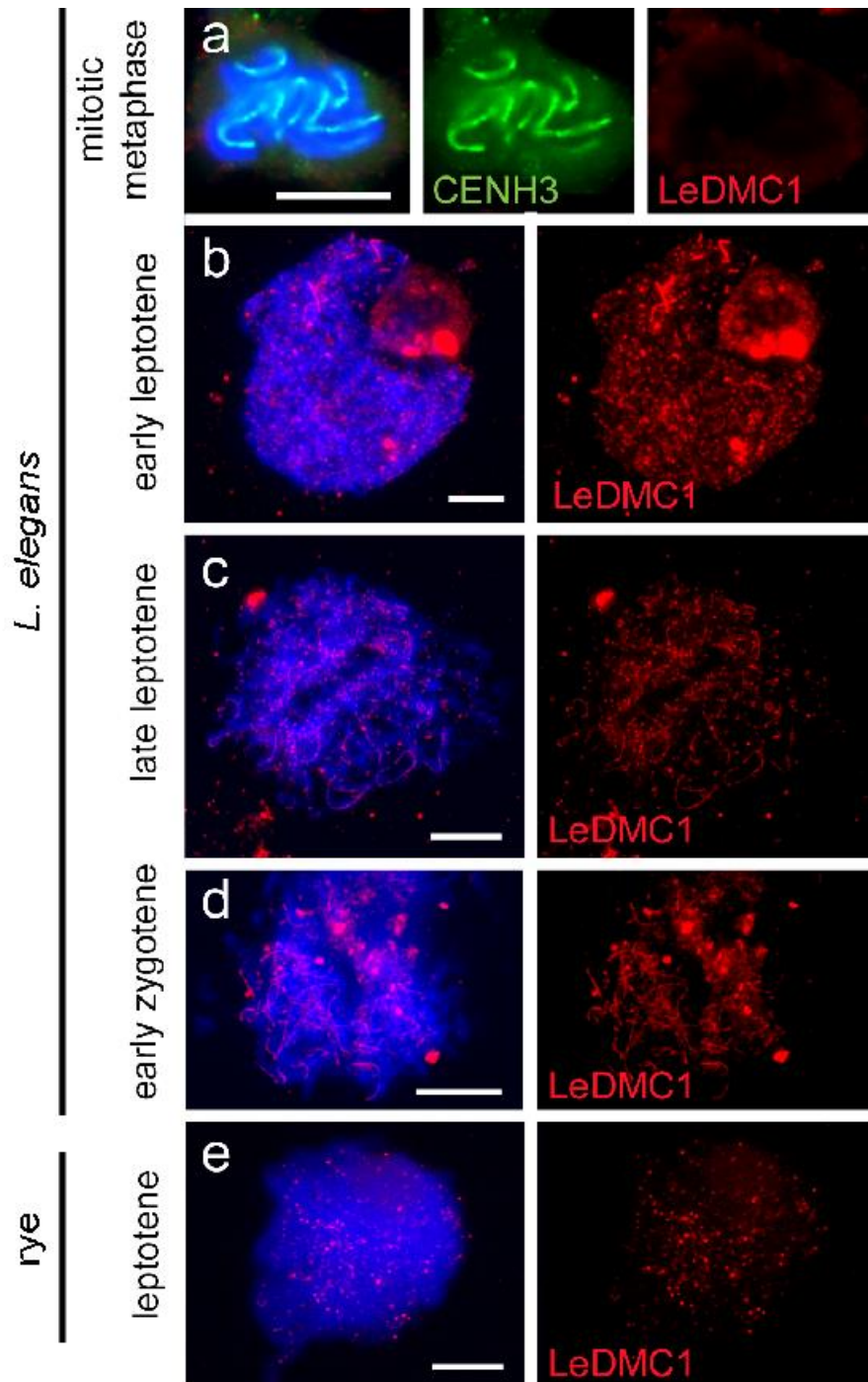


Fig. 25. Distribution of anti-LeDMC1-specific immunosignals.

a) mitotic metaphase, b) early leptotene, c) late leptotene d) early zygotene of *L. elegans* and e) leptotene of rye after immunodetection with CENH3 (green) and LeDMC1 (red). LeDMC1 is present only in meiotic cells, but labelling pattern differs between *L. elegans* and rye. Chromosomes were counterstained with DAPI (blue). Bars = 10 μ m.

4.2.5. LeDMC1 do not mediate the end-to-end connection between homologues in *L. elegans*

To figure out whether the end-to-end connections between homologues are recombination dependent immunostaining with anti-LeDMC1 was performed on meiotic metaphase I. In this stage LeDMC1 signals formed two parallel lines per homologous chromosomes which are colocalized with signals for CENH3 (Fig. 26). Clearly, LeDMC1 specific signal was absent in the end-to-end connection between homologous chromosomes. Thus, DMC1 is not involved in the end-to-end associations of meiotic non-sister chromatids.

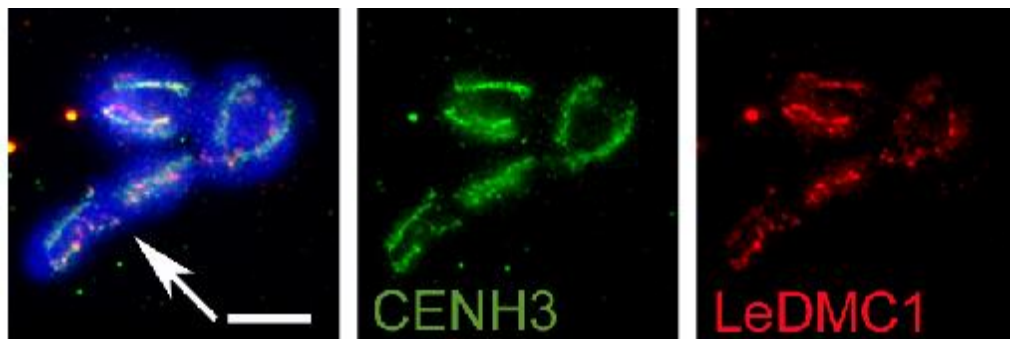


Fig. 26. LeDMC1 does not localize to the end-to-end association between homologues at metaphase I.

Meiotic metaphase I of *L. elegans* after immunodetection with CENH3 (green) and LeDMC1 (red). LeDMC1 signal colocalized with CENH3 signal forming two, parallel lines per homolog. The end-to-end connection between homologues chromosomes is free of both signals (arrow). Chromosomes were counterstained with DAPI (blue). Bars = 10 μ m.

4.3. Karyotype of holocentric species evolves rapidly due to holocentric centromere and efficient telomere healing

4.3.1. X-ray radiation induced dosage dependent chromosomal aberrations

To investigate the frequency of holocentric chromosome fragmentation after X-ray treatment *L. elegans* plantlets were irradiated with various dosages ranking from 10 to 30 Gy. In agreement with previous findings (Prakken, 1959; Li *et al.*, 2010) DNA double strand breaks occurred more frequently within increasing radiation dosage. The plant radiated with 10 Gy did not show any fragmentation and similar to non-irradiated plants possessed 3 equal in the size chromosome pairs. FISH with telomere and terminal satellite - LeSAT7 confirmed the absence of structural changes (Fig. 27a). In contrast, radiation dosage of 20, 25 and 30 Gy induced numerous chromosome breakages detectable already one day after irradiation. The most common number of chromosomes in the plant radiated with 20 Gy was $2n = 7$ (66%, $n = 61$). In this case five out of six chromosomes were unaffected whereas the sixth chromosome was fragmented into two pieces of different size. Additionally, in 18% of cells $2n = 6$ and in 16% $2n = 8$ chromosomes were counted in this plant. The most frequent chromosome complement in the plant irradiated with 25 Gy was $2n = 7$ (70%, $n = 50$), followed by $2n = 8$ (20%) and $2n = 6$ (10%). In the plant irradiated with 30 Gy cells with $2n = 9$ (54%, $n = 67$), $2n = 10$ (22%), $2n = 8$ (19%) and $2n = 11$ (5%) chromosomes were observed. Frequency of chromosome fragmentation in dependence of the radiation dosage is graphically presented on Fig. 27b. The size of the chromosomes/fragments varied from plant to plant and from cell to cell. Although usually small chromosome fragments were observed, in the plant radiated with 25 Gy additionally an extraordinary large chromosome was detected (Fig. 27c). The absence of interstitial telomere or LeSAT7 signals indicates that this chromosome might be a result of a translocation event combining two or more fragments.

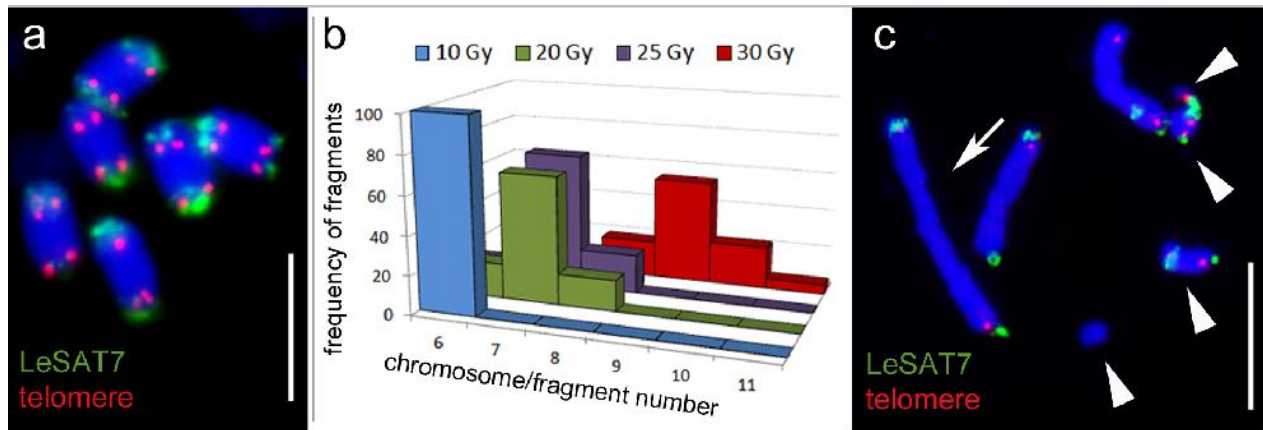


Fig. 27. X-radiation induces chromosome fragmentation in *L. elegans* (Jankowska et al., 2015).

a) Non-irradiated mitotic metaphase with three equally sized chromosome pairs after FISH with telomere (red) and terminal satellite repeat LeSAT7 (green). b) Chromosome fragmentation increase according to increasing irradiation dosage. The plant irradiated with 10 Gy did not show any fragmentation and possess 6 equal in size chromosomes. 7 was the most frequent chromosome/fragment pattern in plants irradiated with 20 Gy (66%, $n = 61$) and 25 Gy (70%, $n = 50$). The most frequent chromosome complement in the plant irradiated with 30 Gy was 9 (54%, $n = 67$). c) Mitotic metaphase of plant irradiated with 25 Gy possessing $2n = 7$ variable in size chromosome/fragments after FISH with telomere (red) and LeSAT7 (green). Arrowheads pointed chromosome fragments. The arrow indicated an unusually large chromosome. Chromosomes were counterstained with DAPI (blue). Bars = 10 μm .

4.3.2. Chromosome fragments have a holokinetic centromere and are stabilized by *de novo* formed telomeres

Next we asked whether the centromere structure differs between broken and unbroken chromosomes. Therefore, the centromeres activity was evaluated by immunostaining with CENH3- or histone H2AThr120ph- specific antibodies. Both antibodies cross-react only if the centromeres are functionally active (Allshire and Karpen, 2008; Kawashima *et al.*, 2010). Immuno-FISH on non-irradiated plants revealed an elongated H2AThr120ph signal alongside the centromere groove which ends before chromosome termini and is bordered by telomere (Fig. 28a). Interestingly, at metaphase chromosome telomeres localized not at the morphological chromosome termini probably due to chromosome termini are folded back. Terminal telomere localization by analysing extended pachytene chromosomes was confirmed (Fig. 28b). Chromosome fragments revealed a centromere groove (Fig. 28c)

and therein colocalized with elongated CENH3/H2AThr120ph signals like in the wild type chromosomes (Fig. 28d, e). The extraordinary long chromosomes observed in the plants radiated with 25 Gy have elongated centromeres along the entire chromosome length (Fig. 28e). No interstitial signal gap in the centromere labelling was found. In addition, the absence of anaphase bridges and micronuclei indicates that fragmented and translocated chromosomes properly segregated in somatic cells due to the activity of the holocentric chromosomes.

The presence of telomeres at both ends of chromosome fragments indicates telomere-based stabilization of the broken chromosome ends. To study in more detail chromosome healing FISH with telomere and subtelomeric- specific probe LeSAT7 on plants radiated with 20 Gy 7, 14 and 21 days after irradiation was performed. It was assumed that chromosome termini carrying both signals for telomere and LeSAT7 were the pre-existing chromosome ends, while LeSAT7- negative chromosome ends but at the same time exhibiting telomere signals were considered as ends with newly synthesized telomeres (Fig. 28f). 7 and 14 days after irradiation none of the examined chromosome fragments termini exhibit *de novo* synthesized telomeres. However, 21 days after irradiation 51% (n = 37) of examined chromosome termini possess newly formed telomere. The hybridization signals intensity differs significantly among newly formed telomeres (Fig. 28g). Small chromosome fragments carrying telomeres and LeSAT7 repeats on both ends, probably as a result of interstitial region deletion or due to translocation of fragmented chromosomes were also observed (Fig. 28h).

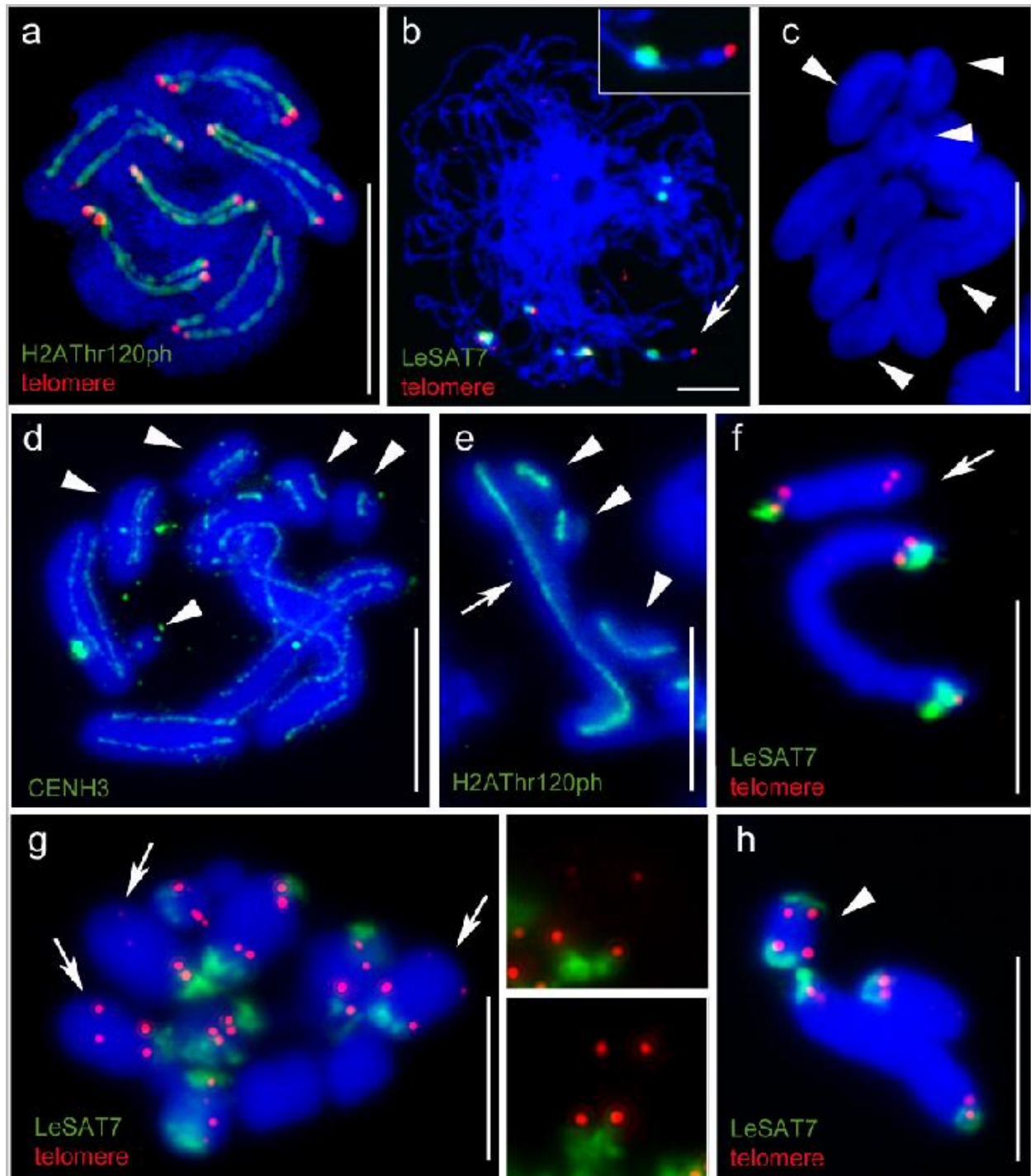


Fig. 28. Chromosome fragments of *L. elegans* possess holocentric centromere and are stabilized by *de novo* formed telomeres.

a) Non-irradiated mitotic metaphase chromosomes after double labelling with anti-H2A Thr120ph immunostaining (green) and FISH with telomere probe (red). The centromeres run along the entire chromosome length from telomere to telomere. Chromosomes were analysed by SIM (Jankowska *et al.*, 2015). b) Extended pachytene chromosomes labelled with LeSAT7 (green) and telomere specific probe (red) by FISH.

Inset and arrow show an enlarged chromosome end (Heckmann *et al.*, 2014). c) Irradiated mitotic metaphase chromosomes. Arrowheads indicate varied in size chromosome fragments with clearly visible groove like structure. Irradiated mitotic metaphase after immunolabelling with (d) anti-CENH3 (green) and (e) anti-H2Athr120ph (green). Both fragmented – (arrowhead) and translocated – (arrow) chromosomes possess active centromere. f) FISH with LeSAT7 (green) and telomere (red) enables to distinguish pre-existing telomere (signal for both probes) from newly formed telomere (signal only for telomere, arrow). g) Arrows and enlargements pointed difference in signal intensity between newly synthesized telomeres. h) Small chromosome fragment possessing pre-existing telomere at the both termini (arrowhead) (Jankowska *et al.*, 2015). Chromosomes were counterstained with DAPI (blue). Bars = 10 μ m.

Three months after radiation, when plants enter meiosis the signal intensity of newly formed telomeres with the pre-existing one of the same chromosome fragment were compared. In 70% (n = 69) hybridization intensity of newly formed telomeres was much weaker than those of the pre-existing one. There were no a significant difference between 'new' and 'old' telomere in 17%. Interestingly, in 9% of cases newly formed telomeres exhibit even stronger telomere signal than the 'old' ones. *De novo* telomere synthesis in 4% of analyzed chromosome fragments was not noticed.

To test whether the newly formed telomeres may be the product of an active telomerase in cooperation with Dr Miloslava Fojtová (Masaryk University, Brno) a PCR-based TRAP assay which allowed the detection of telomerase activity *in vitro* was performed. As shown in Fig. 29, using the TRAP-polyacrylamide gel electrophoresis (TRAP-PRGE) assay, regular hexanucleotide ladder of PCR products detected in both *L. elegans* tissues show the same periodicity as in *A. thaliana* sample which was used as a positive control. Thus, we assumed presence of telomerase in extracts isolated from *L. elegans* seedlings and flower buds. This observation indicates that *de novo* synthesized telomeres observed in somatic and generative cells are potentially the result of a telomerase-based healing mechanism.

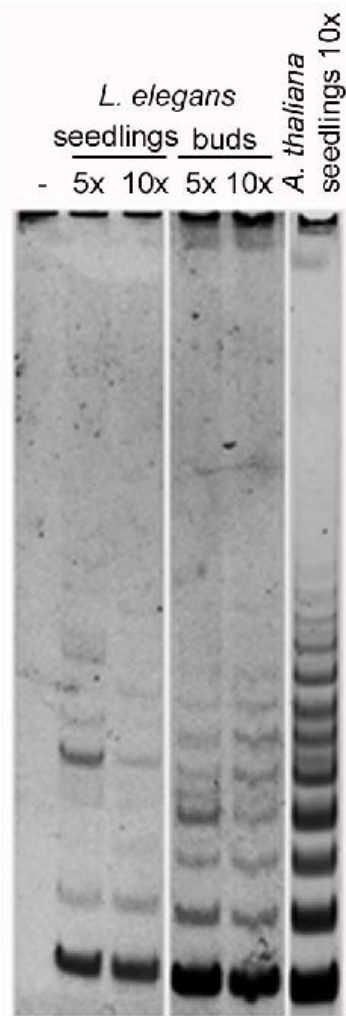


Fig. 29. TRAP assay revealed telomerase activity in seedlings and flower buds of *L. elegans* (Jankowska et al., 2015).

Seedlings and flower buds of *L. elegans* are shown to be positive for telomerase activity, as evidence by the 6-bp incremental TRAP ladder. *L. elegans* total protein extracts from seedlings and flower buds were analyzed in two dilutions 5x and 10x. *A. thaliana* seedlings extract in 10x dilutions was used as a positive control. -) negative control (no extract in the reaction).

Although semi-quantitative analysis of TRAP products exhibited detectable levels of telomerase in extracts isolated from *L. elegans* seedlings and flower buds, the intensity of *L. elegans* TRAP leaders were much weaker in comparison to those of *A. thaliana*. The traditional TRAP quantification can be limited because the PCR amplification efficiency may be inhibited by the proteins in the cell extract. In the next step a control-RTQ-TRAP

assay which is more precise than the conventional TRAP assay was performed (Hou *et al.*, 2001). This assay allowed to verify whether extracts coming from *L. elegans* seedlings and flower buds possess proteins and/or other components inhibiting TRAP reaction. The PCR Ct-values of all analyzed *L. elegans* and *A. thaliana* samples were in similar range indicating the absence of inhibitor factor in both *L. elegans* tissues (Fig. 30a).

To figure out whether irradiation induced a change in telomerase activity a RTQ-TRAP assay was performed. Telomerase activity in non-irradiated *L. elegans* seedlings were compared with seedlings 1, 7, 14 and 21 days after irradiation. It was demonstrated that the Ct values of non-irradiated seedlings and seedlings at different time points after irradiation do not show significant differences (Fig. 30b) pointed to no detectable telomerase activity change after irradiation. Additionally RTQ-TRAP revealed a similar telomerase activity among *L. elegans* seedlings and flower buds. Interestingly, the telomerase activity of *A. thaliana* samples, which were used as a positive control, is significantly much higher than in all *L. elegans* investigated samples (Fig. 30b).

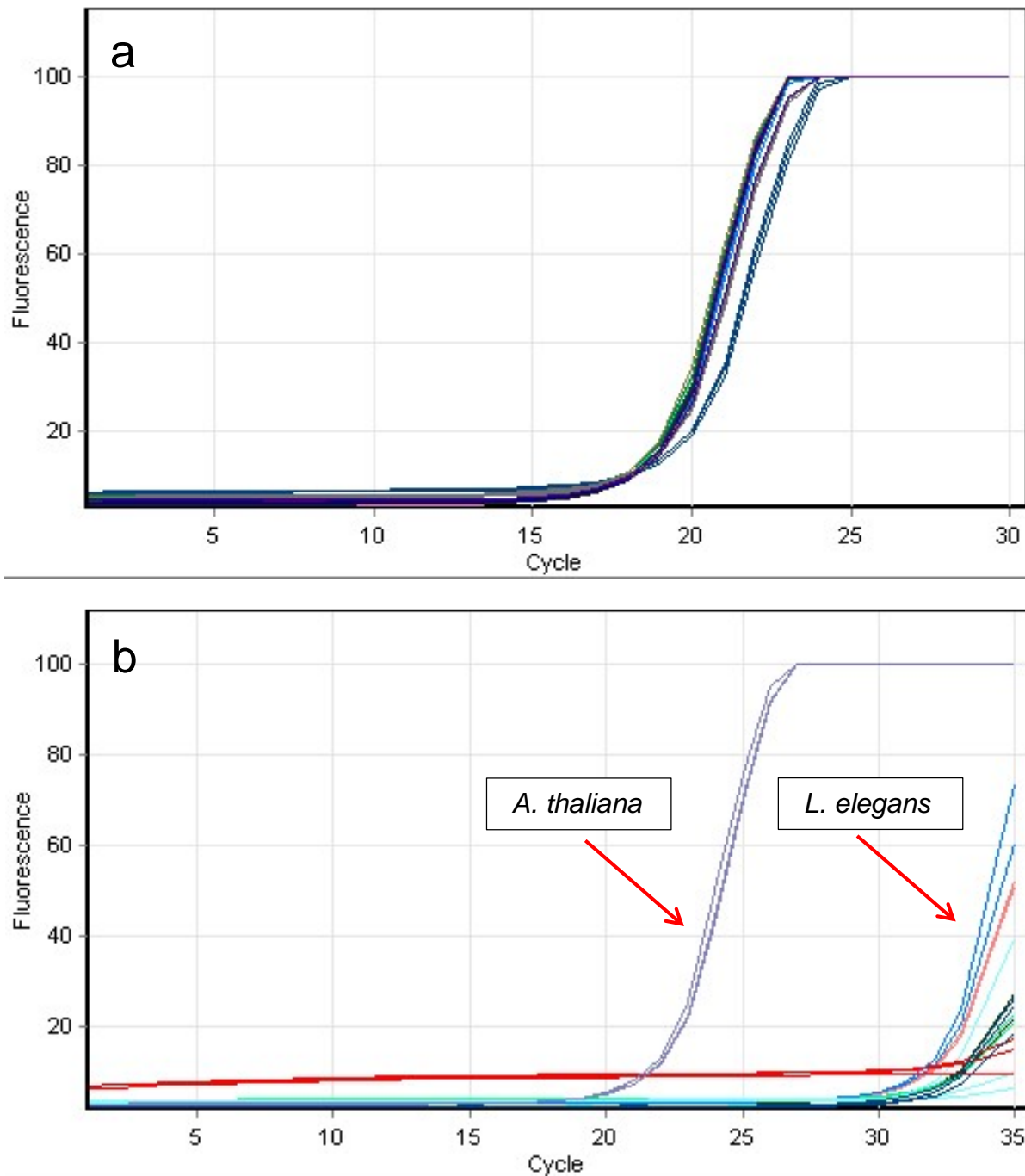


Fig. 30. Determination of inhibitor factors and telomerase activity in different irradiated and non-irradiated *L. elegans* samples by the RTQ-TRAP assay.

a) The cellular protein extracts from *L. elegans* seedlings and flower buds were tested for inhibitor factors using control-RTQ-TRAP assay. Ct values of *A. thaliana* used as a control and *L. elegans* samples are similar pointed lack of inhibitors in *L. elegans* tissue. b) RTQ-TRAP assessment of telomerase activity in irradiated and non-irradiated *L. elegans* seedlings shows no significant different between samples in Ct values indicating no

telomerase activity change after irradiation. Telomerase activity in *L. elegans* seedlings and flowers buds is similar demonstrated by no significant difference in Ct value between tissues. Note, telomerase activity in *A. thaliana* is significantly much higher than in *L. elegans* tissue shows by Ct values diversity. All samples were analyzed in triplicates. ■ - non-irradiated seedlings of *L. elegans*; ■ - *L. elegans* seedlings one day after irradiation; ■ - *L. elegans* seedlings seven days after irradiation; ■ - *L. elegans* seedlings 14 days after irradiation; ■ - *L. elegans* seedlings 21 days after irradiation; ■ - flower buds of *L. elegans*; ■ - *A. thaliana*; ■ - negative control.

4.3.3. Holocentric fragments are successfully transmitted across several generations

To assay whether radiation has an impact on the meiotic chromosome behavior the segregation dynamics of irradiated *L. elegans* plants was analyzed. During zygotene we observed a bouquet-like configuration due to telomere clustering in radiated (Fig. 31a) and non-irradiated plants (Fig. 7g). During pro-metaphase I multivalent (multi-rings and multi-rods) configurations interconnected by terminal satellite repeats were detected (Fig. 31b) in contrast to non-irradiated plants where only rod-, ring- and cruciform- like bivalents were present (Fig. 9b, c, d). In addition, chromosomes with interstitial position of terminal satellite probably as a result of translocation event could be observed (Fig. 31c).

Next, to investigate whether fragments are properly transmitted to the next generation, the DNA content of M1 progeny plants of the plant irradiated with 20 Gy were measured. 19 out of 20 examined M1 plants revealed a genome size comparable to non-irradiated plant ($\pm 1.5\%$) indicating a proper segregation of chromosomes and fragments. FISH analysis confirmed fragments presence in the progeny plants. As shown in Fig. 31d five chromosomes were of standard size and two chromosome fragments of about half of the chromosome size were present. All chromosome fragments in the self-progeny of the irradiated plant possessed telomeres at their newly formed chromosome termini (Fig. 31d). 1 out of 20 examined M1 plants had a 7% bigger genome content compare to non-irradiated plants. Chromosome analysis of this plant in pro-metaphase I showed three bivalents of a standard size and three, different in size chromosome fragments (Fig. 31e). The corresponding tetrads exhibited an unequal number of FISH signals for telomeres and LeSAT7 revealed an unequal fragments distribution to the daughter cells. In 20% of

100 examined tetrads one to three micronuclei were present (Fig 31f). The DNA content of the resulting M2 progeny plants ranged from 7.74 pg/2C (-0.76%) to 8.87 pg/2C (+14%) compared to 7.80 pg/2C of non-irradiated plants. The different DNA content of M2 plants correlated with the number and size of chromosomes and fragments. The various M2 karyotypes reflected a combination of fragments found in the M1 plant. Plants possessing 3.35%, 6.46% and 11.03% bigger genomes harbored chromosome complements with $2n = 6 + 2$ small fragments, $2n = 6 + 2$ big + 2 small fragments and $2n = 7 + 1$ small fragment, respectively (Fig. 31g, h, i) indicating a stable transmission of fragments independent of their size. Despite this severe variation in DNA content and karyotype constitution, no obvious phenotypic differences could be observed.

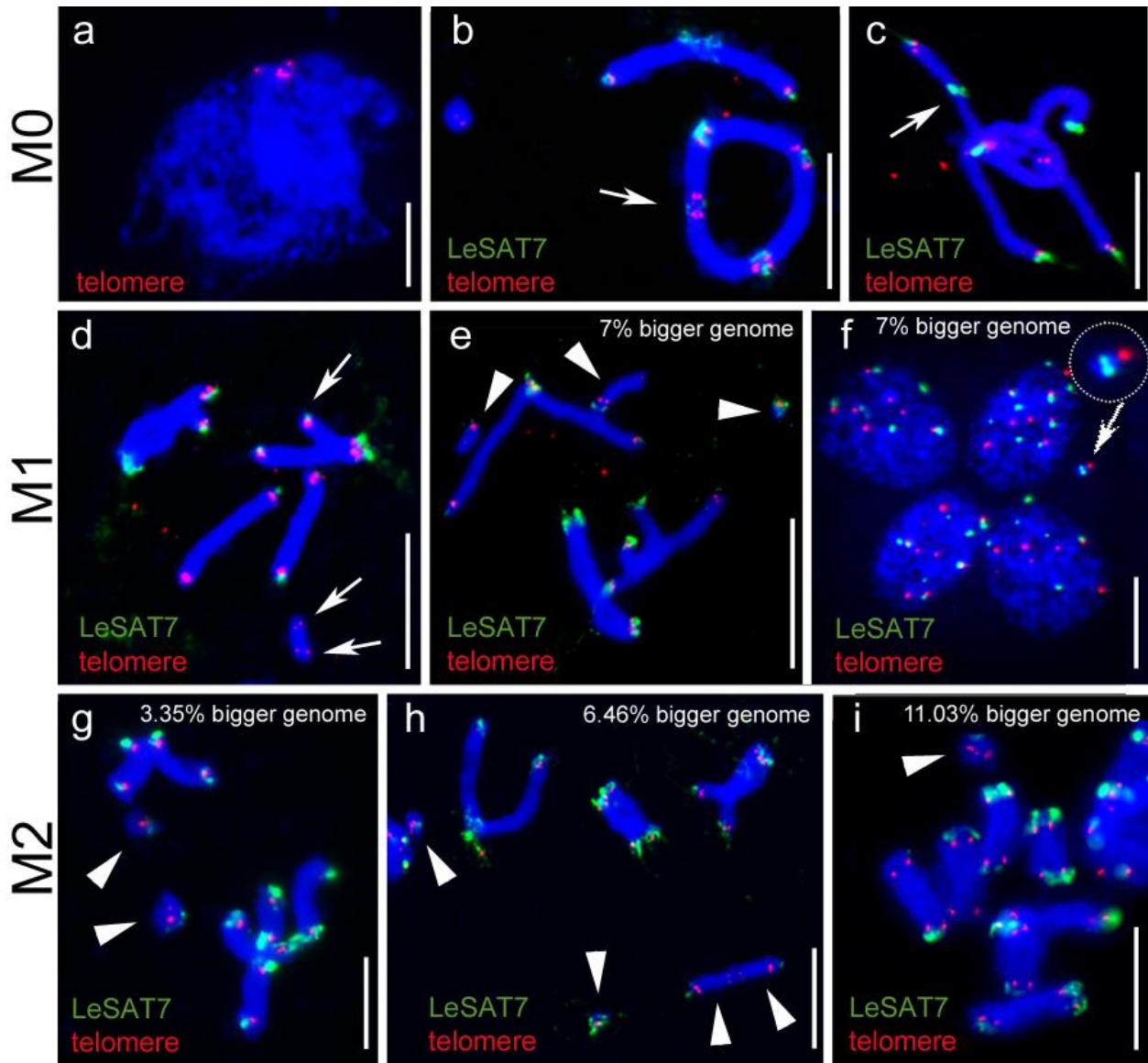
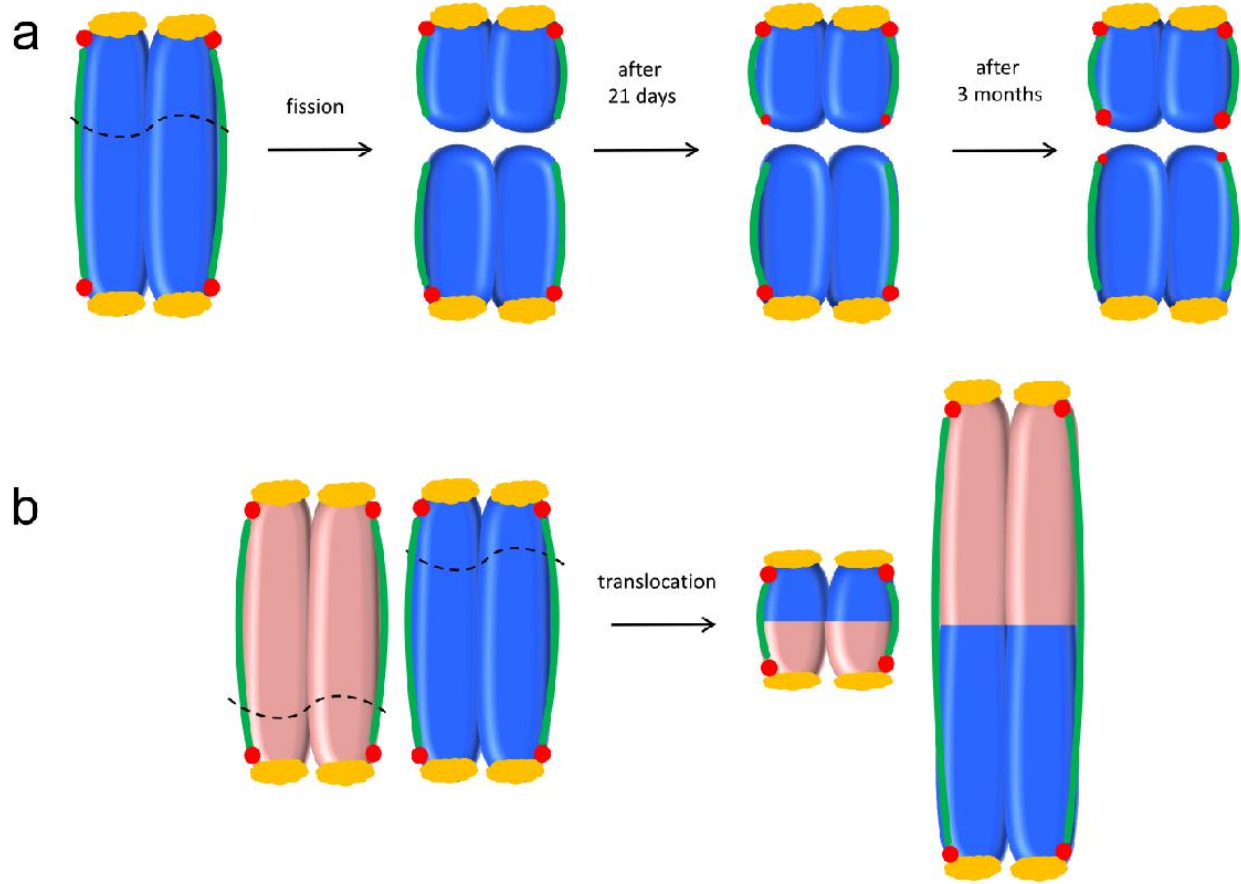


Fig. 31. Holocentric fragments are stably transmitted to the next generations (Jankowska *et al.*, 2015).

a) Telomeres clustering in a bouquet configuration during zygotene is not impaired by the radiation, b) irradiation causes multivalent configuration formation during pro-metaphase I (arrow). c) A translocation event caused by irradiation is indicated by the interstitial localization of the terminal satellite LeSAT7 (arrow). d) Chromosome fragments are stably transmitted to the M1 progeny plants as indicated by the somatic metaphase plate with 5 standard in size chromosomes and two fragments of about half of the chromosome size ($2n = 7$) and the genome content comparable to the non-irradiated plants. Note, all chromosome fragments possess new telomere repeats at the break points (arrows). e) Pro-metaphase plate of the M1 progeny plant with 7% bigger genome content revealed three bivalents and three, different in size chromosome fragments (arrowheads). f) In the tetrads of corresponding mutant micronuclei are present (arrow and insert). g, h, i) M2 offspring of M1 with 7% bigger genome content exhibit different combination of fragments

(arrowhead) occurring in the mother plant. Number and size of fragments correlate with the estimated genome size: $2n = 6 + 2$ small fragments (3.4% enlarged genome), $2n = 6 + 2$ big + 2 small fragments (6.5% enlarged genome) and $2n = 7 + 1$ small fragment (11.0% enlarged genome). FISH with the terminal satellite LeSAT7 and the telomere repeat. Chromatin was counterstained with DAPI (blue). Bars = 10 μm .

In summary, we demonstrated that the combination of holokinetic centromeres and the rapid formation of new telomeres at the break points enable chromosome fragments to be properly transmitted across several generations. Thus, holocentric species are characterized by a rapid karyotype evolution involving chromosome fragmentation (Fig. 32a) and translocation (Fig. 32b).



chromosome / fragment, centromere, telomere, subtelomeric satellite

Fig. 32. Model illustrating possible ways of holocentric karyotype evolution based on the interplay between holokinetic centromeres and rapid telomere healing (Jankowska *et al.*, 2015).

Irradiation induces chromosome fragmentation. Fragments are of different size and have a centromere activity (green). Break points are labelled by black, dotted lines. a) Broken ends are negative for a terminal satellite repeats (yellow) and are gradually healed by *de novo* telomere formation (red). b) Translocation between chromosomes (blue/orange) form different in size fragments which are stabilized by pre-existing telomere.

5. Discussion

5.1. *L. elegans* performs an inverted meiosis

5.1.1. Prophase I is conserved in *Luzula* species

Based on the distribution of Asy1 and Zyp1 immunolabelling pattern we could confirm the presence of axial elements and SCs in *L. elegans* similar to that found in holocentric *C. elegans* (Colaiacovo *et al.*, 2003; Nabeshima *et al.*, 2005), *Pyrrhocoris apterus*, *Graphosoma italicum* (Suja *et al.*, 2000), *R. pubera* (Cabral *et al.*, 2014), in the autosome chromosomes of heteropteran species (Suja *et al.*, 2000) and various monocentric species (Armstrong *et al.*, 2002; Higgins *et al.*, 2005; Sanchez-Moran *et al.*, 2008). In contrast to *C. elegans* (Phillips and Dernburg, 2006) clustering of *Arabidopsis*-type telomeres and the subterminal region (e.g. LeSAT7) in one nuclear hemisphere forming a bouquet like configuration was observed in both *L. elegans* and *L. luzuloides*, like in many species with monocentric chromosomes (Scherthan, 2001; Bass, 2003; Loidl *et al.*, 2012; Tiang *et al.*, 2012). The presence of axial elements, SCs and the zygotene- typical bouquet- like configuration during prophase I in *L. elegans* and *L. luzuloides* provided evidence that early meiotic events until the onset of metaphase I are conserved in *Luzula*.

5.1.2. *L. elegans* exhibits a restricted crossover frequency and localization

In agreement with previous reports for *L. elegans* (Nordenskiöld, 1962) during early metaphase I two dominant bivalent types i.e. rod and ring like configurations, as a result of one or two terminal crossover, respectively were observed. In addition, other holocentric species like *C. elegans* (Barnes *et al.*, 1995), *R. pubera* (Cabral *et al.*, 2014) or *Triatoma infestans* (Perez *et al.*, 1997) usually show a limited crossover frequency to one or two per homologue which are mostly present at the distal chromosome region (Fig. 33) (Halkka, 1964; White, 1973; Nokkala *et al.*, 2004). Sporadic crossovers in interstitial regions of *L. elegans* are manifested by the occasional occurrence of cruciform-like bivalents. Similar, monocentric species undergo usually limited recombination events per homolog which are in general excluded from centromeric and pericentromeric regions (Schnable *et al.*, 1998; Gerton *et al.*, 2000; Borde *et al.*, 2004; Phillips *et al.*, 2013).

Therefore, precise control of crossover frequency and localization seems to be common feature independent of the centromere type.

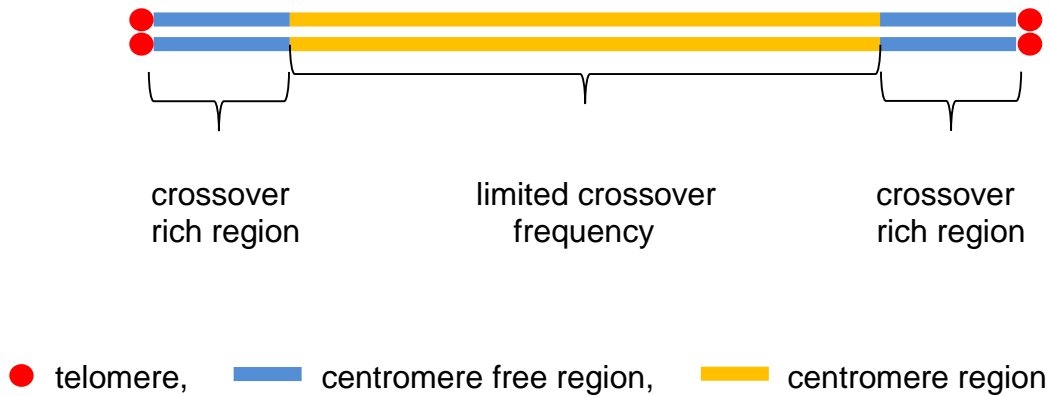


Fig. 33. Model illustrating crossover distribution along a holocentric chromosome.

In holocentric chromosomes crossover occurs preferentially at the terminal chromosome region and is mainly excluded from the centromere region.

5.1.3. Centromeres of *L. elegans* are holocentric during the entire meiotic division

Immunolabelling with the centromere-specific markers CENH3, H2AThr120phos and α -tubulin antibodies demonstrated that the chromosomes of *L. elegans* are holocentric during the first and second meiosis division. Each sister chromatid revealed a longitudinal centromere which like in mitosis interacts with spindle microtubules (Nagaki *et al.*, 2005; Heckmann *et al.*, 2011). In contrast, spindle microtubules of *C. elegans* (Monen *et al.*, 2005; Nabeshima *et al.*, 2005; Dumont *et al.*, 2010), *Heteroptera* (Hughes-Schrader and Schrader, 1961; Perez *et al.*, 2000; Viera *et al.*, 2009) and *Parascaris* (Pimpinelli and Goday, 1989) attach to a restricted kinetochore region at the chromosome termini. Hence, chromosomes exhibit a telokinetic-like behavior during meiosis. These data underline striking differences in the kinetochore geometry during meiosis between holocentric species.

Our results clearly demonstrated four, elongated centromeres per bivalent in *L. elegans*, each representing a centromere per single chromatid. This observation indicates the absence of sister chromatid centromeres cohesion during meiosis I which is different to the situation present in monocentric species (Kerrebrock *et al.*, 1995; Sakuno and Watanabe, 2009; Nogueira *et al.*, 2014). Indeed, the genes of monopolin complex – the kinetochore proteins required for sister centromere fusion in monocentric species (Toth *et al.*, 2000; Rabitsch *et al.*, 2003) are not detectable in the pollen mother cell transcriptome of *L. elegans* (Jankowska, unpublished). Interestingly, in species with monocentric chromosomes, mutations in genes involved in kinetochore fusion such as MIS12 (Li and Dawe, 2009) or REC8 (Watanabe and Nurse, 1999; Shao *et al.*, 2011) and genes involved in protection of centromere fusions such as Shugoshin (Cromer *et al.*, 2013; Zamariola *et al.*, 2014) cause unfused centromeres during meiosis I and premature division of sister chromatids. Since REC8 and Shugoshin-like genes are detectable in the *L. elegans* meiotic transcriptome (Jankowska and Ma, unpublished), we suspect that the fusion of sister centromeres during meiosis I is likely prevented due to the groove-like structure of the holocentromeres. It is known that sister centromere fusion plays an essential role in co-orientation of sister chromatids and allows the two-step release of sister chromatid cohesion in monocentric species (Nasmyth, 2001; Sakuno and Watanabe, 2009; Sakuno *et al.*, 2011). Thus, as an adaptation to holocentricity, *L. elegans* needs to follow an alternative process of meiotic division.

5.1.4. An inverted sequence of meiotic sister chromatid segregation in *L. elegans*

Through visualization of centromere specific proteins and microtubules during meiosis we confirmed the previously assumed inverted order of meiotic divisions in *L. elegans* (Malheiros *et al.*, 1947; Kusanagi, 1962; Nordenskiöld, 1962; Nordenskiöld, 1963; Kusanagi, 1973). During metaphase I, bivalents are oriented perpendicular to the spindle microtubules. Non-fused sister centromeres reveal a bipolar orientation and are attached to microtubules from opposite spindle poles. Subsequently, during anaphase I sister chromatids separated to opposite cells poles and non-sister chromatids, end-to-end connected, migrated to the same pole (equational division). After degradation of the end-

to-end association of homologues, non-sister chromatids segregated to daughter cells during second meiosis division (reductional division).

To confirm the occurrence of inverted meiosis, x-ray induced chromosome fragments of *L. elegans* were included in the study of meiosis. Random fragmentation of *Luzula* chromosomes caused by x-ray irradiation has been already successfully performed in the past (Nordenskiöld, 1962; Nordenskiöld, 1963; Nordenskiöld, 1964). Breakage of chromosomes allowed distinguishing of homologs and therefore of sisters and non-sisters chromatids during meiosis. Large chromosome fragments formed an end-to-end connection with their broken homologues. During anaphase I, end-to-end connected chromatids of different length migrated to the same cell pole illustrating that at meiosis I sister chromatids are separated and not homologues. Thus, in *L. elegans* the inverted sequence of chromatid segregation occurred in contrast to the typical sequence observed in monocentric species (John, 1990). Inverted meiosis has been previously indicated also in other holocentric plants like *L. campestris* (Nordenskiöld, 1961) *R. pubera* and *R. tenuis* (Cabral *et al.*, 2014), *Cuscuta babylonica* (Pazy and Plitmann, 1987), *Cuscuta approximate* (Guerra and Garcia, 2004) *E. subarticulata* (Da Silva *et al.*, 2005) and in animals, like mealybug (Hemiptera), some dragonflies and arachnids (Chandra, 1962; Bongiorno *et al.*, 2004; Viera *et al.*, 2009). Interestingly, genotyping using around 300.000 genetic markers, human polar bodies and oocytes showed frequently occurring reversed order of monocentric chromatid segregation during female meiosis (Ottolini *et al.*, 2015) resembling this of *L. elegans*. Therefore, both holocentric and monocentric chromosomes can undergo remarkable changes in the process of canonical meiotic division.

5.1.5. Heterochromatin fibers connect homologous non-sister chromatids

During metaphase I we observed in *L. elegans*, two thin chromatin threads representing an end-to-end association between homologues chromosomes. Interestingly, this connection persists till the second meiosis division where homologous non-sister chromatids were connected by one fiber. Such fibers have been also observed in holocentric species *R. pubera* and *R. tenuis* (Cabral *et al.*, 2014). In contrast to meiosis, we did not find such connections in mitotic chromosomes of *L. elegans*, like it was also

not present in *R. pubera* and *R. tenuis* (Cabral *et al.*, 2014), *L. nivea* (Bokhari and Godward, 1980), *Oncopeltus* (Comings and Okada, 1972) nor in *G. italicum* (GonzalezGarcia *et al.*, 1996). Interestingly, during mitosis in monocentric chaffinch, the interchromosomal fibers, rich in highly repeated centromere sequences connect centromeres of different chromosomes and therefore are probably involved in the maintenance of nuclear architecture (Saifitdinova *et al.*, 2000; Saifitdinova *et al.*, 2001). Although, the nature, composition and regulation of meiotic end-to-end association are unknown, it is tempting to speculate that the sticky threads are necessary components for successful inverted meiosis of holocentric chromosomes.

Different to monocentric species (Watanabe, 2004), in *L. elegans*, *R. pubera* and *R. tenuis* (Cabral *et al.*, 2014) and in mealybugs (Bongiorni *et al.*, 2004) sister chromatid cohesion seems to be released in one step along the entire chromatid length before anaphase I. However, terminal chromatid segments might not lose their cohesion thereby the region between homologous chromatids can be held together by remnants of sister chromatid cohesion. A two-step loss of cohesion was observed in holocentric *C. elegans*. In this case, crossover divided bivalents into two subunits (long and short arms) which harbor a distinct complement of proteins (Schwarzstein *et al.*, 2010). During meiosis I cohesion is released only between short arms and afterwards during meiosis II it is also lost between the long arms (Kaitna *et al.*, 2002; Rogers *et al.*, 2002; Nabeshima *et al.*, 2005; Schwarzstein *et al.*, 2010). If the end-to-end association in *L. elegans* is recombination dependent, it can be speculated that, crossover would divide chromosomes into two subunits (long segment and short, involved in the end-to-end connection of segments) and subsequently each of them would obtain a different set of cohesion proteins (Fig. 34a, b). Possibly, during meiosis I cohesion might be released along long segments enabling sister chromatids segregation and at the same time can be retained in the short segment mediating end-to-end connection between homologs (Fig. 34c, d). Subsequently, during meiosis II cohesion could be released from end-to-end connection (Fig. 34e) allowing homologous non-sister chromatid segregation (Fig. 34f). Thereby, contrary to current assumptions a mechanism of two-step loss of cohesion might also work in *L. elegans*.

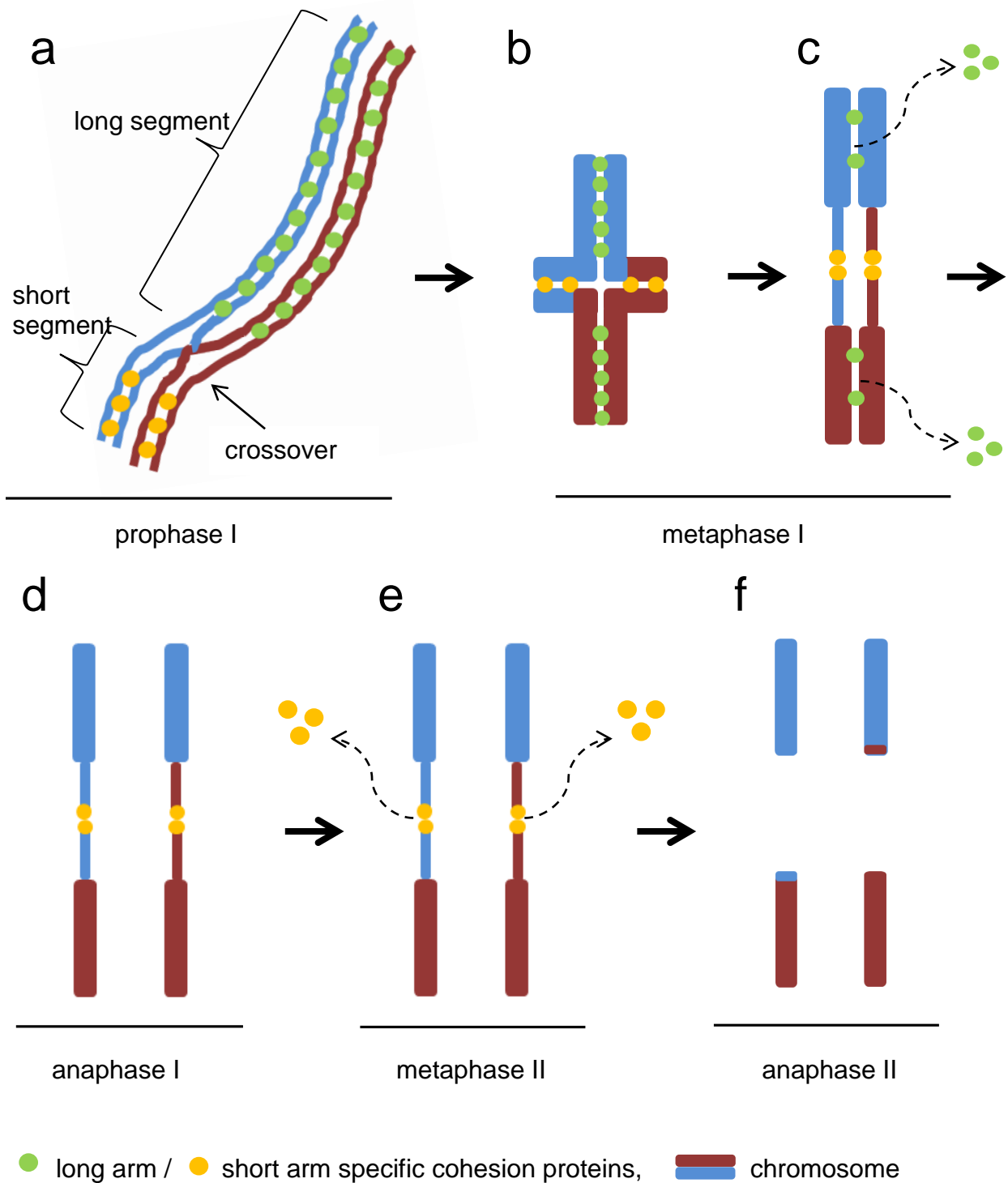


Fig. 34. Crossover-triggered differentiation of bivalent subdomains dictates chromosome organization and behavior during meiosis.

a) Different cohesion proteins become localized in a crossover-dependent manner between sister chromatids of the short and long chromosome segments during prophase

I. b) Homologous chromosome pair undergoes reorganization into a cruciform bivalent configuration at metaphase I. c) Cohesion along long segments is released and at the same time is retained in the short segments, mediating an end-to-end association between homologs. d) Sister chromatid segregated during anaphase I. e) Proteins involved in the end-to-end connection are released during metaphase II and f) homologous non-sister chromatids segregate to the daughter cells during anaphase II.

Presence of axial elements, synaptonemal complex and bouquet-like configuration suggest that crossovers might be established along the whole chromosome length in *L. elegans*. Until anaphase I all interstitial chiasmata can be resolved like in monocentrics (John, 1990) and only terminal chiasmata last, connecting homologous chromosomes. Depending on whether one or two terminal chiasmata persist rod- or ring-like configurations can be observed, respectively. Rarely interstitial chiasmata are not resolved what causes a cruciform bivalent formation. Cruciform bivalents, as a result of one, interstitial crossover are usually present in *C. elegans* (Barnes *et al.*, 1995; Meneely *et al.*, 2002; Phillips and Dernburg, 2006; Wignall and Villeneuve, 2009; Dumont *et al.*, 2010). On the other hand, recombination might occur preferentially in terminal, centromere free regions of the chromosomes as observed in monocentric species, where the centromere is a region with reduced crossover frequency (Schnable *et al.*, 1998; Gerton *et al.*, 2000; Borde *et al.*, 2004; Higgins *et al.*, 2012; Yelina *et al.*, 2012). It seems to be a common phenomenon in *L. elegans* and in other holocentric species, e.g. *L. nivea* (Nagaki *et al.*, 2005) and *C. elegans* (Buchwitz *et al.*, 1999; Moore *et al.*, 1999) that terminal chromosome regions are free of centromere activity. Thus, one can speculate that in holocentric species and in monocentric ones crossovers preferentially take place in non-centromeric regions.

Another possibility for the origin of end-to-end associations between homologous chromosomes is based on an achiasmatic mechanism. Chromosomes of *R. tenuis* do not undergo recombination during meiosis. Nevertheless homologous non-sister chromatids are held together by thin chromatin threads (Cabral *et al.*, 2014). Interestingly, in monocentric *Drosophila melanogaster* oocytes the 4th chromosomes are always non-exchanged but connected via elastic, heterochromatin tether (Dernburg *et al.*, 1996; Hughes *et al.*, 2009). Similarly, FISH with different terminal satellite repeats revealed that

these repetitive sequences localize to the chromatin threads underlining the heterochromatic character of the fibers in *L. elegans*. In contrast to monocentrics where heterochromatin and high copy repeats are mostly clustered at centromere region and various other sites (Schmidt and Heslop-Harrison, 1998; Mola and Papeschi, 2006; Lamb *et al.*, 2007), terminal localization of heterochromatin seems to be a common feature in holocentric plants (Sheikh and Kondo, 1995; Vanzela and Guerra, 2000; Guerra and Garcia, 2004; Heckmann *et al.*, 2013) and animals (Tartarotti and de Azeredo-Oliveira, 1999; Mola and Papeschi, 2006; Hill *et al.*, 2009). Comparative FISH analyses of the end-to-end connection of rod bivalents in *S. cereale* and *H. vulgare* revealed in contrast to *L. elegans* only one heterochromatin fiber per one end-to-end connection during metaphase I. It is likely that one fiber is the result of a physical connection between homologous non-sisters chromatids established via proteins involved in chiasmata resolution thus, implying that the end-to-end connections in monocentrics are recombination dependent.

In addition, heterochromatin fibers connecting two or more bivalents were observed in rye (Gonzalez-Garcia *et al.*, 2006). Such associations could be a result of ectopic recombination where crossovers would take place between homologous sequences (e.g. subtelomeric heterochromatin) of different bivalents. Our obtained data suggest that holocentric and also some monocentric species can use different strategies to mediate the end-to-end association between homologs, although in both cases satellite repeats are involved.

5.1.6. Chromosome end looping is likely important for telomere protection as well as to establish an end-to-end connection between homologs

By applying FISH with probes to detect *Arabidopsis*-type telomere and terminal satellite repeats on metaphase I chromosomes both in holocentric *L. elegans* and monocentric *S. cereale* and *H. vulgare*, we demonstrated that heterochromatin fibers run always between telomeres of homologs, similar to the observations obtained with spermatocytes of crane-fly (LaFountain *et al.*, 2002). As the telomere in *L. elegans* during prophase I are mapped at the extreme chromosome ends, distal from terminal satellite repeats, it seems that chromosome ends fold back during the process of chromosome condensation. Similar

observations have been reported in rye (Gonzalez-Garcia *et al.*, 2006) as well as in budding yeast (Poschke *et al.*, 2012), tomato (Zhong *et al.*, 1998), pea, field bean (Rawlins *et al.*, 1991) and grasshoppers (Suja and Rufas, 1994). The mechanism of chromosome end looping is unknown, although it is tempting to speculate that telomeres could be looped into the protein rich ends of the chromosome axis, so-called telochores. Chromosome axes, do not reach the chromosome termini, and are surrounded by radial-loop arrangement chromatin (Suja and Rufas, 1994). In *L. elegans* from late prophase I to telophase II telomeres are attached to the termini of the centromere. Unpublished data (Wei Ma, personal communication) indicated that the cohesion complex Rad21 colocalizes with the centromere during meiosis favoring the hypothesis that telomeres in *L. elegans* might interact with cohesion proteins localized in the centromere. Interestingly, during meiosis in grasshoppers it was observed that a subunit of the SCC3 cohesion complex- SA1 (homolog Rad21) is accumulated both at the centromere region and at telochores (Calvente *et al.*, 2013). Furthermore, in contrast to other cohesion complexes, the SA1 subunit is established at zygotene and persists until telophase II (Valdeolmillos *et al.*, 2007; Calvente *et al.*, 2013) exactly when chromosome ends looping takes place in *L. elegans*. Additionally, the presence of SA1 has been described in telomeres of human HeLa cells and a possible interaction of this cohesion subunit with telomeric proteins, such as TIN1 and TRF1, has been suggested (Canudas and Smith, 2009). Likewise, the SMC1 β cohesion complex is crucial for telomere structure and meiotic function in mammalian cells (Adelfalk *et al.*, 2009). Therefore, we suspect that the telomeres of *L. elegans* are looped to reach telochores cohesion proteins which border centromeres. The subterminal position of the telomere is suggested to be related with their protection from exonucleolytic degradation, fusion and recombination (Poschke *et al.*, 2012). The seemingly reversed order of telomeres and terminal satellite repeats implies that the region rich in subtelomeric repeat is the extreme end, suggesting that looping might play a role not only in telomere protection, but also in mediation of the end-to-end association between homologs during meiosis.

In summary, based on the distribution of centromere specific proteins, microtubules, telomeres and different satellite repeats during meiosis we propose that variable

mechanisms can act together to perform a proper division of genetic material to the daughter cells in holocentric species. In addition, we suggest that terminal satellite DNA repeat-enriched chromatin threads fulfill the key function in correct joining of homologous non-sister chromatids enabling successful genome haploidization.

5.2. DMC1 is present in *L. elegans* pollen mother cells

5.2.1. DMC1 exhibits a meiosis- specific expression pattern in *L. elegans*

Based on the LeDMC1 transcription activity analysis and the distribution of LeDMC1 immunolabelling patterns during meiosis and mitosis we demonstrate that the expression of DMC1 protein is restricted to meiotically active cells in *L. elegans*. Meiosis specific expression of DMC1 was previously observed for yeast (Bishop *et al.*, 1992a; Schwacha and Kleckner, 1997; Grishchuk *et al.*, 2004), *A. thaliana* (Klimyuk and Jones, 1997; Vignard *et al.*, 2007) *O. sativa* (Ding *et al.*, 2001), *Lilium longiflorum* (Kobayashi *et al.*, 1993), *T. aestivum* (Devisetty *et al.*, 2010), mouse and human (Sato *et al.*, 1995; Habu *et al.*, 1996; Yoshida *et al.*, 1998). DMC1 protein is supposed to catalyze meiotic recombination in contrast to Rad51 - another homologue of the bacterial recombinase RecA (Bishop *et al.*, 1992a; Shinohara *et al.*, 1992) which is required for both mitotic and meiotic recombination (Bishop *et al.*, 1992a; Yamamoto *et al.*, 1996; Shinohara and Shinohara, 2004; Busygina *et al.*, 2012; Cloud *et al.*, 2012).

5.2.2. LeDMC1 shows a line-like specific immunolabelling pattern

Immunolabelling with a LeDMC1- specific antibody demonstrated that in *L. elegans* DMC1 exhibits a disperse distribution during leptotene. In agreement with data from *A. thaliana* (Kurzbaue *et al.*, 2012), *L. longiflorum* (Terasawa *et al.*, 1995) and mouse (Yoshida *et al.*, 1998; Moens *et al.*, 2002) numerous DMC1 foci exist. It is assumed that DMC1 appears at the same time when DSBs occur and require DSBs formation to initiate their assembly (Roeder, 1997). Quantification of the number of DMC1 foci observed at early prophase I in *A. thaliana* showed a mean number of around 250 per cell. Subsequently, DMC1 signals tend to disappear and during pachytene only a few residual DMC1 foci can be detected which reflect sites of meiotic recombination events (Chelysheva *et al.*, 2007;

Vignard *et al.*, 2007; Kurzbauer *et al.*, 2012). In contrast, in *L. elegans* LeDMC1 signals do not decrease during leptotene and zygotene but gradually linearize. A linear distribution of DMC1 immuno signals has been never found in other species (Bishop, 1994; Terasawa *et al.*, 1995; Moens *et al.*, 2002; Chelysheva *et al.*, 2007; Sheridan *et al.*, 2008; Kurzbauer *et al.*, 2012). To confirm the specificity of LeDMC1 antibody we tested its cross-reactivity with early prophase I chromosomes of rye. In contrast to the linear pattern observed in *L. elegans*, immunolabelling of rye with LeDMC1 showed randomly distributed dot-like signal. Therefore, the line-like distribution of DMC1 in *L. elegans* is likely not caused by an unspecific labelling of the antibody but revealed a typical staining for *L. elegans*.

Co-localization experiments using DMC1 and Rad51 antibodies in *A. thaliana* documented that these two proteins do not precisely colocalize, as assumed previously (Bishop, 1994; Shinohara *et al.*, 1997; Tarsounas *et al.*, 1999), but closely associate (Kurzbauer *et al.*, 2012). The total number of DMC1 and Rad51 foci are nearly the same (Bishop, 1994) suggesting that these two proteins work together in DSBs repair probably by occupying two different ends of DSBs (Shinohara *et al.*, 2000; Hunter and Kleckner, 2001; Kurzbauer *et al.*, 2012; Pradillo *et al.*, 2012). Other than in *L. elegans*, in the holocentric nematode *C. elegans* DMC1 protein is absent although Rad51 is present and mediated interhomolog meiotic recombination (Rinaldo *et al.*, 2002; Alpi *et al.*, 2003). The cytological localization of Rad51 in *C. elegans* (Alpi *et al.*, 2003) as well as in *R. pubera* and *R. tenuis* (Cabral *et al.*, 2014) revealed that most of Rad51 dot-like signal appear at leptotene and then disappear before late pachytene (Alpi *et al.*, 2003). Similar in monocentric maize (Franklin *et al.*, 1999) and *L. longiflorum* (Terasawa *et al.*, 1995) immunosignals of Rad51 appear at leptotene and subsequently decrease during progression of prophase I to disappear after pachytene. Other than LeDMC1 in *L. elegans*, Rad51 does not linearize neither in holocentric *C. elegans*, *R. pubera*, *R. tenuis* (Alpi *et al.*, 2003; Cabral *et al.*, 2014) nor in monocentric species (Terasawa *et al.*, 1995; Franklin *et al.*, 1999) indicating that linearization of RecA homologues is not a specific pattern related to a holocentric chromosome type.

Although a linear pattern of RecA signals has been not observed neither in monocentric nor in holocentric species, REC8 a meiosis-specific cohesion protein occurs as dots during early prophase I which subsequently fuse and form continuous lines (Klein *et al.*,

1999; Eijpe *et al.*, 2003; Lee *et al.*, 2003; Ji *et al.*, 2013) like the observed LeDMC1 immunodetection pattern. Despite REC8's important role in chromosome segregation, the *rec8* mutant in *S. pombe* revealed a strong reduction in meiotic recombination indicating a close relation between cohesion and recombination (Ponticelli and Smith, 1989). More recent investigations of *rec8* mutants confirmed that REC8 is required for DSBs formation and recombination (Ellermeier and Smith, 2005). Moreover, immunolabelling experiments using Rad51/DMC1 and REC8 antibodies revealed co-localization of these two proteins both in *O. sativa* (Ji *et al.*, 2013) and in rat (Eijpe *et al.*, 2003) during meiosis. In addition, in rats Rad51 and DMC1 proteins co-immunoprecipitate with REC8 (Eijpe *et al.*, 2003). Therefore, we would like to propose that REC8 can attract proteins that are involved in homologous recombination. Therefore, the line like LeDMC1 in *L. elegans* might be due to a potential interaction with the REC8 cohesion protein.

5.2.3. LeDMC1 localizes with CENH3 but does not mediate the meiotic end-to-end connection between homologous non-sister chromatids

Our immunolabelling results clearly demonstrated four elongated LeDMC1 signals per one bivalent during meiotic metaphase I which are co-localized with the centromere of each chromatid. Recent analysis of *dmc1* and *rad51* mutants of *A. thaliana* showed that DMC1 protein is required for pairing of homologous chromosome centromere regions. In contrast, RAD51 and its paralogs XRCC3 and RAD51C are mainly involved in pairing of chromosome arms (Da Ines *et al.*, 2012). Since fusion of sister centromeres in *L. elegans* does not occur we suspect that LeDMC1 is required for fusion of individual centromere units. Ultrastructural investigations demonstrated that holocentric centromeres consist of a high number of discrete centromere units, which resemble a beads-on-a-string-like structure (Nagaki *et al.*, 2005; Steiner and Henikoff, 2014; Wanner *et al.*, 2015). In interphase nuclei and early prophase I immunolabelling with the centromere specific marker CENH3 revealed numerous and dispersed signals which gradually linearize to form a continuous centromeric line at metaphase (Heckmann *et al.*, 2014). The dot-like immunolabelling patterns of CENH3 and LeDMC1 during meiotic interphase (Fig. 35a), gradual linearize during prophase I (Fig. 35b) and subsequent co-localization of CENH3

and LeDMC1 at metaphase I occurs (Fig. 35c). Hence, a cooperation of both proteins in the maintenance of the centromere structure is likely.

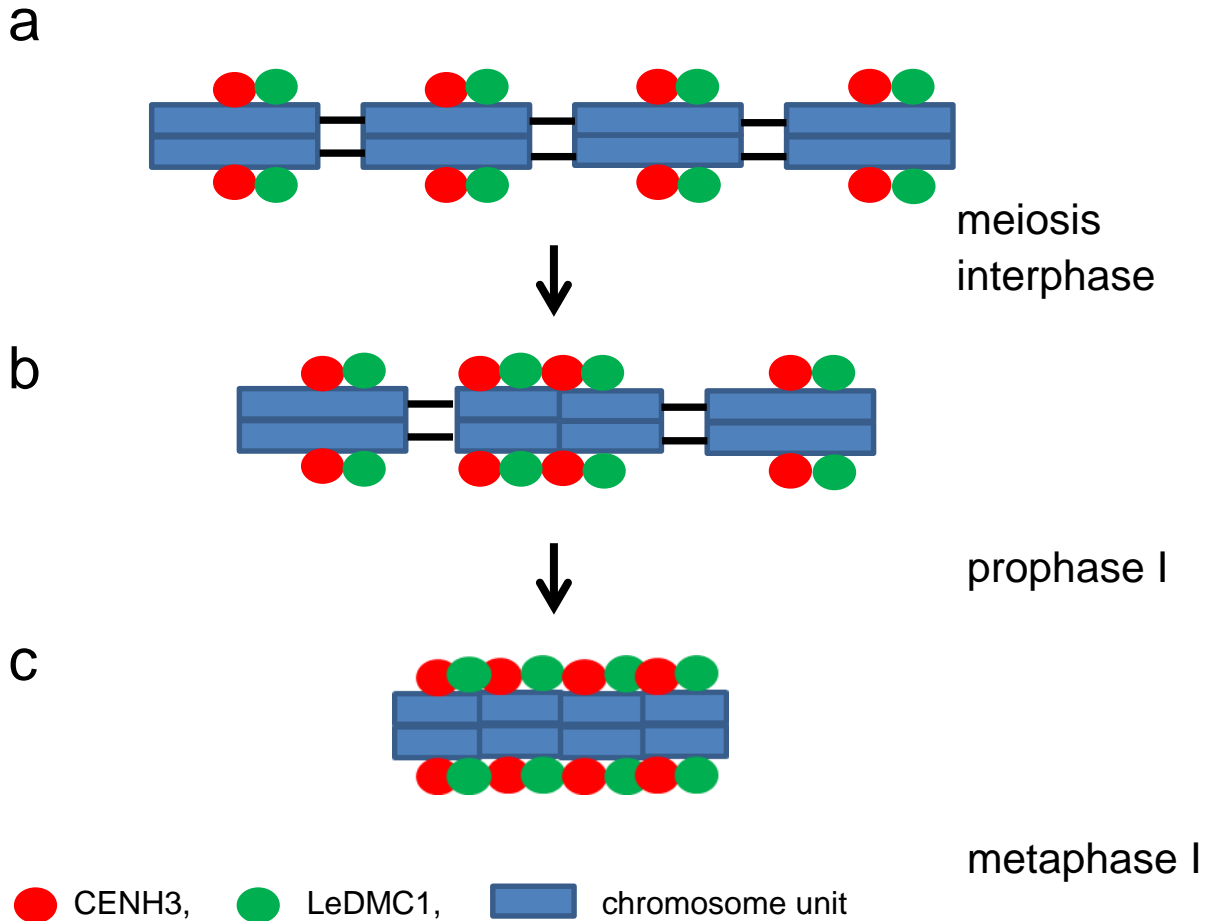


Fig. 35. Scheme showing the likely dynamics of CENH3 and LeDMC1 proteins in holocentric centromeres at different stages of meiosis.

a) CENH3 and LeDMC1 proteins reveal numerous and disperse localization at interphase before meiosis. b) Both proteins linearize gradually during prophase I due to the stepwise association of centromere units. c) At metaphase I a line-like distribution of CENH3 and LeDMC1 signals occurs.

In our study we observed that LeDMC1 specific immunolabelling signals do not localize to the end-to-end association of homologues metaphase I chromosomes. This observation indicates that DMC1 is not involved in the establishment of the connection between meiotic non-sister chromatids, excluding that meiotic recombination is involved in the end-to-end association. Alternative mechanisms of mediating connections between homologs are discussed in paragraph 5.1.5.

5.3. Karyotype of holocentric species evolves rapidly due to holokinetic centromeres and efficient telomere healing

5.3.1. X-ray radiation induced dosage dependent chromosomal aberrations

In agreement with previous reports for *L. elegans* (Nordenskiöld, 1963; Nordenskiöld, 1964; Sengupta and Sharma, 1988) we observed that DNA double-strand breaks occur more frequently with increasing X-ray irradiation dosage. The first reported evidence that X-ray induced chromosomal aberrations come from early genetic studies of *Drosophila* (Painter and Müller, 1929). Subsequently in numerous experiments chromosomal aberrations like: dicentric chromosomes, centric rings, acentric fragments, reciprocal/ non-reciprocal translocations, insertions, premature chromosome condensation or micronuclei were caused by ionizing irradiations (eg. γ -, X-rays) and UV irradiation in a dosage dependent manner (Schultz, 1936; Sax, 1940; Wolff and Atwood, 1954; Prakken, 1959; Manti *et al.*, 1997; Manual, 2001; Li *et al.*, 2010). It should be noted that the relation between irradiation dose and chromosomal mutations is not linear. Numerous experiments showed an exponential increase of chromosome mutations with increasing dosage (Muller, 1932; Oliver, 1932; Bauer *et al.*, 1938; Sax, 1938). Interestingly, many studies demonstrated that irradiation had a stimulating effect on plants' growth. Exposition of seeds or plants to low doses of irradiation stimulates seed germination, induction of faster seedlings growth, earlier flowering and contribute to the production of larger plants and greater yields (Sax, 1963; Woodstoc.Lw and Justice, 1967; Wiendl *et al.*, 1995; Paull, 1996; Charbaji and Nabulsi, 1999; Al-Safadi *et al.*, 2000; Li *et al.*, 2005; Al-Safadi and Elias, 2011). Thus, the effect of irradiation on plants in dependence of dosage can be either positive or negative.

5.3.2. Chromosome fragmentation in *L. elegans* is sequence independent

In our study we observed that plants after irradiation were chimeric showing different chromosomal patterns in different cells. Radiation induced chromosome fragments varied in size. It seems that the distribution of break points occurs randomly along the whole chromosome length. Although, many studies demonstrate a non-random distribution of chromosome breaks with a higher frequency in repetitive DNA such as centromeric and

telomeric chromatin (Buckton, 1976; Brøgger, 1977; Bauchinger and Gotz, 1979). Often interstitial telomeric repeats, which probably originated from ancestral chromosomal fusions (Holmquist and Dancis, 1979; Meyne *et al.*, 1990; Lee *et al.*, 1993; Maeda *et al.*, 2012) are characterized by increased frequencies of spontaneous (Bertoni *et al.*, 1994; Slijepcevic *et al.*, 1996) and induced (Alvarez *et al.*, 1993; Balajee *et al.*, 1994; Slijepcevic *et al.*, 1996) chromosomal breakages. Based on FISH with an *Arabidopsis*-type telomere probe we did not observe interstitial telomere signals as a potential hot spot of chromosome fragmentation in *L. elegans*. Also interstitial telomeres were not found in other holocentric species e.g. aphids (Monti *et al.*, 2011), *L. luzuloides* (Fuchs *et al.*, 1995) *R. tenuis* (Vanzela *et al.*, 2003) and *M. brassicae* (Mandrioli, 2002). Therefore, we suspect that the breakage of chromosomes via radiation in many holocentric species might occur independently of interstitial telomeric repeats. Although, various blocks of heterochromatin distributed along the chromosome length in holocentric chromosomes (Vanzela and Guerra, 2000; Guerra and Garcia, 2004; Heckmann *et al.*, 2013) might exhibit higher chromosome fragility.

5.3.3. Chromosome fragments have holokinetic centromeres

Using centromere-specific markers, we demonstrated that fragmented and translocated chromosomes of *L. elegans*, independent of their size possess centromere activity over the entire length of the chromosomes. Similar to the wild type chromosomes each chromosome fragment revealed a groove-like structure where the centromere is located. The absence of anaphase bridges and micronuclei indicates that fragmented and translocated chromosomes properly segregate in somatic cells due to the activity of the holocentric centromeres. Likewise, no abnormalities during mitotic division were found in irradiated *R. pubera* (Vanzela and Colaço, 2002), *Cuscuta* (Pazy and Plitmann, 1994), *Spirogyra* (Godward, 1954), *C. elegans* (Albertson and Thomson, 1982) or *Tetranychus urticae* (Tempelaar, 1979). In contrast, irradiation induced chromosome rearrangements in organisms with monocentric chromosomes, often results in the formation of acentric and dicentric fragments which fail to segregate in a correct manner (Bauer *et al.*, 1938; McClintock, 1939; Sax, 1941; Manti *et al.*, 1997).

5.3.4. Chromosome fragments are stabilized by *de novo* formed telomeres

Based on FISH with an *Arabidopsis*-type telomere probe, we detected telomeric repeats at ~50% of broken termini already 21 days after radiation induced chromosome fragmentation and up to 96% after 3 months. Moreover, analysis of TRAP products indicated detectable levels of telomerase in extracts isolated from *L. elegans* generative and vegetative tissue like it was observed for *A. thaliana*, barley (Heller *et al.*, 1996) or *Nicotiana tabacum* (Fajkus *et al.*, 1996). Our results suggest that *de novo* synthesized telomeres are most likely the outcome of a telomerase-mediated healing process. Likewise, the telomerase-based mechanism of chromosome healing was observed for holocentric *Myzus persicae* (Monti *et al.*, 2011) and *Bombyx mori* (Fujiwara *et al.*, 2000) as well as in monocentric human (Chabchoub *et al.*, 2007), *Tetrahymena* (Harrington and Harrington, 1991; Yu and Blackburn, 1991), *S. cerevisiae* (Jager and Philippsen, 1989) and wheat (Tsujiimoto, 1993; Tsujiimoto *et al.*, 1997; Friebe *et al.*, 2001). Similar, as observed for *L. elegans*, 50% of the chromosome fragments of maize were stabilized by telomeres 3 weeks and up to 93% 10 weeks after fragmentation (Zheng *et al.*, 1999). Also in wheat, 2 - 4 weeks after chromosome fragmentation telomeres at the break points were rarely observed, although during meiosis, all broken ends displayed detectable telomeres (Friebe *et al.*, 2001). Therefore, we suspect that chromosome healing occurs gradually and cells have to pass through several cell divisions to acquire a cytologically detectable telomere.

Measurements of telomerase activity by TRAP assay at several time points after radiation in *L. elegans* did not reveal changes in enzymatic activity compared to non-irradiated plants. In contrast, in mouse spermatocytes a three to five fold increase in telomerase activity was observed immediately after x-irradiation (Hande *et al.*, 1998). A dosage-dependent increase of telomerase activity was also observed in human (Joo *et al.*, 1998; Neuhofer *et al.*, 2001) and Chinese hamster (Hande *et al.*, 1997). It is supposed that the upregulation of telomerase activity after radiation can be a DNA-damage induced cell response and also indicates the role of telomerase in the process of DNA repair and chromosome healing (Hande *et al.*, 1998). We suspect that telomerase activity in *L. elegans* tissues is sufficient for chromosome break point stabilization and an increase in

their activity is not necessary. Eventually, activity changes were not detected by the TRAP assay due to the weak activity of the telomerase.

The absence of detectable telomeres and the differences in intensity of newly synthesized telomeric FISH signals at some termini of chromosome fragments might indicate a preferential binding of the telomerase to specific repeats/sequences at break points. Previously, it was shown, that in *S. cerevisiae* the *de novo* telomere synthesis occurs more likely at TG-rich sequences (Putnam *et al.*, 2004). Additionally, the telomerase might preferentially elongate shorter telomeres than the longer ones causing differences in telomere size. The preferential prolongation of shorter telomeres has been observed in yeast (Teixeira *et al.*, 2004), mouse (Hemann *et al.*, 2001) and human (Britt-Compton *et al.*, 2009). The presence of new telomeres with similar FISH signal intensity as the pre-existing ones in a short time after irradiation, as well as the occurrence of small chromosomal fragments carrying pre-existing telomeres at both ends suggest the action of an additional, telomerase independent mechanisms of chromosome healing, such as terminal translocation or recombination. Indeed, in human chromosome fragments are simultaneously stabilized by telomerase dependent and independent mechanisms (Chabchoub *et al.*, 2007).

5.3.5. Chromosome fragments are successfully transmitted across several generations

Our observations demonstrated that irradiation- induced chromosome fragmentation and translocations as well as multivalent configurations do not affect the process of inverted meiosis in *L. elegans*, similarly to holocentric *C. babylonica* (Pazy and Plitmann, 1994), *Cyperus eragrostis* (Bokhari, 1976) and *R. pubera* (Vanzela and Colaço, 2002). In contrast, in monocentric species numerous meiotic irregularities caused by induced chromosomal rearrangements were observed e.g. *Capsicum annuum* (Dhamayanthi and Reddy, 2000), barley (Caldecott and Smith, 1952) or *Delphinium malabaricum* (Kolar *et al.*, 2013). Similar like in *L. elegans*, the presence of irradiation-induced multivalent configurations, probably as a result of multiple translocations involving terminal heterochromatic region, were also observed in holocentric *E. subarticulata* (Da Silva *et*

al., 2005), *Philosamia ricini* (Padhy, 1986) and in scorpions from the family Buthidae (Shanahan, 1989; Schneider *et al.*, 2009). Faithful transmission of aberrated holocentric chromosomes to the next generation contributes to the high divergence in chromosome number and size in close related species with holocentric chromosomes (Heilborn, 1924; Brown *et al.*, 2004; Kuta *et al.*, 2004; Da Silva *et al.*, 2008; Hipp *et al.*, 2009). Indeed, e.g. in the genus *Luzula* the haploid chromosome number varies in a broad range and species with 3, 6–16, 18, 21, 23, 24, 26, 31, 33, 35, 36, and 42 chromosomes were found (Nordenskiöld, 1951; Kuta *et al.*, 2004; Závěská Drábková, 2013).

We observed that all size variants of chromosome fragments present in the progeny of irradiated plants possessed telomere repeats at their break points. This data indicate the importance of telomeres in chromosome fragment stabilization. Telomere repeats added to the broken chromosome ends protect them from end-to-end fusion and future degradation. Furthermore telomeres bind to the nuclear envelope to form a bouquet like configuration which is a crucial event for the correct synapsis of homologs during meiosis (Day *et al.*, 1993). The importance of telomeres in chromosome fragment end stabilization was demonstrated in holocentric *B. mori*. In this case, fragments with telomeres are present only at the one chromosome end were lost more often (56%) during gametogenesis than fragments with telomeres at the both ends (25%) (Fujiwara *et al.*, 2000). The absence of chromosome healing leads to the programmed cell death, as reported for yeast (Sandell and Zakian, 1993) or to the activation of proto-oncogenes, as described for mammals (Lee and Myung, 2009). Beside the telomeres also the presence of terminal satellite repeats might influence the process of chromosome fragment stabilization. Indeed, our study on inverted meiosis in *L. elegans* underlines the significant role of the terminal satellites LeSAT7, LeSAT11 and LeSAT28 in proper meiotic segregation. The occasional presence of micronuclei in the post-meiotic cells and the increase of the DNA content in some progeny plants might suggest sporadic abnormalities in the meiotic segregation of chromosome fragments. Different factors like fragment size, inappropriate attachment of spindle microtubules, kinetochore damage or defects in the cell cycle control system can result in micronuclei formation (Luzhna *et al.*, 2013).

Our data confirm that the combination of a holocentric chromosome structure and rapid *de novo* telomeres formation at the break points enable chromosome fragments to be successfully transmitted across generations. Thus, species with holocentric chromosomes may undergo a rapid karyotype evolution involving chromosome translocation and fragmentation.

6. Outlook

1) To determine the distribution of meiotic recombination events along chromosomes antibodies specific for proteins involved in crossover formation like, MLH1, MLH3, MUS81 should be generated and used in future. In addition, the localization of crossovers could be visualized by marking individual chromatids with the help of incorporated 5-Bromdesoxyuridine (BrdU). Each exchange between non-sister chromatids (recombination) of bivalent could be visualized as differentially labelled chromatid segment.

2) The distribution and timing of proteins involved in sister chromatid cohesion during meiosis should be determined. Immunostaining with antibodies against cohesion proteins such as REC8, SCC3 and proteins involved in protection of centromere cohesion such as Shugoshin should be performed. The analysis of cohesion related proteins within the end-to-end connection would indicate the cohesion nature of this chromosomal association during meiosis.

3) To explain the line-like distribution of the meiosis specific recombination protein LeDMC1, a co-localization study with proteins involved in cohesion should be performed. Dual-immunostaining with LeDMC1 and REC8 antibodies would reveal whether both proteins localize in the same manner on meiotic chromosomes. Spatial overlapping of the analyzed proteins would indicate that recombination and cohesion proteins cooperate to ensure a proper recombination and therefore successful meiotic division in *L. elegans*.

4) To better understand the biology of holocentric chromosomes comparative and functional genomics study should be performed in *L. elegans* and other holocentric species. Determination of the genomic DNA sequence, gene order and their function within holocentric species would open new perspectives to analyse the mechanisms of karyotype rearrangements and origin of holocentricity.

7. References

- Adelfalk, C., Janschek, J., Revenkova, E., Blei, C., Liebe, B., Gob, E., Alsheimer, M., Benavente, R., de Boer, E., Novak, I., Hoog, C., Scherthan, H., Jessberger, R., 2009. Cohesin SMC1 beta protects telomeres in meocytes. *Journal of Cell Biology* 187, 185-199.
- Al-Safadi, B., Ayyoubi, Z., Jawdat, D., 2000. The effect of gamma irradiation on potato microtuber production in vitro. *Plant Cell Tiss Org* 61, 183-187.
- Al-Safadi, B., Elias, R., 2011. Improvement of caper (*Capparis spinosa* L.) propagation using in vitro culture and gamma irradiation. *Scientia Horticulturae* 127, 290-297.
- Albertson, D.G., Thomson, J.N., 1982. The kinetochores of *Caenorhabditis-elegans*. *Chromosoma* 86, 409-428.
- Albertson, D.G., Thomson, J.N., 1993. Segregation of holocentric chromosomes at meiosis in the nematode, *Caenorhabditis elegans*. *Chromosome Research* 1, 15-26.
- Albini, S.M., Jones, G.H., 1987. Synaptonemal Complex Spreading in *Allium-cepa* and *Allium-fistulosum* - .1. The Initiation and Sequence of Pairing. *Chromosoma* 95, 324-338.
- Alfenito, M.R., Birchler, J.A., 1993. Molecular characterization of a maize B-chromosome centric sequence. *Genetics* 135, 589-597.
- Allshire, R.C., Karpen, G.H., 2008. Epigenetic regulation of centromeric chromatin: old dogs, new tricks? *Nature reviews. Genetics* 9, 923-937.
- Alpi, A., Pasierbek, P., Gartner, A., Loidl, J., 2003. Genetic and cytological characterization of the recombination protein RAD-51 in *Caenorhabditis elegans*. *Chromosoma* 112, 6-16.
- Alvarez, L., Evans, J.W., Wilks, R., Lucas, J.N., Brown, J.M., Giaccia, A.J., 1993. Chromosomal radiosensitivity at intrachromosomal telomeric sites. *Genes Chromosomes and Cancer* 8, 8-14.
- AragonAlcaide, L., Miller, T., Schwarzacher, T., Reader, S., Moore, G., 1996. A cereal centromeric sequence. *Chromosoma* 105, 261-268.
- Armstrong, S.J., Caryl, A.P., Jones, G.H., Franklin, F.C.H., 2002. Asy1, a protein required for meiotic chromosome synapsis, localizes to axis-associated chromatin in Arabidopsis and Brassica. *Journal of Cell Science* 115, 3645-3655.
- Bačič, T., Jogan, N., Koce, J.D., 2007. *Luzula* sect. *Luzula* in the south-eastern Alps—karyology and genome size. *Taxon* 56, 129-136.
- Balajee, A.S., Oh, H.J., Natarajan, A.T., 1994. Analysis of restriction enzyme-induced chromosome-aberrations in the interstitial telomeric repeat sequences of Cho and Che cells by fish. *Mutation research* 307, 307-313.
- Barnes, T.M., Kohara, Y., Coulson, A., Hekimi, S., 1995. Meiotic recombination, noncoding DNA and genomic organization in *Caenorhabditis elegans*. *Genetics* 141, 159-179.
- Bass, H.W., 2003. Telomere dynamics unique to meiotic prophase: formation and significance of the bouquet. *Cellular and Molecular Life Sciences* 60, 2319-2324.
- Bass, H.W., Marshall, W.F., Sedat, J.W., Agard, D.A., Cande, W.Z., 1997. Telomeres cluster de novo before the initiation of synapsis: a three-dimensional spatial analysis of telomere positions before and during meiotic prophase. *Journal of Cell Biology* 137, 5-18.
- Bauchinger, M., Gotz, G., 1979. Distribution of radiation-induced lesions in human-chromosomes and dose-effect relation analyzed with G-banding. *Radiation and environmental biophysics* 16, 355-366.
- Bauer, H., 1967. Die kinetische Organisation der Lepidopteren-Chromosomen. *Chromosoma* 22, 101-125.
- Bauer, H., Demerec, M., Kaufmann, B., 1938. X-ray induced chromosomal alterations in *Drosophila melanogaster*. *Genetics* 23, 610.

Bertoni, L., Attolini, C., Tessera, L., Mucciolo, E., Giulotto, E., 1994. Telomeric and nontelomeric (Ttagcc)(N) sequences in gene amplification and chromosome stability. *Genomics* 24, 53-62.

Bishop, D.K., 1994. RecA homologs Dmc1 and Rad51 interact to form multiple nuclear-complexes prior to meiotic chromosome synapsis. *Cell* 79, 1081-1092.

Bishop, D.K., Park, D., Xu, L., Kleckner, N., 1992a. DMC1: a meiosis-specific yeast homolog of *E. coli* recA required for recombination, synaptonemal complex formation, and cell cycle progression. *Cell* 69, 439-456.

Bishop, D.K., Park, D., Xu, L.Z., Kleckner, N., 1992b. Dmc1 - a meiosis-specific yeast homolog of *Escherichia-coli* RecA required for recombination, synaptonemal complex-formation, and cell-cycle progression. *Cell* 69, 439-456.

Blackburn, E.H., 1991. Structure and function of telomeres. *Nature* 350, 569-573.

Blat, Y., Protacio, R.U., Hunter, N., Kleckner, N., 2002. Physical and functional interactions among basic chromosome organizational features govern early steps of meiotic chiasma formation. *Cell* 111, 791-802.

Blower, M.D., Sullivan, B.A., Karpen, G.H., 2002. Conserved organization of centromeric chromatin in flies and humans. *Developmental Cell* 2, 319-330.

Bokhari, F.S., 1976. Meiosis in untreated and irradiated *Cyperus-eragrostis* Vahl. *Cytologia* 41, 607-614.

Bokhari, F.S., Godward, M.B.E., 1980. The ultrastructure of the diffuse kinetochore in *Luzula-nivea*. *Chromosoma* 79, 125-136.

Bongiorni, S., Fiorenzo, P., Pippoletti, D., Prantera, G., 2004. Inverted meiosis and meiotic drive in mealybugs. *Chromosoma* 112, 331-341.

Borde, V., Lin, W., Novikov, E., Petrini, J.H., Lichten, M., Nicolas, A., 2004. Association of Mre11p with double-strand break sites during yeast meiosis. *Molecular Cell* 13, 389-401.

Bozek, M., Leitch, A.R., Leitch, I.J., Závěská Drábková, L., Kuta, E., 2012. Chromosome and genome size variation in *Luzula* (Juncaceae), a genus with holocentric chromosomes. *Botanical Journal of the Linnean Society* 170, 529-541.

Braselton, 1971. Ultrastructure of non-localized kinetochores of *Luzula* and *Cyperus*. *Chromosoma* 36, 89-&.

Britt-Compton, B., Capper, R., Rowson, J., Baird, D.M., 2009. Short telomeres are preferentially elongated by telomerase in human cells. *FEBS letters* 583, 3076-3080.

Brøgger, A., 1977. Non-random localization of chromosome damage in human cells and targets for clastogenic action. *Chromosomes today*. Volume 6.

Brown, J., Keith, S., Von Schoultz, B., Suomalainen, E., 2004. Chromosome evolution in neotropical Danainae and Ithomiinae (Lepidoptera). *Hereditas* 141, 216-236.

Brown, S.W., 1954. Mitosis and meiosis in *Luzula campestris*. University of California Publication in Botany 27, 231-278.

Brown, W.R.A., Mackinnon, P.J., Villasante, A., Spurr, N., Buckle, V.J., Dobson, M.J., 1990. Structure and polymorphism of human telomere-associated DNA. *Cell* 63, 119-132.

Buchwitz, B.J., Ahmad, K., Moore, L.L., Roth, M.B., Henikoff, S., 1999. A histone-H3-like protein in *C. elegans*. *Nature* 401, 547-548.

Buckton, K.E., 1976. Identification with G and R banding of position of breakage points induced in human-chromosomes by invitro X-irradiation. *International journal of radiation biology* 29, 475-488.

Bureš, P., Zedek, F., Marková, M., 2013. Holocentric chromosomes. In: Greilhuber, J., Dolezel, J., Wendel, J.F. (Eds.), *Plant Genome Diversity Volume 2*. Springer Vienna, pp. 187-208.

Busygina, V., Saro, D., Williams, G., Leung, W.K., Say, A.F., Sehorn, M.G., Sung, P., Tsubouchi, H., 2012. Novel attributes of Hed1 affect dynamics and activity of the Rad51 presynaptic filament during meiotic recombination. *Journal of Biological Chemistry* 287, 1566-1575.

Cabral, G., Marques, A., Schubert, V., Pedrosa-Harand, A., Schlogelhofer, P., 2014. Chiasmatic and achiasmatic inverted meiosis of plants with holocentric chromosomes. *Nature communications* 5.

Caldecott, R.S., Smith, L., 1952. A study of X-ray-induced chromosomal aberrations in barley. *Cytologia* 17, 224-242.

Calvente, A., Viera, A., Parra, M.T., de la Fuente, R., Suja, J.A., Page, J., Santos, J.L., de la Vega, C.G., Barbero, J.L., Rufas, J.S., 2013. Dynamics of cohesin subunits in grasshopper meiotic divisions. *Chromosoma* 122, 77-91.

Cangiano, G., Lavolpe, A., 1993. Repetitive DNA-sequences located in the terminal portion of the *Caenorhabditis-elegans* chromosomes. *Nucleic acids research* 21, 1133-1139.

Canudas, S., Smith, S., 2009. Differential regulation of telomere and centromere cohesion by the Scc3 homologues SA1 and SA2, respectively, in human cells. *Journal of Cell Biology* 187, 165-173.

Castro, D.d., Camara, A., Malheiros, N., 1949. X-rays in the centromere problem of *Luzula purpurea* Link. *Genetica iberica* 1, 49-54.

Chabchoub, E., Rodriguez, L., Galan, E., Mansilla, E., Martinez-Fernandez, M.L., Martinez-Frias, M.L., Fryns, J.P., Vermeesch, J.R., 2007. Molecular characterisation of a mosaicism with a complex chromosome rearrangement: evidence for coincident chromosome healing by telomere capture and neo-telomere formation. *Journal of medical genetics* 44, 250-256.

Chandra, H.S., 1962. Inverse meiosis in triploid females of *Mealy bug, Planococcus citri*. *Genetics* 47, 1441-&.

Charbaji, T., Nabulsi, I., 1999. Effect of low doses of gamma irradiation on in vitro growth of grapevine. *Plant Cell Tiss* 57, 129-132.

Cheeseman, I.M., Desai, A., 2008. Molecular architecture of the kinetochore-microtubule interface. *Nature Reviews Molecular Cell Biology* 9, 33-46.

Chelysheva, L., Gendrot, G., Vezon, D., Doutriaux, M.P., Mercier, R., Grelon, M., 2007. Zip4/Spo22 is required for class ICO formation but not for synapsis completion in *Arabidopsis thaliana*. *PLoS genetics* 3, 802-813.

Chomczynski, P., Sacchi, N., 1987. Single-step method of RNA isolation by acid guanidinium thiocyanate phenol chloroform extraction. *Analytical Biochemistry* 162, 156-159.

Choo, K.H., 1997. The centromere. Oxford: Oxford University Press.

Clarke, L., Carbon, J., 1985. The structure and function of yeast centromeres. *Annual Review of Genetics* 19, 29-56.

Cloud, V., Chan, Y.L., Grubb, J., Budke, B., Bishop, D.K., 2012. Rad51 is an accessory factor for Dmc1-mediated joint molecule formation during meiosis. *Science* 337, 1222-1225.

Colaiacono, M.P., MacQueen, A.J., Martinez-Perez, E., McDonald, K., Adamo, A., La Volpe, A., Villeneuve, A.M., 2003. Synaptonemal complex assembly in *C-elegans* is dispensable for loading strand-exchange proteins but critical for proper completion of recombination. *Developmental Cell* 5, 463-474.

Comings, D.E., Okada, T.A., 1972. Holocentric chromosomes in *Oncopeltus* - kinetochore plates are present in mitosis but absent in meiosis. *Chromosoma* 37, 177-&.

Cooper, J.L., Henikoff, S., 2004. Adaptive evolution of the histone fold domain in centromeric histones. *Molecular Biology and Evolution* 21, 1712-1718.

Coyne, J.A., Orr, H.A., 2004. Speciation. Sinauer Associates Sunderland, MA.

Cromer, L., Jolivet, S., Horlow, C., Chelysheva, L., Heyman, J., De Jaeger, G., Koncz, C., De Veylder, L., Mercier, R., 2013. Centromeric cohesion is protected twice at meiosis, by shugoshins at anaphase I and by patronus at interkinesis. *Current Biology* 23, 2090-2099.

Cuadrado, A., Vitellozzi, F., Jouve, N., Ceoloni, C., 1997. Fluorescence in situ hybridization with multiple repeated DNA probes applied to the analysis of wheat-rye chromosome pairing. *Theoretical and Applied Genetics* 94, 347-355.

Da Ines, O., Abe, K., Goubely, C., Gallego, M.E., White, C.I., 2012. Differing requirements for RAD51 and DMC1 in meiotic pairing of centromeres and chromosome arms in *Arabidopsis thaliana*. *PLoS genetics* 8, e1002636.

Da Silva, C.R.M., González-Elizondo, M.S., Vanzela, A.L.L., 2005. Reduction of chromosome number in *Eleocharis subarticulata* (Cyperaceae) by multiple translocations. *Botanical Journal of the Linnean Society* 149, 457-464.

Da Silva, C.R.M., González-Elizondo, M.S., Vanzela, A.L.L., 2008. Chromosome reduction in *Eleocharis maculosa* (Cyperaceae). *Cytogenetic and Genome Research* 122, 175-180.

Day, J.P., Marder, B.A., Morgan, W.F., 1993. Telomeres and their possible role in chromosome stabilization. *Environmental and Molecular Mutagenesis* 22, 245-249.

Dernburg, A.F., 2001. Here, there, and everywhere: kinetochore function on holocentric chromosomes. *The Journal of Cell Biology* 153, 33-38.

Dernburg, A.F., Sedat, J.W., Hawley, R.S., 1996. Direct evidence of a role for heterochromatin in meiotic chromosome segregation. *Cell* 86, 135-146.

Devisetty, U.K., Mayes, K., Mayes, S., 2010. The RAD51 and DMC1 homoeologous genes of bread wheat: cloning, molecular characterization and expression analysis. *BMC research notes* 3, 245.

Dhamayanthi, K., Reddy, V., 2000. Cytogenetic effects of gamma rays and ethyl methane sulphonate in chilli pepper (*Capsicum annum* L.). *Cytologia* 65, 129-133.

Ding, Z.-j., Wang, T., Chong, K., Bai, S., 2001. Isolation and characterization of OsDMC1, the rice homologue of the yeast DMC1 gene essential for meiosis. *Sexual Plant Reproduction* 13, 285-288.

Doherty, A.J., Serpell, L.C., Ponting, C.P., 1996. The helix-hairpin-helix DNA-binding motif: A structural basis for non-sequence-specific recognition of DNA. *Nucleic acids research* 24, 2488-2497.

Doležel, J., Greilhuber, J., Lucretti, S., Meister, A., Lysák, M., Nardi, L., Obermayer, R., 1998. Plant genome size estimation by flow cytometry: inter-laboratory comparison. *Annals Of Botany* 82, 17-26.

Dougan, D.A., Mogk, A., Zeth, K., Turgay, K., Bukau, B., 2002. AAA plus proteins and substrate recognition, it all depends on their partner in crime. *Febs Letters* 529, 6-10.

Dresser, M.E., Ewing, D.J., Conrad, M.N., Dominguez, A.M., Barstead, R., Jiang, H., Kodadek, T., 1997. DMC1 functions in a *Saccharomyces cerevisiae* meiotic pathway that is largely independent of the RAD51 pathway. *Genetics* 147, 533-544.

Dumont, J., Oegema, K., Desai, A., 2010. A kinetochore-independent mechanism drives anaphase chromosome separation during acentrosomal meiosis. *Nature cell biology* 12, 894-901.

Dundas, J., Ling, M., 2012. Reference genes for measuring mRNA expression. *Theory In Biosciences* 131, 215-223.

Eichler, E.E., Sankoff, D., 2003. Structural dynamics of eukaryotic chromosome evolution. *Science* 301, 793-797.

Eijpe, M., Offenbergh, H., Jessberger, R., Revenkova, E., Heyting, C., 2003. Meiotic cohesin REC8 marks the axial elements of rat synaptonemal complexes before cohesins SMC1 beta and SMC3. *Journal of Cell Biology* 160, 657-670.

Ellermeier, C., Smith, G.R., 2005. Cohesins are required for meiotic DNA breakage and recombination in *Schizosaccharomyces pombe*. *Proceedings of the National Academy of Sciences of the United States of America* 102, 10952-10957.

Erzberger, J.P., Berger, J.M., 2006. Evolutionary relationships and structural mechanisms of AAA plus proteins. *Annual Review of Biophysics* 35, 93-114.

Fajkus, J., Fulnečková, J., Hulánová, M., Berková, K., Říha, K., Matyášek, R., 1996. Plant cells express telomerase activity upon transfer to callus culture, without extensively changing telomere lengths. *Molecular and General Genetics* 260, 470-474.

Fajkus, J., Kovarik, A., Kralovics, R., 1998. Telomerase activity in plant cells. *Febs Letters* 391, 307-309.

Feng, C., Liu, Y., Su, H., Wang, H., Birchler, J., Han, F., 2015. Recent advances in plant centromere biology. *Science China. Life sciences* 58, 240-245.

Fitzgerald, M.S., McKnight, T.D., Shippen, D.E., 1996. Characterization and developmental patterns of telomerase expression in plants. *Proceedings of the National Academy of Sciences of the United States of America* 93, 14422-14427.

Franklin, A.E., McElver, J., Sunjevaric, I., Rothstein, R., Bowen, B., Cande, W.Z., 1999. Three-dimensional microscopy of the Rad51 recombination protein during meiotic prophase (vol 11, pg 809, 1999). *Plant Cell* 11, 1811-1811.

Friebe, B., Kynast, R.G., Zhang, P., Qi, L.L., Dhar, M., Gill, B.S., 2001. Chromosome healing by addition of telomeric repeats in wheat occurs during the first mitotic divisions of the sporophyte and is a gradual process. *Chromosome Research* 9, 137-146.

Fuchs, J., Brandes, A., Schubert, I., 1995. Telomere sequence localization and karyotype evolution in higher-plants. *Plant Systematics and Evolution* 196, 227-241.

Fuchs, J., Jovtchev, G., Schubert, I., 2008. The chromosomal distribution of histone methylation marks in gymnosperms differs from that of angiosperms. *Chromosome Research* 16, 891-898.

Fujiwara, H., Nakazato, Y., Okazaki, S., Ninaki, O., 2000. Stability and telomere structure of chromosomal fragments in two different mosaic strains of the silkworm, *Bombyx mori*. *Zoological Science* 17, 743-750.

Galbraith, D.W., Harkins, K.R., Maddox, J.M., Ayres, N.M., Sharma, D.P., Firoozabady, E., 1983. Rapid flow cytometric analysis of the cell-cycle in intact plant-tissues. *Science* 220, 1049-1051.

Gascoigne, K.E., Cheeseman, I.M., 2011. Kinetochores assembly: if you build it, they will come. *Current Opinion in Cell Biology* 23, 102-108.

Gassmann, R., Rechtsteiner, A., Yuen, K.W., Muroyama, A., Egelhofer, T., Gaydos, L., Barron, F., Maddox, P., Essex, A., Monen, J., Ercan, S., Lieb, J.D., Oegema, K., Strome, S., Desai, A., 2012. An inverse relationship to germline transcription defines centromeric chromatin in *C. elegans*. *Nature* 484, 534-U166.

Gerton, J.L., DeRisi, J., Shroff, R., Lichten, M., Brown, P.O., Petes, T.D., 2000. Global mapping of meiotic recombination hotspots and coldspots in the yeast *Saccharomyces cerevisiae*. *Proceedings of the National Academy of Sciences of the United States of America* 97, 11383-11390.

Gerton, J.L., Hawley, R.S., 2005. Homologous chromosome interactions in meiosis: diversity amidst conservation. *Nature Reviews Genetics* 6, 477-487.

Giroux, C.N., Dresser, M.E., Tiano, H.F., 1989. Genetic control of chromosome synapsis in yeast meiosis. *Genome / National Research Council Canada = Genome / Conseil national de recherches Canada* 31, 88-94.

Godward, M.B.E., 1954. The diffuse centromere or polycentric chromosomes in *Spirogyra*. *Annals Of Botany* 18, 143-155.

Gonzalez-Garcia, M., Gonzalez-Sanchez, M., Puertas, M.J., 2006. The high variability of subtelomeric heterochromatin and connections between nonhomologous chromosomes, suggest frequent ectopic recombination in rye meiocytes. *Cytogenetic and Genome Research* 115, 179-185.

GonzalezGarcia, J.M., Benavente, R., Rufas, J.S., 1996. Cytochemical and immunocytochemical characterization of kinetochores in the holocentric chromosomes of *Graphosoma italicum*. *European Journal of Cell Biology* 70, 352-360.

Grant, V., 1981. *Plant speciation*. New York: Columbia University Press xii, 563p.-illus., maps, chrom. nos.. En 2nd edition. Maps, Chromosome numbers. General (KR, 198300748).

Grishchuk, A.L., Kraehenbuehl, R., Molnar, M., Fleck, O., Kohli, J., 2004. Genetic and cytological characterization of the RecA-homologous proteins Rad51 and Dmc1 of *Schizosaccharomyces pombe*. *Current Genetics* 44, 317-328.

Guerra, M., Cabral, G., Cuacos, M., Gonzalez-Garcia, M., Gonzalez-Sanchez, M., Vega, J., Puertas, M.J., 2010. Neocentrics and holokinetics (holocentrics): chromosomes out of the centromeric rules. *Cytogenetic and Genome Research* 129, 82-96.

Guerra, M., Garcia, M.A., 2004. Heterochromatin and rDNA sites distribution in the holocentric chromosomes of *Cuscuta approximata* Bab. (Convolvulaceae). *Genome / National Research Council Canada = Genome / Conseil national de recherches Canada* 47, 134-140.

Habu, T., Taki, T., West, A., Nishimune, Y., Morita, T., 1996. The mouse and human homologs of DMC1, the yeast meiosis-specific homologous recombination gene, have a common unique form of exon-skipped transcript in meiosis. *Nucleic acids research* 24, 470-477.

Håkansson, A., 1954. Meiosis and pollen mitosis in X-rayed and untreated spikelets of *Eleocharis palustris*. *Hereditas* 40, 325-345.

Håkansson, A., 1958. Holocentric chromosomes in *Eleocharis*. *Hereditas* 44, 531-540.

Halkka, O., 1964. Recombination in 6 homopterous families. *Evolution* 18, 81-&.

Hamant, O., Ma, H., Cande, W.Z., 2006. Genetics of meiotic prophase I in plants. *Annual Review of Plant Biology* 57, 267-302.

Hande, M.P., Balajee, A.S., Natarajan, A.T., 1997. Induction of telomerase activity by UV-irradiation in *Chinese hamster* cells. *Oncogene* 15, 1747-1752.

Hande, M.P., Lansdorp, P.M., Natarajan, A.T., 1998. Induction of telomerase activity by in vivo x-irradiation of mouse splenocytes and its possible role in chromosome healing. *Mutation Research-Fundamental And Molecular Mechanisms Of Mutagenesis* 404, 205-214.

Harrington, L.A., Harrington, L.A., 1991. Telomerase primer specificity and chromosome healing. *Nature* 353, 451-454.

Heckmann, S., Houben, A., 2013. Holokinetic centromeres. In: J. Jiang and J. Birchler (eds.), *Plant Centromere Biology*, Vol 1. Wiley-Blackwell in press.

Heckmann, S., Jankowska, M., Schubert, V., Kumke, K., Ma, W., Houben, A., 2014. Alternative meiotic chromatid segregation in the holocentric plant *Luzula elegans*. *Nature communications* 5, 4979.

Heckmann, S., Macas, J., Kumke, K., Fuchs, J., Schubert, V., Ma, L., Novák, P., Neumann, P., Taudien, S., Platzer, M., Houben, A., 2013. The holocentric species *Luzula elegans* shows interplay between centromere and large-scale genome organization. *The Plant Journal* 73, 555-565.

Heckmann, S., Schroeder-Reiter, E., Kumke, K., Ma, L., Nagaki, K., Murata, M., Wanner, G., Houben, A., 2011. Holocentric chromosomes of *Luzula elegans* are characterized by a longitudinal centromere groove, chromosome bending, and a terminal nucleolus organizer region. *Cytogenetic and Genome Research* 134, 220-228.

Heilborn, O., 1924. Chromosome numbers and dimensions, species-formation and phylogeny in the genus *Carex*. *Hereditas* 5, 129-216.

Heller, K., Kilian, A., Piatyszek, M.A., Kleinhofs, A., 1996. Telomerase activity in plant extracts. *Molecular & General Genetics* 252, 342-345.

Hemann, M.T., Strong, M.A., Hao, L.-Y., Greider, C.W., 2001. The shortest telomere, not average telomere length, is critical for cell viability and chromosome stability. *Cell* 107, 67-77.

Herbert, B.S., Hochreiter, A.E., Wright, W.E., Shay, J.W., 2006. Nonradioactive detection of telomerase activity using the telomeric repeat amplification protocol. *Nature Protocols* 1, 1583-1590.

Heyting, C., 1996. Synaptonemal complexes: structure and function. *Current Opinion in Cell Biology* 8, 389-396.

Higgins, J.D., Perry, R.M., Barakate, A., Ramsay, L., Waugh, R., Halpin, C., Armstrong, S.J., Franklin, F.C.H., 2012. Spatiotemporal asymmetry of the meiotic program underlies the predominantly distal distribution of meiotic crossovers in Barley. *Plant Cell* 24, 4096-4109.

Higgins, J.D., Sanchez-Moran, E., Armstrong, S.J., Jones, G.H., Franklin, F.C., 2005. The Arabidopsis synaptonemal complex protein ZYP1 is required for chromosome synapsis and normal fidelity of crossing over. *Genes & Development* 19, 2488-2500.

Hill, C.A., Guerrero, F.D., Van Zee, J.P., Geraci, N.S., Walling, J.G., Stuart, J.J., 2009. The position of repetitive DNA sequence in the southern cattle tick genome permits chromosome identification. *Chromosome Research* 17, 77-89.

Hipp, A.L., Rothrock, P.E., Roalson, E.H., 2009. The evolution of chromosome arrangements in *Carex* (Cyperaceae). *The Botanical Review* 75, 96-109.

Holmquist, G.P., Dancis, B., 1979. Telomere replication, kinetochore organizers, and satellite DNA evolution. *Proceedings of the National Academy of Sciences of the United States of America* 76, 4566-4570.

Hoshino, T., Okamura, K., 1994. Cytological studies on meiotic configurations of intraspecific aneuploids of *Carex blepharicarpa* (Cyperaceae) in Japan. *Journal of Plant Research* 107, 1-8.

Hou, M., Xu, D.W., Bjorkholm, M., Gruber, A., 2001. Real-time quantitative telomeric repeat amplification protocol assay for the detection of telomerase activity. *Clinical Chemistry* 47, 519-524.

Houben, A., Schroeder-Reiter, E., Nagaki, K., Nasuda, S., Wanner, G., Murata, M., Endo, T., 2007. CENH3 interacts with the centromeric retrotransposon *cereba* and GC-rich satellites and locates to centromeric substructures in barley. *Chromosoma* 116, 275-283.

Houben, A., Schubert, I., 2003. DNA and proteins of plant centromeres. *Current Opinion in Plant Biology* 6, 554-560.

Houben, A., Wako, T., Furushima-Shimogawara, R., Presting, G., Künzel, G., Schubert, I., Fukui, K., 1999. The cell cycle dependent phosphorylation of histone H3 is correlated with the condensation of plant mitotic chromosomes. *Plant Journal* 18, 675-679.

Hughes-Schrader, S., Schrader, F., 1961. The kinetochore of the Hemiptera. *Chromosoma* 12, 327-350.

Hughes-Schrader, S., Ris, H., 1941. The diffuse spindle attachment of coccids, verified by the mitotic behavior of induced chromosome fragments. *Journal of Experimental Zoology* 87, 429-456.

Hughes, S.E., Gilliland, W.D., Cotitta, J.L., Takeo, S., Collins, K.A., Hawley, R.S., 2009. Heterochromatic Threads connect oscillating chromosomes during prometaphase I in *Drosophila* oocytes. *PLoS genetics* 5, e1000348.

Hunter, N., Kleckner, N., 2001. The single-end invasion: an asymmetric intermediate at the double-strand break to double-holliday junction transition of meiotic recombination. *Cell* 106, 59-70.

Ijdo, J.W., Wells, R.A., Baldini, A., Reeders, S.T., 1991. Improved telomere detection using a telomere repeat probe (Ttaggg)N generated by Pcr. *Nucleic acids research* 19, 4780-4780.

Jager, D., Philippsen, P., 1989. Stabilization of dicentric chromosomes in *Saccharomyces-cerevisiae* by telomere addition to broken ends or by centromere deletion. *The EMBO Journal* 8, 247-254.

Jankowska, M., Fuchs, J., Klocke, E., Fojtova, M., Polanska, P., Fajkus, J., Schubert, V., Houben, A., 2015. Holokinetic centromeres and efficient telomere healing enable rapid karyotype evolution. *Chromosoma*.

Ji, J.H., Tang, D., Wang, M., Li, Y.F., Zhang, L., Wang, K.J., Li, M., Cheng, Z.K., 2013. MRE11 is required for homologous synapsis and DSB processing in rice meiosis. *Chromosoma* 122, 363-376.

Jiang, J., Nasuda, S., Dong, F., Scherrer, C.W., Woo, S.S., Wing, R.A., Gill, B.S., Ward, D.C., 1996. A conserved repetitive DNA element located in the centromeres of cereal chromosomes. *Proceedings of the National Academy of Sciences of the United States of America* 93, 14210-14213.

Jiang, J.M., Birchler, J.A., Parrott, W.A., Dawe, R.K., 2003. A molecular view of plant centromeres. *Trends in Plant Science* 8, 570-575.

John, B., 1990. Meiosis. Book Cambridge University Press 1990, Cambridge, New York, Post Chester, Melbourne, Sydney, 396 pp.

Jones, G.H., 1984. The control of chiasma distribution. *Symposia of the Society for Experimental Biology* 38:293-320.

Joo, O.H., Hande, M.P., Lansdorp, P.M., Natarajan, A.T., 1998. Induction of telomerase activity and chromosome aberrations in human tumour cell lines following X-irradiation. *Mutation Research-Fundamental And Molecular Mechanisms Of Mutagenesis* 401, 121-131.

Kaitna, S., Pasierbek, P., Jantsch, M., Loidl, J., Glotzer, M., 2002. The aurora B kinase AIR-2 regulates kinetochores during mitosis and is required for separation of homologous chromosomes during meiosis. *Current biology* 12, 798-812.

Kalitsis, P., Choo, K.H., 2012. The evolutionary life cycle of the resilient centromere. *Chromosoma* 121, 327-340.

Karpen, G.H., Allshire, R.C., 1997. The case for epigenetic effects on centromere identity and function. *Trends in Genetics* 13, 489-496.

Kawashima, S.A., Yamagishi, Y., Honda, T., Ishiguro, K., Watanabe, Y., 2010. Phosphorylation of H2A by Bub1 prevents chromosomal instability through localizing shugoshin. *Science* 327, 172-177.

Keeney, S., Giroux, C.N., Kleckner, N., 1997. Meiosis-specific DNA double-strand breaks are catalyzed by Spo11, a member of a widely conserved protein family. *Cell* 88, 375-384.

Kerrebrock, A.W., Moore, D.P., Wu, J.S., Orrweaver, T.L., 1995. Mei-S332, a *Drosophila* protein required for sister-chromatid cohesion, can localize to meiotic centromere regions. *Cell* 83, 247-256.

Klein, F., Mahr, P., Galova, M., Buonomo, S.B.C., Michaelis, C., Nairz, K., Nasmyth, K., 1999. A central role for cohesions in sister chromatid cohesion, formation of axial elements, and recombination during yeast meiosis. *Cell* 98, 91-103.

Klimyuk, V.I., Jones, J.D.G., 1997. AtDMC1, the Arabidopsis homologue of the yeast DMC1 gene: characterization, transposon-induced allelic variation and meiosis-associated expression. *Plant Journal* 11, 1-14.

Kobayashi, T., Hotta, Y., Tabata, S., 1993. Isolation and characterization of a yeast gene that is homologous with a meiosis-specific Cdna from a plant. *Molecular & General Genetics* 237, 225-232.

Kolar, F.R., Pai, S.R., Dixit, G.B., 2013. EMS, sodium azide and gamma rays induced meiotic anomalies in *Delphinium malabaricum* (Huth) Munz. *Israel Journal of Plant Sciences* 61, 64-72.

Kurzbauer, M.T., Uanschou, C., Chen, D., Schlogelhofer, P., 2012. The Recombinases DMC1 and RAD51 are functionally and spatially separated during meiosis in Arabidopsis. *Plant Cell* 24, 2058-2070.

Kusanagi, A., 1962. Mechanism of post-reductional meiosis in *Luzula*. *Journal of Genetics* 37, 396-&.

Kusanagi, A., 1973. Preferential orientation of interchange multiples in *Luzula elegans*. *Journal of Genetics* 48, 175-183.

Kuta, E., Bohanec, B., Dubas, E., Vižintin, L., Przywara, L., 2004. Chromosome and nuclear DNA study on *Luzula* - a genus with holokinetic chromosomes. *Genome / National Research Council Canada = Genome / Conseil national de recherches Canada* 47, 246-256.

LaChance, L.E., Degrugillier, M., 1969. Chromosomal fragments transmitted through three generations in *Oncopeltus* (Hemiptera). *Science* 166, 235-236.

LaCour, F.L., 1953. The *Luzula* system analyzed by x-rays. *Heredity* 6, 77-81.

LaFountain, J.R., Cole, R.W., Rieder, C.L., 2002. Partner telomeres during anaphase in crane-fly spermatocytes are connected by an elastic tether that exerts a backward force and resists poleward motion. *Journal of Cell Science* 115, 1541-1549.

Lamb, J.C., Yu, W.C., Han, F.P., Birchler, J.A., 2007. Plant chromosomes from end to end: telomeres, heterochromatin and centromeres. *Current Opinion in Plant Biology* 10, 116-122.

Lee, C., Sasi, R., Lin, C.C., 1993. Interstitial localization of telomeric DNA-sequences in the *Indian muntjac* chromosomes - *Fu* 63, 156-159.

Lee, J., Iwai, T., Yokota, T., Yamashita, M., 2000. Further Evidence for tandem chromosome fusions in the karyotypic evolution of the Asian Muntjacs. *Cytogenetics and cell genetics* 3. Temporally and spatially selective loss of Rec8 protein from meiotic chromosomes during mammalian meiosis. *Journal of Cell Science* 116, 2781-2790.

Lee, S.E., Myung, K., 2009. Faithful after break-up: suppression of chromosomal translocations. *Cellular and Molecular Life Sciences* 66, 3149-3160.

Li, H., Zhou, W., Zhang, Z., Gu, H., Takeuchi, Y., Yoneyama, K., 2005. Effect of γ -radiation on development, yield and quality of microtubers in vitro in *Solanum tuberosum* L. *Biologia plantarum* 49, 625-628.

Li, R., Bruneau, A.H., Qu, R., 2010. Morphological mutants of *St. Augustinegrass* induced by gamma ray irradiation. *Plant Breeding* 129, 412-416.

Li, X., Dawe, R.K., 2009. Fused sister kinetochores initiate the reductional division in meiosis I. *Nature Cell Biology* 11, 1103-1108.

Lima-de-Faria, A., 1949. Genetics, origin and evolution of kinetochores. *Hereditas* 35, 422-444.

Lo, A.W., Magliano, D.J., Sibson, M.C., Kalitsis, P., Craig, J.M., Choo, K.H., 2001. A novel chromatin immunoprecipitation and array (CIA) analysis identifies a 460-kb CENP-A-binding neocentromere DNA. *Genome research* 11, 448-457.

Loidl, J., Lukaszewicz, A., Howard-Till, R.A., Koestler, T., 2012. The tetrahymena meiotic chromosome bouquet is organized by centromeres and promotes interhomolog recombination. *Journal of Cell Science* 125, 5873-5880.

Luceño, M., Vanzela, A.L.L., Guerra, M., 1998. Cytotaxonomic studies in Brazilian *Rhynchospora* (Cyperaceae), a genus exhibiting holocentric chromosomes. *Canadian Journal of Botany* 76, 440-449.

Lundblad, V., 2002. Telomere maintenance without telomerase. *Oncogene* 21, 522-531.

Luzhna, L., Kathiria, P., Kovalchuk, O., 2013. Micronuclei in genotoxicity assessment: from genetics to epigenetics and beyond. *Frontiers in genetics* 4, 131.

Macas, J., Kejnovsky, E., Neumann, P., Novak, P., Koblizkova, A., Vyskot, B., 2011. Next generation sequencing-based analysis of repetitive DNA in the model dioecious plant *Silene latifolia*. *PloS one* 6.

Macas, J., Neumann, P., Navratilova, A., 2007. Repetitive DNA in the pea (*Pisum sativum* L.) genome: comprehensive characterization using 454 sequencing and comparison to soybean and *Medicago truncatula*. *Bmc Genomics* 8.

Maddox, P.S., Oegema, K., Desai, A., Cheeseman, I.M., 2004. "Holo"er than thou: chromosome segregation and kinetochore function in *C. elegans*. *Chromosome Research* 12, 641-653.

Maeda, J., Yurkon, C.R., Fujisawa, H., Kaneko, M., Genet, S.C., Roybal, E.J., Rota, G.W., Saffer, E.R., Rose, B.J., Hanneman, W.H., Thamm, D.H., Kato, T.A., 2012. Genomic instability and telomere fusion of Canine Osteosarcoma Cells. *PloS one* 7.

Malheiros-Garde, N., Garde, A., 1950. Fragmentation as a possible evolutionary process in the genus *Luzula* DC. *Genetica Iberica* 2, 257-262.

Malheiros, N., de Castro, K., Camara, A., 1947. Chromosomas sem centromero localizado. O caso da *Luzula purpurea* Link. *Agronomia Lusitana* 9, 51-74.

Malik, H.S., Henikoff, S., 2001. Adaptive evolution of cid, a centromere-specific histone in *Drosophila*. *Genetics* 157, 1293-1298.

Malik, H.S., Henikoff, S., 2002. Conflict begets complexity: the evolution of centromeres. *Current opinion in genetics & development* 12, 711-718.

Malik, H.S., Vermaak, D., Henikoff, S., 2002. Recurrent evolution of DNA-binding motifs in the *Drosophila* centromeric histone. *Proceedings of the National Academy of Sciences of the United States of America* 99, 1449-1454.

Mandrioli, M., 2002. Cytogenetic characterization of telomeres in the holocentric chromosomes of the lepidopteran *Mamestra brassicae*. *Chromosome Research* 10, 279-286.

Manti, L., Jamali, M., Prise, K.M., Michael, B.D., Trott, K.R., 1997. Genomic instability in *Chinese hamster* cells after exposure to X rays or alpha particles of different mean linear energy transfer. *Radiation research* 147, 22-28.

Manual, A., 2001. Cytogenetic analysis for radiation dose assessment. Technical Report Series- International Atomic Energy Agency.

Marston, A.L., Tham, W.H., Shah, H., Amon, A., 2004. A genome-wide screen identifies genes required for centromeric cohesion. *Science* 303, 1367-1370.

Matsumoto, T., Fukui, K., Niwa, O., Sugawara, N., Szostak, J.W., Yanagida, M., 1987. Identification of healed terminal DNA fragments in linear minichromosomes of *Schizosaccharomyces-pombe*. *Molecular and cellular biology* 7, 4424-4430.

McClintock, B., 1939. The behavior in successive nuclear divisions of a chromosome broken at meiosis. *Proceedings of the National Academy of Sciences of the United States of America* 25, 405.

McClintock, B., 1941. The stability of broken ends of chromosomes in *Zea mays*. *Genetics* 26, 234.

McClintock, B., 1942. The fusion of broken ends of chromosomes following nuclear fusion. *Proceedings of the National Academy of Sciences of the United States of America* 28, 458.

Melek, M., Shippen, D.E., 1996. Chromosome healing: spontaneous and programmed *de novo* telomere formation by telomerase. *BioEssays : news and reviews in molecular, cellular and developmental biology* 18, 301-308.

Melters, D.P., Paliulis, L.V., Korf, I.F., Chan, S.W., 2012. Holocentric chromosomes: convergent evolution, meiotic adaptations, and genomic analysis. *Chromosome Research* 20, 579-593.

Meltzer, P.S., Guan, X.Y., Trent, J.M., 1993. Telomere capture stabilizes chromosome breakage. *Nature Genetics* 4, 252-255.

Meneely, P.M., Farago, A.F., Kauffman, T.M., 2002. Crossover distribution and high interference for both the X chromosome and an autosome during oogenesis and spermatogenesis in *Caenorhabditis elegans*. *Genetics* 162, 1169-1177.

Meyne, J., Baker, R.J., Hobart, H.H., Hsu, T.C., Ryder, O.A., Ward, O.G., Wiley, J.E., Wursterhill, D.H., Yates, T.L., Moyzis, R.K., 1990. Distribution of nontelomeric sites of the (Ttaggg)_n telomeric sequence in vertebrate chromosomes. *Chromosoma* 99, 3-10.

Moens, P.B., Kolas, N.K., Tarsounas, M., Marcon, E., Cohen, P.E., Spyropoulos, B., 2002. The time course and chromosomal localization of recombination-related proteins at meiosis in the mouse are compatible with models that can resolve the early DNA-DNA interactions without reciprocal recombination. *Journal of cell science* 115, 1611-1622.

Mola, L., Papeschi, A., 2006. Holokinetic chromosomes at a glance. *Journal of Basic and Applied Genetics* 17, 17-33.

Monen, J., Maddox, P.S., Hyndman, F., Oegema, K., Desai, A., 2005. Differential role of CENP-A in the segregation of holocentric *C. elegans* chromosomes during meiosis and mitosis. *Nature Cell Biology* 7, 1148-1155.

Monti, V., Giusti, M., Bizzaro, D., Manicardi, G.C., Mandrioli, M., 2011. Presence of a functional (TTAGG)_n telomere-telomerase system in aphids. *Chromosome Research* 19, 625-633.

Moore, L.L., Morrison, M., Roth, M.B., 1999. HCP-1, a protein involved in chromosome segregation, is localized to the centromere of mitotic chromosomes in *Caenorhabditis elegans*. *Journal of Cell Biology* 147, 471-480.

Morris, C.A., Moazed, D., 2007. Centromere assembly and propagation. *Cell* 128, 647-650.

Muller, H., 1938. The remaking of chromosomes. *Collecting net* 13, 181-195.

Muller, H.J., 1932. Further studies on the nature and causes of gene mutations. *Proceedings of the 6th International Congress of Genetics. Brooklyn Botanic Gardens Menasha, Wisconsin*, pp. 213-255.

Nabeshima, K., Villeneuve, A.M., Colaicovo, M.P., 2005. Crossing over is coupled to late meiotic prophase bivalent differentiation through asymmetric disassembly of the SC. *Journal of Cell Biology* 168, 683-689.

Nagaki, K., Kashihara, K., Murata, M., 2005. Visualization of diffuse centromeres with centromere-specific histone H3 in the holocentric plant *Luzula nivea*. *Plant Cell* 17, 1886-1893.

Nasmyth, K., 2001. Disseminating the genome: joining, resolving, and separating sister chromatids during mitosis and meiosis. *Annual Review of Genetics* 35, 673-745.

Nasuda, S., Hudakova, S., Schubert, I., Houben, A., Endo, T.R., 2005. Stable barley chromosomes without centromeric repeats. *Proceedings of the National Academy of Sciences of the United States of America* 102, 9842-9847.

Neuhof, D., Ruess, A., Wenz, F., Weber, K.J., 2001. Induction of telomerase activity by irradiation in human lymphoblasts. *Radiation research* 155, 693-697.

Neumann, P., Navratilova, A., Koblizkova, A., Kejnovsky, E., Hribova, E., Hobza, R., Widmer, A., Dolezel, J., Macas, J., 2011. Plant centromeric retrotransposons: a structural and cytogenetic perspective. *Mobile DNA-Uk* 2.

Neumann, P., Navratilova, A., Schroeder-Reiter, E., Koblizkova, A., Steinbauerova, V., Chocholova, E., Novak, P., Wanner, G., Macas, J., 2012. Stretching the Rules: Monocentric Chromosomes with Multiple Centromere Domains. *PLoS genetics* 8.

Nietzel, A., Rocchi, M., Starke, H., Heller, A., Fiedler, W., Wlodarska, I., Loncarevic, I.F., Beensen, V., Claussen, U., Liehr, T., 2001. A new multicolor-FISH approach for the characterization of marker chromosomes: centromere-specific multicolor-FISH (cenM-FISH). *Human Molecular Genetics* 108, 199-204.

Nogueira, C., Kashevsky, H., Pinto, B., Clarke, A., Orr-Weaver, T.L., 2014. Regulation of centromere localization of the Drosophila Shugoshin MEI-S332 and sister-chromatid cohesion in meiosis. *G3-Genes Genom Genet* 4, 1849-1858.

Nokkala, S., Kuznetsova, V.G., Maryanska-Nadachowska, A., Nokkala, C., 2004. Holocentric chromosomes in meiosis. I. Restriction of the number of chiasmata in bivalents. *Chromosome Research* 12, 733-739.

Nordenskiöld, H., 1962. Studies of meiosis in *Luzula purpurea*. *Hereditas* 48, 503-&.

Nordenskiöld, H., 1951. Cyto-taxonomical studies in the genus *Luzula*. *Hereditas* 37, 325-355.

Nordenskiöld, H., 1961. Tetrad analysis and course of meiosis in three hybrids of *Luzula campestris*. *Hereditas* 47, 203-238.

Nordenskiöld, H., 1962. Studies of meiosis in *Luzula purpurea*. *Hereditas* 48, 503-519.

Nordenskiöld, H., 1963. A study of meiosis in progeny of X-irradiated *Luzula purpurea*. *Hereditas* 49, 33-47.

Nordenskiöld, H., 1964. The effect of x-irradiation on diploid and polyploid *Luzula*. *Hereditas* 51, 344-374.

Oliver, C.P., 1932. An analysis of the effect of varying the duration of X-ray treatment upon the frequency of mutations. *Molecular and General Genetics MGG* 61, 447-488.

Ottolini, C.S., Newnham, L.J., Capalbo, A., Natesan, S.A., Joshi, H.A., Cimadomo, D., Griffin, D.K., Sage, K., Summers, M.C., Thornhill, A.R., Housworth, E., Herbert, A.D., Rienzi, L., Ubaldi, F.M., Handyside, A.H., Hoffmann, E.R., 2015. Genome-wide maps of recombination and chromosome segregation in human oocytes and embryos show selection for maternal recombination rates. *Nature Genetics* 47, 727-+.

Padhy, K.B., 1986. Chromosome aberrations in the holocentric chromosomes of *Philosamia ricini* (Saturniidae). *Journal of Research on the Lepidoptera* 25, 63-66.

Painter, T.S., Müller, H., 1929. Parallel cytology and genetics of induced translocations and deletions in *Drosophila*. *Journal of Heredity* 20, 287-298.

Palmer, D.K., Oday, K., Wener, M.H., Andrews, B.S., Margolis, R.L., 1987. A 17-Kd Centromere protein (Cenp-a) copurifies with nucleosome core particles and with histones. *Journal of Cell Biology* 104, 805-815.

Paull, R.E., 1996. Ripening behavior of papaya (*Carica papaya* L.) exposed to gamma irradiation. *Postharvest Biology and Technology* 7, 359-370.

Pazy, B., Plitmann, U., 1987. Persisting demibivalents - a unique meiotic behavior in *Cuscuta-babylonica* Choisy. *Genome / National Research Council Canada = Genome / Conseil national de recherches Canada* 29, 63-66.

Pazy, B., Plitmann, U., 1991. Unusual chromosome separation in meiosis of *Cuscuta* L. *Genome / National Research Council Canada = Genome / Conseil national de recherches Canada* 34, 533-536.

Pazy, B., Plitmann, U., 1994. Holocentric chromosome behavior in *Cuscuta* (Cuscutaceae). *Plant Systematics and Evolution* 191, 105-109.

Pazy, B., Plitmann, U., 1995. Chromosome divergence in the genus *Cuscuta* and its systematic implications. *Caryologia* 48, 173-180.

Perez, R., Panzera, F., Page, J., Suja, J.A., Rufas, J.S., 1997. Meiotic behaviour of holocentric chromosomes: orientation and segregation of autosomes in *Triatoma infestans* (Heteroptera). *Chromosome Research* 5, 47-56.

Perez, R., Rufas, J.S., Suja, J.A., Page, J., Panzera, F., 2000. Meiosis in holocentric chromosomes: orientation and segregation of an autosome and sex chromosomes in *Triatoma infestans* (Heteroptera). *Chromosome Research* 8, 17-25.

Pfaffl, M.W., 2004. Quantification strategies in real-time PCR. *AZ of quantitative PCR* 1, 89-113.

Phillips, C.M., Dernburg, A.F., 2006. A family of zinc-finger proteins is required for chromosome-specific pairing and synapsis during meiosis in *C. elegans*. *Developmental Cell* 11, 817-829.

Phillips, D., Wnetrzak, J., Nibau, C., Barakate, A., Ramsay, L., Wright, F., Higgins, J.D., Perry, R.M., Jenkins, G., 2013. Quantitative high resolution mapping of HvMLH3 foci in barley pachytene nuclei reveals a strong distal bias and weak interference. *Journal of Experimental Botany* 64, 2139-2154.

Pimpinelli, S., Goday, C., 1989. Unusual kinetochores and chromatin diminution in *Parascaris*. *Trends in Genetics* 5, 310-315.

Ponticelli, A.S., Smith, G.R., 1989. Meiotic recombination-deficient mutants of *Schizosaccharomyces-pombe*. *Genetics* 123, 45-54.

Poschke, H., Dees, M., Chang, M., Amberkar, S., Kaderali, L., Rothstein, R., Luke, B., 2012. Rif2 promotes a telomere fold-back structure through Rpd3L recruitment in budding yeast. *PLoS genetics* 8.

Pradillo, M., Lopez, E., Linacero, R., Romero, C., Cunado, N., Sanchez-Moran, E., Santos, J.L., 2012. Together yes, but not coupled: new insights into the roles of RAD51 and DMC1 in plant meiotic recombination. *Plant Journal* 69, 921-933.

Prakken, R., 1959. Induced mutation. *Euphytica* 8, 270-322.

Putnam, C.D., Pennaneach, V., Kolodner, R.D., 2004. Chromosome healing through terminal deletions generated by *de novo* telomere additions in *Saccharomyces cerevisiae*. *Proceedings of the National Academy of Sciences of the United States of America* 101, 13262-13267.

Rabitsch, K.P., Petronczki, M., Javerzat, J.P., Genier, S., Chwalla, B., Schleiffer, A., Tanaka, T.U., Nasmyth, K., 2003. Kinetochore recruitment of two nucleolar proteins is required for homolog segregation in meiosis I (vol 4, pg 535, 2003). *Developmental Cell* 5, 523-523.

Rawlins, D.J., Highett, M.I., Shaw, P.J., 1991. Localization of telomeres in plant interphase nuclei by insitu hybridization and 3d confocal microscopy. *Chromosoma* 100, 424-431.

Ray, J.H., Venketeswaran, S., 1979. DNA-replication, Crna-H-3 insitu hybridization and C-band patterns in the polycentric chromosomes of *Luzula-purpurea* Link. *Chromosoma* 74, 337-346.

Raynard, S., Niu, H.Y., Sung, P., 2008. DNA double-strand break processing: the beginning of the end. *Genes & Development* 22, 2903-2907.

Richards, E.J., Goodman, H.M., Ausubel, F.M., 1991. The centromere region of *Arabidopsis-thaliana* chromosome-1 contains telomere-similar sequences. *Nucleic acids research* 19, 3351-3357.

Rinaldo, C., Bazzicalupo, P., Ederle, S., Hilliard, M., La Volpe, A., 2002. Roles for *Caenorhabditis elegans* rad-51 in meiosis and in resistance to ionizing radiation during development. *Genetics* 160, 471-479.

Rivadavia, F., Kondo, K., Kato, M., Hasebe, M., 2003. Phylogeny of the sundews, *Drosera* (Droseraceae), based on chloroplast rbcL and nuclear 18S ribosomal DNA sequences. *American Journal of Botany* 90, 123-130.

Roeder, G.S., 1997. Meiotic chromosomes: it takes two to tango. *Genes & Development* 11, 2600-2621.

Rogers, E., Bishop, J.D., Waddle, J.A., Schumacher, J.M., Lin, R.L., 2002. The aurora kinase AIR-2 functions in the release of chromosome cohesion in *Caenorhabditis elegans* meiosis. *Journal of Cell Biology* 157, 219-229.

Saffery, R., Irvine, D.V., Griffiths, B., Kalitsis, P., Wordeman, L., Choo, K.H.A., 2000. Human centromeres and neocentromeres show identical distribution patterns of > 20 functionally important kinetochore-associated proteins. *Human Molecular Genetics* 9, 175-185.

Saifitdinova, A.F., Derjusheva, S.E., Malykh, A.G., Zhurov, V.G., Andreeva, T.F., Gaginskaya, E.R., 2001. Centromeric tandem repeat from the chaffinch genome: isolation and molecular characterization. *Genome / National Research Council Canada = Genome / Conseil national de recherches Canada* 44, 96-103.

Saifitdinova, A.F., Timofejeva, L.P., Zhurov, V.G., Guginskaya, E.R., 2000. A highly repeated FCP centromeric sequence from chaffinch (*Fringilla coelebs*: Aves) genome is revealed within interchromosomal connectives during mitosis. *Tsitologiya* 42, 581-586.

Sakuno, T., Tanaka, K., Hauf, S., Watanabe, Y., 2011. Repositioning of Aurora B promoted by chiasmata ensures sister chromatid mono-orientation in meiosis I. *Developmental Cell* 21, 534-545.

Sakuno, T., Watanabe, Y., 2009. Studies of meiosis disclose distinct roles of cohesion in the core centromere and pericentromeric regions. *Chromosome Research* 17, 239-249.

Sanchez-Moran, E., Osman, K., Higgins, J.D., Pradillo, M., Cunado, N., Jones, G.H., Franklin, F.C., 2008. ASY1 coordinates early events in the plant meiotic recombination pathway. *Cytogenetic and Genome Research* 120, 302-312.

Sandell, L.L., Zakian, V.A., 1993. Loss of a yeast telomere: arrest, recovery, and chromosome loss. *Cell* 75, 729-739.

Sato, S., Kobayashi, T., Hotta, Y., Tabata, S., 1995. Characterization of a mouse recA-like gene specifically expressed in testis. *DNA research : an international journal for rapid publication of reports on genes and genomes* 2, 147-150.

Sax, K., 1938. Chromosome aberrations induced by X-rays. *Genetics* 23, 494.

Sax, K., 1940. An analysis of X-ray induced chromosomal aberrations in *Tradescantia*. *Genetics* 25, 41.

Sax, K., 1941. The behavior of x-ray induced chromosomal aberrations in *Allium* root tip cells. *Genetics* 26, 418-425.

Sax, K., 1963. The stimulation of plant growth by ionizing radiation. *Radiation Botany* 3, 179-186.

Schagger, H., Vonjagow, G., 1987. Tricine sodium dodecyl-sulfate polyacrylamide-gel electrophoresis for the separation of proteins in the range from 1-Kda to 100-Kda. *Analytical Biochemistry* 166, 368-379.

Scherthan, H., 2001. A bouquet makes ends meet. *Nature Reviews Molecular Cell Biology* 2, 621-627.

Scherthan, H., Weich, S., Schwegler, H., Heyting, C., Harle, M., Cremer, T., 1996. Centromere and telomere movements during early meiotic prophase of mouse and man are associated with the onset of chromosome pairing. *Journal of Cell Biology* 134, 1109-1125.

Schmidt, T., Heslop-Harrison, J.S., 1998. Genomes, genes and junk: the large-scale organization of plant chromosomes. *Trends in Plant Science* 3, 195-199.

Schnable, P.S., Hsia, A.P., Nikolau, B.J., 1998. Genetic recombination in plants. *Current Opinion in Plant Biology* 1, 123-129.

Schneider, M.C., Zacaro, A.A., Pinto-da-Rocha, R., Candido, D.M., Cella, D.M., 2009. Complex meiotic configuration of the holocentric chromosomes: the intriguing case of the scorpion *Tityus bahiensis*. *Chromosome Research* 17, 883-898.

Schönswetter, P., Suda, J., Popp, M., Weiss-Schneeweiss, H., Brochmann, C., 2007. Circumpolar phylogeography of *Juncus biglumis* (Juncaceae) inferred from AFLP fingerprints, cpDNA sequences, nuclear DNA content and chromosome numbers. *Molecular Phylogenetics and Evolution* 42, 92-103.

Schrader, F., 1947. The Role of the Kinetochore in the chromosomal evolution of the Heteroptera and Homoptera. *Evolution* 1, 134-142.

Schubert, I., Lysak, M.A., 2011. Interpretation of karyotype evolution should consider chromosome structural constraints. *Trends in Genetics* 27, 207-216.

Schuermann, D., Molinier, J., Fritsch, O., Hohn, B., 2005. The dual nature of homologous recombination in plants. *Trends in Genetics* 21, 172-181.

Schultz, J., 1936. *Radiation and the study of mutations in animals. Biological Effects of Radiation*", IIMcGraw-Hill, New York, 1209-1261.

Schwarzstein, M., Wignall, S.M., Villeneuve, A.M., 2010. Coordinating cohesion, co-orientation, and congression during meiosis: lessons from holocentric chromosomes. *Genes & Development* 24, 219-228.

Schwacha, A., Kleckner, N., 1997. Interhomolog bias during meiotic recombination: meiotic functions promote a highly differentiated interhomolog-only pathway. *Cell* 90, 1123-1135.

Sengupta, J., Sharma, A.K., 1988. Response to radiation and invitro Growth of 2 species of *Luzula* with non-localized centromere. *P Indian as-Plant Science* 98, 489-493.

Shakes, D.C., Wu, J.C., Sadler, P.L., LaPrade, K., Moore, L.L., Noritake, A., Chu, D.S., 2009. Spermatogenesis-specific features of the meiotic program in *Caenorhabditis elegans*. *PLoS genetics* 5.

Shanahan, C.M., 1989. Cytogenetics of australian scorpions .1. Interchange polymorphism in the family Buthidae. *Genome / National Research Council Canada = Genome / Conseil national de recherches Canada* 32, 882-889.

Shao, T., Tang, D., Wang, K., Wang, M., Che, L., Qin, B., Yu, H., Li, M., Gu, M., Cheng, Z., 2011. OsREC8 is essential for chromatid cohesion and metaphase I monopolar orientation in rice meiosis. *Plant Physiology* 156, 1386-1396.

Sheikh, S.A., Kondo, K., 1995. Differential staining with Orcein, Giemsa, Cma, and Dapi for comparative chromosome study of 12 species of australian *Drosera* (Droseraceae). *American Journal of Botany* 82, 1278-1286.

Shelby, R.D., Vafa, O., Sullivan, K.F., 1997. Assembly of CENP-A into centromeric chromatin requires a cooperative array of nucleosomal DNA contact sites. *Journal of Cell Biology* 136, 501-513.

Sheridan, S.D., Yu, X., Roth, R., Heuser, J.E., Sehorn, M.G., Sung, P., Egelman, E.H., Bishop, D.K., 2008. A comparative analysis of Dmc1 and Rad51 nucleoprotein filaments. *Nucleic acids research* 36, 4057-4066.

Shinohara, A., Gasior, S., Ogawa, T., Kleckner, N., Bishop, D.K., 1997. *Saccharomyces cerevisiae* recA homologues RAD51 and DMC1 have both distinct and overlapping roles in meiotic recombination. *Genes Cells* 2, 615-629.

Shinohara, A., Ogawa, H., Ogawa, T., 1992. Rad51 Protein involved in repair and recombination in *Saccharomyces-cerevisiae* is a recA-like protein. *Cell* 69, 457-470.

Shinohara, A., Shinohara, M., 2004. Roles of RecA homologues Rad51 and Dmc1 during meiotic recombination. *Cytogenetic and Genome Research* 107, 201-207.

Shinohara, M., Gasior, S.L., Bishop, D.K., Shinohara, A., 2000. Tid1/Rdh54 promotes colocalization of Rad51 and Dmc1 during meiotic recombination. *Proceedings of the National Academy of Sciences of the United States of America* 97, 10814-10819.

Slijepcevic, P., Bryant, P.E., 1998. Chromosome healing, telomere capture and mechanisms of radiation-induced chromosome breakage. *International journal of radiation biology* 73, 1-13.

Slijepcevic, P., Xiao, Y., Dominguez, I., Natarajan, A.T., 1996. Spontaneous and radiation-induced chromosomal breakage at interstitial telomeric sites. *Chromosoma* 104, 596-604.

Stebbins Jr, C., 1950. Variation and evolution in plants. *Variation and evolution in plants*.

Steiner, F.A., Henikoff, S., 2014. Holocentromeres are dispersed point centromeres localized at transcription factor hotspots. *Elife* 3.

Steiner, N.C., Clarke, L., 1994. A novel epigenetic effect can alter centromere function in fission yeast. *Cell* 79, 865-874.

Suja, J.A., del Cerro, A.L., Page, J., Rufas, J.S., Santos, J.L., 2000. Meiotic sister chromatid cohesion in holocentric sex chromosomes of three heteropteran species is maintained in absence of axial elements. *Chromosoma* 109, 35-43.

Suja, J.A., Rufas, J.S., 1994. The telochore: a telomeric differentiation of the chromosome axis. *Chromosome Research* 2, 361-368.

Sykorova, E., Lim, K.Y., Chase, M.W., Knapp, S., Leitch, I.J., Leitch, A.R., Fajkus, J., 2003. The absence of Arabidopsis-type telomeres in *Cestrum* and closely related genera *Vestia* and *Sessea* (Solanaceae): first evidence from eudicots. *Plant Journal* 34, 283-291.

Szostak, J.W., Orrweaver, T.L., Rothstein, R.J., Stahl, F.W., 1983. The double-strand-break repair model for recombination. *Cell* 33, 25-35.

Talbert, P.B., Masuelli, R., Tyagi, A.P., Comai, L., Henikoff, S., 2002. Centromeric localization and adaptive evolution of an Arabidopsis histone H3 variant. *Plant Cell* 14, 1053-1066.

Tanaka, N., Tanaka, N., 1977. Chromosome studies in *Chionographis* (Liliaceae) .1. Holokinetic nature of chromosomes in *Chionographis-japonica*-Maxim. *Cytologia* 42, 753-763.

Tarsounas, M., Morita, T., Pearlman, R.E., Moens, P.B., 1999. RAD51 and DMC1 form mixed complexes associated with mouse meiotic chromosome cores and synaptonemal complexes. *Journal of Cell Biology* 147, 207-219.

Tartarotti, E., de Azeredo-Oliveira, M.T.V., 1999. Heterochromatin patterns in triatomines of the genus *Panstrongylus*. *Cytobios* 99, 113-122.

Teixeira, M.T., Arneric, M., Sperisen, P., Lingner, J., 2004. Telomere length homeostasis is achieved via a switch between telomerase-extendible and-nonextendible states. *Cell* 117, 323-335.

Tek, A.L., Jiang, J.M., 2004. The centromeric regions of potato chromosomes contain megabase-sized tandem arrays of telomere-similar sequence. *Chromosoma* 113, 77-83.

Tempelaar, M.J., 1979. Fate of fragments and properties of translocations of holokinetic chromosomes after x-irradiation of mature sperm of *Tetranychus urticae* Koch (Acari, Tetranychidae). *Mutation research* 63, 301-316.

Terasawa, M., Shinohara, A., Hotta, Y., Ogawa, H., Ogawa, T., 1995. Localization of RecA-like recombination proteins on chromosomes of the Lily at various meiotic stages. *Genes & Development* 9, 925-934.

Tiang, C.L., He, Y., Pawlowski, W.P., 2012. Chromosome organization and dynamics during interphase, mitosis, and meiosis in plants. *Plant Physiology* 158, 26-34.

Toth, A., Rabitsch, K.P., Galova, M., Schleiffer, A., Buonomo, S.B.C., Nasmyth, K., 2000. Functional genomics identifies Monopolin: A kinetochore protein required for segregation of homologs during meiosis I. *Cell* 103, 1155-1168.

Tsujimoto, H., 1993. Molecular cytological evidence for gradual telomere synthesis at the broken chromosome ends in wheat. *Journal of Plant Research* 106, 239-244.

Tsujimoto, H., Yamada, T., Sasakuma, T., 1997. Molecular structure of a wheat chromosome end healed after gametocidal gene-induced breakage. *Proceedings of the National Academy of Sciences of the United States of America* 94, 3140-3144.

Valdeolillos, A.M., Viera, A., Page, J., Prieto, I., Santos, J.L., Parra, M.T., Heck, M.M.S., Martinez, C., Barbero, J.L., Suja, J.A., Rufas, J.S., 2007. Sequential loading of cohesin subunits during the first meiotic prophase of grasshoppers. *PLoS genetics* 3, 204-215.

Vanzela, A.L.L., Colaço, W., 2002. Mitotic and meiotic behavior of γ irradiated holocentric chromosomes of *Rhynchospora pubera* (Cyperaceae). *Acta Scientiarum* 24, 611-614.

Vanzela, A.L.L., Cuadrado, A., Guerra, M., 2003. Localization of 45S rDNA and telomeric sites on holocentric chromosomes of *Rhynchospora tenuis* Link (Cyperaceae). *Genetics And Molecular Biology* 26, 199-201.

Vanzela, A.L.L., Guerra, M., 2000. Heterochromatin differentiation in holocentric chromosomes of *Rhynchospora* (Cyperaceae). *Genetics And Molecular Biology* 23, 453-456.

Viera, A., Page, J., Rufas, J.S., 2009. Inverted meiosis: the true bugs as a model to study. *Genome dynamics and stability Journal* 5, 137-156.

Vignard, J., Siwiec, T., Chelysheva, L., Vrielynck, N., Gonord, F., Armstrong, S.J., Schlogelhofer, P., Mercier, R., 2007. The interplay of RecA-related proteins and the MND1-HOP2 complex during meiosis in *Arabidopsis thaliana*. *PLoS genetics* 3, 1894-1906.

Villasante, A., Abad, J.P., Mendez-Lago, M., 2007. Centromeres were derived from telomeres during the evolution of the eukaryotic chromosome. *Proceedings of the National Academy of Sciences of the United States of America* 104, 10542-10547.

Wanner, G., Schroeder-Reiter, E., Ma, W., Houben, A., Schubert, V., 2015. The ultrastructure of mono- and holocentric plant centromeres: an immunological investigation by structured illumination microscopy and scanning electron microscopy. *Chromosoma* 503-17.

Watanabe, Y., 2004. Modifying sister chromatid cohesion for meiosis. *Journal of Cell Science* 117, 4017-4023.

Watanabe, Y., Nurse, P., 1999. Cohesin Rec8 is required for reductional chromosome segregation at meiosis. *Nature* 400, 461-464.

White, M.J.D., 1973. *Animal cytology and evolution* / M. J. D. White. University Press, Cambridge, [Eng.].

Wiendl, F.M., Wiendl, F.W., Wiendl, J.A., Vedovatto, A., Arthur, V., 1995. Increase of onion yield through low-dose of gamma-irradiation of its seeds. *Radiation Physics and Chemistry* 46, 793-795.

Wignall, S.M., Villeneuve, A.M., 2009. Lateral microtubule bundles promote chromosome alignment during acentrosomal oocyte meiosis. *Nature Cell Biology* 11, 839-U135.

Wolff, S., Atwood, K., 1954. Independent x-ray effects on chromosome breakage and reunion. *Proceedings of the National Academy of Sciences of the United States of America* 40, 187.

Woodstoc.Lw, Justice, O.L., 1967. Radiation-induced changes in respiration of corn wheat sorghum and radish seeds during initial stages of germination in relation to subsequent seedling growth. *Radiation Botany* 7, 129-&.

Wrensch, D.L., Kethley, J.B., Norton, R.A., 1994. Cytogenetics of holokinetic chromosomes and inverted meiosis: keys to the evolutionary success of mites, with generalizations on eukaryotes. *Mites*. Springer, pp. 282-343.

Wright, W.E., Shay, J.W., 1992. Telomere positional effects and the regulation of cellular senescence. *Trends in Genetics* 8, 193-197.

Yamamoto, A., Yagi, H., Habu, T., Yoshimura, Y., Matsushiro, A., Nishimune, Y., Morita, T., Taki, T., Yoshida, K., Yamamoto, K., 1996. Cell cycle-dependent expression of the mouse Rad51 gene in proliferating cells. *Molecular and General Genetics MGG* 251, 1-12.

Yano, O., Hoshino, T., 2006. Cytological studies of aneuploidy in *Eleocharis kamtschatica* (Cyperaceae). *Cytologia* 71, 141-147.

Yelina, N.E., Choi, K., Chelysheva, L., Macaulay, M., de Snoo, B., Wijnker, E., Miller, N., Drouaud, J., Grelon, M., Copenhaver, G.P., Mezard, C., Kelly, K.A., Henderson, I.R., 2012. Epigenetic remodeling of meiotic crossover frequency in *Arabidopsis thaliana* DNA methyltransferase mutants. *PLoS genetics* 8, e1002844.

Yoshida, K., Kondoh, G., Matsuda, Y., Habu, T., Nishimune, Y., Morita, T., 1998. The mouse RecA-like gene Dmc1 is required for homologous chromosome synapsis during meiosis. *Molecular Cell* 1, 707-718.

Yu, G.-L., Blackburn, E.H., 1991. Developmentally programmed healing of chromosomes by telomerase in *Tetrahymena*. *Cell* 67, 823-832.

Zakian, V.A., 1995. Telomeres - beginning to understand the end. *Science* 270, 1601-1607.

Zamariola, L., De Storme, N., Vannerum, K., Vandepoele, K., Armstrong, S.J., Franklin, F.C.H., Geelen, D., 2014. Shugoshins and Patronus protect meiotic centromere cohesion in *Arabidopsis thaliana*. *The Plant Journal* 77, n/a-n/a.

Záveská Drábková, L., 2013. A survey of karyological phenomena in the Juncaceae with emphasis on chromosome number variation and evolution. *Botanical Review* 79, 401-446.

Zedek, F., Šmerda, J., Šmarda, P., Bureš, P., 2010. Correlated evolution of LTR retrotransposons and genome size in the genus *Eleocharis*. *Bmc Plant Biology* 10.

Zheng, Y.Z., Roseman, R.R., Carlson, W.R., 1999. Time course study of the chromosome-type breakage-fusion-bridge cycle in maize. *Genetics* 153, 1435-1444.

Zhong, X.B., Fransz, P.F., Wennekes-van Eden, J., Ramanna, M.S., van Kammen, A., Zabel, P., de Jong, J.H., 1998. FISH studies reveal the molecular and chromosomal organization of individual telomere domains in tomato. *Plant Journal* 13, 507-517.

https://www.neb.com/~media/NebUs/Files/Chart%20image/cleavage_olignucleotides_old.pfd

<http://www.ncbi.nlm.nih.gov/Structure/cdd/wrpsb.cgi?RID=GWVVOAPY01R&mode=all>

http://web.expasy.org/compute_pi/

<http://primer3.ut.ee/>

List of publications related to this thesis

Heckmann, S., **Jankowska, M.**, Schubert, V., Kumke, K., Ma, W., Houben, A., 2014. Alternative meiotic chromatid segregation in the holocentric plant *Luzula elegans*. Nature communications 5, 4979.

Jankowska, M., Fuchs, J., Klocke, E., Fojtova, M., Polanska, P., Fajkus, J., Schubert, V., Houben, A., 2015. Holokinetic centromeres and efficient telomere healing enable rapid karyotype evolution. Chromosoma, 1432-0886.

Curriculum Vitae

Personal details

Name Maja Jankowska
Gender female
Nationality Poland
Present address Corrensstrasse 3
06466 Gatersleben, Germany
Date of birth 12.05.1987

Contact information

Phone +49(0)15738489787
E-mail jankowskam@ipk-gatersleben.de

Education

since April 2012 PhD at the **Leibniz Institute of Plant Genetics and Crop Plant Research (IPK)**, Gatersleben, Germany. Department of Breeding Research, Chromosome Structure and Function Group (Dr. habil. A. Houben) Topic: Functional consequence of chromosome holocentricity.

September 2010-May 2011 Erasmus student at **Institute of Biological, Rural and Environmental Sciences**, Aberystwyth University, UK.

October 2009-June 2011 MSc at the **University of Silesia**, Katowice, Poland. Department of Plant Anatomy and Cytology, Biotechnology of Crop Plants (Prof. R. Hasterok) Topic: Comparative analysis of the distribution of centromeric and telomeric domains during different stages of mitosis and meiosis in *Brachypodium* species.

October 2009-October 2011 MSc at the **University of Silesia**, Katowice, Poland. Department of Animals Physiology, Environmental Protection (Prof. P. Migula) Topic: The metallothionein level in selected organs of *Sinanodonta woodiana* exposed to cadmium and copper.

October 2006-June 2009 BSc at the **University of Silesia**, Katowice, Poland. Department of Plant Anatomy and Cytology, Biotechnology of Crop Plants (Prof. J. Małuszynska) Topic: Structure and function of synaptonemal complex.

Stays in other Research

Centers

February 2015

Masaryk University, Brno, Czech Republic. Research group Molecular Complex of Chromatin (Prof. J. Fajkus).

January 2012 – February 2012

University of Jaén, Jaén, Spain. Department of Animal, Plant Biology and Ecology (Dr. A. J. Manzaneda).

Oral presentations

Jankowska, M. Title: *Luzula elegans* – a holocentric species with an inverted sequence of meiotic events? (2.06.2014) Plant Science Student Conference, Leibniz Institute of Plant Genetics and Crop Plant Research, Gatersleben, Germany

Jankowska, M. Title: Alternative meiotic chromatid segregation in the holocentric plant *Luzula elegans* (19.12.2014) Jagiellonian University, Krakow, Poland

Jankowska, M. Title: *Luzula elegans* – a holocentric species with an inverted sequence of meiotic events? (20.02.2015) Masaryk University, Brno, Czech Republic

Jankowska, M. Title: Functional consequences of chromosome holocentricity. (17.07.2015) Martin-Luther University, Halle/Saale, Germany

Poster presentations

Jankowska, M., Heckmann, S., Houben, A. Title: Inverted meiosis in the holocentric plant *Luzula elegans*. (04.06 – 07.06.2012) Plant Science Student Conference 2012, Leibniz Institute of Plant Genetics and Crop Plant Research, Gatersleben, Germany

Jankowska, M., Heckmann, S., Houben, A. Title: Inverted meiosis in the holocentric plant *Luzula elegans*. (03.09 – 05.09.2012) The International PhD Student Conference on Experimental Plant Biology, Mendel Museum, Brno, Czech Republic

Heckmann, S., **Jankowska, M.**, Houben, A. Title: How does holocentricity influence meiosis and the genome organization of *Luzula elegans*? (24.09 – 26.09.2012) Institutes day IPK, Gatersleben, Germany

Jankowska, M., Houben, A. Title: *Luzula elegans* – a holocentric species with an inverted sequence of meiotic events. (28.05 – 31.05.2013) Plant science student conference, Halle/Salle, Germany

Jankowska, M., Ma, W., Heckmann, S., Houben, A. Title: *Luzula elegans* – a holocentric species with an inverted sequence of meiotic events. (14.11 – 19.11.2013) EMBO Conference Series - MEIOSIS, Dresden, Germany

Jankowska, M., Ma, W., Heckmann, S., Houben, A. Title: Inverted meiosis in the holocentric plant *Luzula elegans*. (02.04 – 03.04.2014) Meiosis meeting SPP1384, Heidelberg, Germany

Ma, W., **Jankowska, M.**, Schubert, V., Scholz, U., Houben, A. Title: Unraveling an alternative meiosis (17.05.2014) Institutes day IPK, Gatersleben, Germany

Jankowska, M., Ma, W., Heckmann, S., Kumke, K., Schubert, V., Houben, A. Title: Alternative meiotic chromatid segregation in the holocentric plant *Luzula elegans* (23.09 – 24.09.2014) Plant molecular cytogenetics in genomic and postgenomic era, Katowice, Poland

Awards

1st price poster: The 10th International Ph.D. Student Conference on Experimental Plant Biology (2012) Brno, Czech Republic.

Audience price best talk: Plant Science Student Conference (2014) Leibniz Institute of Plant Genetics and Crop Plant Research, Gatersleben, Germany.

2nd price poster: Plant Science Student Conference (2012) Leibniz Institute of Plant Genetics and Crop Plant Research, Gatersleben, Germany.

I hereby declare that all information stated above is true

Maja Jankowska

Declarations

Eidesstattliche Erklärung / Declaration under Oath

Ich erkläre an Eides statt, dass ich die Arbeit selbstständig und ohne fremde Hilfe verfasst, keine anderen als die von mir angegebenen Quellen und Hilfsmittel benutzt und die den benutzten Werken wörtlich oder inhaltlich entnommenen Stellen als solche kenntlich gemacht habe.

I declare under penalty of perjury that this thesis is my own work entirely and has been written without any help from other people. I used only the sources mentioned and included all the citations correctly both in word or content.

Datum / Date

Unterschrift des Antragstellers / Signature of the applicant

Erklärung über bestehende Vorstrafen und anhängige Ermittlungsverfahren / Declaration concerning Criminal Record and Pending Investigations

Hiermit erkläre ich, dass ich weder vorbestraft bin noch dass gegen mich Ermittlungsverfahren anhängig sind. / *I hereby declare that I have no criminal record and that no preliminary investigations are pending against me.*

Datum / Date

Unterschrift des Antragstellers / Signature of the applicant